Behavior of interface between concrete-PCM at elevated temperature at material and member level

高温下の材料および部材レベルでのコンクリートとPCMとの付着界面挙動

Khuram Rashid

March 2016

Behavior of interface between concrete-PCM at elevated temperature at material and member level

高温下の材料および部材レベルでのコンクリートとPCMとの付着界面挙動

By

Khuram Rashid

A thesis submitted in partial fulfillment of the requirements for the Degree of Doctor of Philosophy in Engineering

English Engineering Program (e3)

Laboratory of Engineering for Maintenance System

Division of Engineering and Policy for Sustainable Environment

Graduate School of Engineering

Hokkaido University

March 2016

ACKNOWLEDGEMENTS

Up and above anything else, praises are due to Almighty ALLAH alone, the omnipotent, and the omnipresent.

I would like to express my deepest and heartfelt gratitude and indebtedness to my supervisor, Prof. Tamon UEDA, for his continuous support, expert guidance, dearly encouragement and constructive criticism during my entire research period. It was a lifetime experience to work under his excellent supervision with a joy of learning and exploring new things each and every time.

I would also like to extend my sincere gratitude to Associate Prof. Dawei ZHANG for providing valuable suggestions and innovative ideas throughout my research. My sincere thankfulness is extended to all esteemed members of the doctoral committee, Prof. Hiroshi YOKOTA and Prof. Takafumi SUGIYAMA for their valuable comments and guidance during yearly evaluations.

My appreciation also goes to Prof. Toshifumi SATOH, Prof. Weiliang JIN, Associate Prof. Yasuhiko SATO and Dr. Hitoshi FURUUCHI for their support in conducting my experiments in respective laboratories. It would have been truly impossible to carry out such an extensive experimental work without our lab technicians Mr. Tsutomu Kimura and Ohta Masaichi. My sincere thanks to both of them for generous help offered throughout my long experimental program.

I am also grateful to Mr. Katsushi MIYAGUCHI and Seiji FUJIMA of Denki Kagaku Kogyo Kabushiki Kaisha (DENKA) and Mr. Hiroshi Nakai of Maeda Kosen Co. Limited for providing polymer cement mortar along with some useful information.

I would like to acknowledge our past e3 coordinator Mrs. Werawan Manakul for providing me an opportunity to be a part of e3 family and the present coordinator Ms. Natalya Shmakova for their continuous support and encouragement during my stay in Japan.

I am really indebted to University of Engineering and Technology, Lahore, Pakistan for the scholarship to support my three years stay in Japan for Ph.D.

I would also like to appreciate the contributions of all my lab members for providing good cooperation and assistance during my experimental works. Their support contributes in many ways for the completion of this study.

No acknowledgement would ever adequately express my obligation to my parents and family who have always wished to see me flying high up at the skies of success. Without their prayers, sacrifices and encouragements the present work have been a merry dream.

ABSTRACT

Strengthening, retrofitting, upgrading and rehabilitation of ageing infrastructure by Polymer Cement Mortar (PCM) is one of viable, economical and environment friendly solutions. Although PCM has superior properties than ordinary mortar in terms of mechanical strength, durability and good adhesive strength with concrete, the weakest zone in the concrete-PCM specimen is the interfacial zone. PCM after placing over treated substrate concrete surface is properly cured and after designed curing period, composite specimens/structures were exposed to severe environmental deterioration mechanisms. This fact causes the degradation of interface more rapidly than constituent materials and is responsible for significant reduction of intended service life of repaired structures. Therefore, it is necessary to investigate the behavior of interface under severe environmental conditions, which can be used for designing of repaired structures. For such aim, detailed experimental and analytical study were conducted, in which influence of moisture and temperature were investigated on composite specimens along with the constituents.

Primary goal of this work is to strengthening of concrete structure in hot regions, where temperature increases to higher than 60 ℃ in peak summer. So environmental conditions were selected, which have resemblance to real environment. Day night variation and seasonal variation with short and long temperature duration were considered as exposure conditions. PCM and composite specimens were exposed to such conditions and were tested for interfacial tensile strength at designed conditions. Polymers from PCM were extracted after conducting interfacial split tensile strength test and tested for molecular weight, glass transition temperature and melting point. It was observed that testing condition significantly affected the tensile strength of PCM and composite specimens. Severe degradation at high temperature and recovery under lowering temperature were observed. Short temperature duration, about 16 hours, is long enough to have pronounced effect on tensile strength. Maximum reduction in tensile strength was observed under the combined action of temperature and moisture and tested at high temperature. Failure mode of composite specimen was shifted from adhesive interface failure to cohesive PCM at elevated temperature, which is considered as the indication of degradation of PCM. Whereas, molecular weight, glass transition temperature and melting point of polymers were still almost the same after different exposures.

Because of the observed severe influence of moisture and temperature on interfacial tensile strength, more detailed experiments were designed, in which properties of bulk specimens and composite specimens were investigated under moisture and temperature variation separately and then combined variation. Tensile strength of concrete, PCM and concrete-PCM specimens was decreased with increase in temperature and moisture have only marginal effect. Degradation in tensile strength of PCM was significant at elevated temperature. Prediction formula of interfacial tensile strength was also proposed which was the function of the tensile strength of constituent materials and applicable for the temperature range from 20 ℃ to 60 ℃. Failure mode of all

composite specimens under both types of environmental conditions was adhesive interface failure. To increase the interfacial strength, interfacial zone was enhanced by adding primer at interface and also by increasing the roughness level of substrate concrete surface. Along with interfacial tensile strength of bulk and composite specimens at elevated temperature, interfacial shear strength was also investigated for both types of specimens. Prediction formula of interfacial tensile strength was verified by incorporating the effect of primer and enhanced surface treatment. All data lies within ±10% of experimental results when compared with the predicted interfacial tensile strength. Prediction formula of interfacial shear strength was also proposed and applicable for temperature range of 20 ℃ to 60 ℃. Small variation was observed but average experimental data lies within ±10% of predicted results, which verifies the applicability of proposed formula.

For real application of the current work, behavior of interface was also investigated at member level by conducting loading test of RC beams strengthened by PCM overlaying with different amount of reinforcement. All beams, strengthened and unstrengthened, were exposed to different temperature levels and tested at exposed temperature and humidity condition in four points loading test. Failure load of all strengthened beams were observed more than the unstrengthened beams but decreased with the increase in temperature level. Failure mode at elevated temperature was also varied from classical failure mode of conventional RC beam to debonding at overlay end as increase in the amount of reinforcement. Ductility, first crack load, yield load and ultimate load also decreased with the increase in temperature. Prediction model for debonding strength was proposed by incorporating interfacial tensile and shear strength of composite specimens, which were investigated at material level. Truss analogy approach was used for prediction of ultimate shear load and failure mode for overlay beams and close agreement was observed at all temperature levels. Serviceability of strengthened RC beams at elevated temperature was also investigated by investigating flexural crack spacing in constant moment zone at different temperature level and by measuring crack width at temperature level of 20 and 40 ℃. Crack spacing and crack width was increased with the increase in temperature.

Keywords: PCM, Temperature, Interfacial Bond Strength, Debonding Strength, Failure Modes, Serviceability.

Table of Contents

List of Figures

List of Tables

Chapter 1

INTRODUCTION

1.1 BACKGROUND

Reinforced concrete (RC) structures are considered as most durable structures and used to build from houses to bridges. Hundreds of thousands of RC structures are annually constructed worldwide. Large number of structures deteriorated before the end of intended service life due to different reasons viz. inadequacy of design detailing, poor construction, overloading, corrosion of rebar, fatigue effect, severe environmental condition, natural disaster (earthquake, storm or flood), change in use, change in configuration, etc. Maintenance or rehabilitation is most suitable solution, economically and environmentally, for restoration of such deteriorated RC structures. Concrete repaired structures are exposed to severe environmental conditions along with the various loading impacts.

Durability of concrete repair is the key issue of present scenario. Various repairing materials have been produced and commercially available in large area of the world, e.g. Fiber Reinforced Polymers (FRP), Polymer Cement Mortar (PCM), Engineering Cementitious Composites (ECC). Almost all repairing materials have superior properties than ordinary concrete. But, in repaired structures the bond between substrate concrete and repairing materials was considered as the weakest link between two materials. And may deteriorated more rapidly than intended service life. Some factors, which affect the durability of concrete repairs is presented in Fig. 1.1 [1].

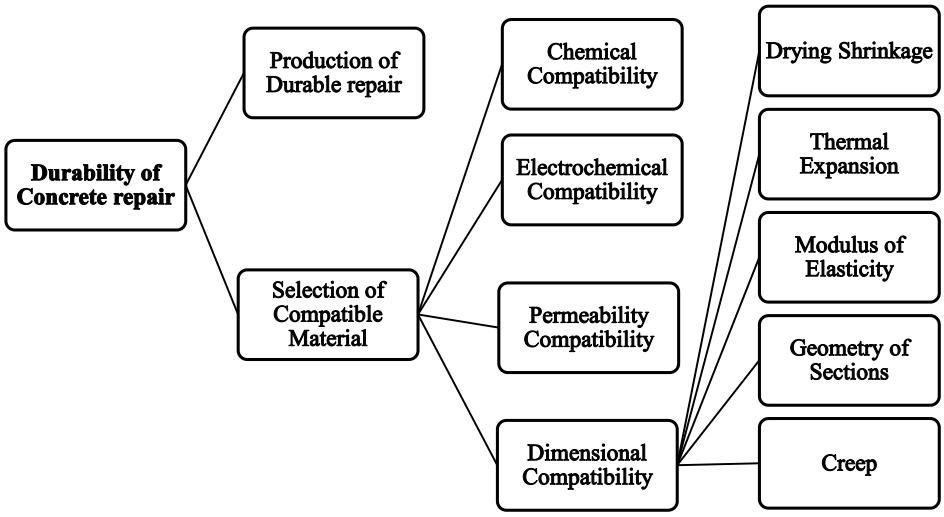

Fig. 1.1 Factors affecting durability of Concrete repairs. [1]

The adhesive mechanism of cementitious materials with the substrate concrete is considered as the first step for the compatibility or repairing structure. The ‘adhesive’ mechanism is related to chemical forces, which are responsible for the embedding action or mechanical anchorage between

the reactive matrix of new material and old substrate concrete. Adhesion at interface is improved by adding different binder which makes it dense and reduces the porosity at the interface [2, 3]. Among all cementitious materials, polymer modified cement mortar gives the good adhesion at interface due to the fact that polymer films surround the hydration products and aggregates. Coalescence of polymer particles fills all the pores and reduces the porosity and increases the adhesive strength [4-6]. Polymer cement mortar (PCM) is more durable and having strong resistance against chloride ion penetration and freezing and thawing than ordinary mortar. Due to its favorable usage and superior properties in repairing, PCM is widely used as repairing material [7].

The intense growth in construction industry has been noticed in the Gulf States from last two decades. Large quantity of concrete was used in making bridges, runways and high-rise buildings. All structures undergo daily high fluctuation of temperature and moisture. In summer, temperature in the above region and also in some regions of North America exceeds 50 ℃ and may rise to 60 ℃ [8, 9], which may deteriorate concrete structure rapidly. Concerns related to concrete durability problems should culminate in efforts to check the durability of available repairing material and compatibility with concrete in such condition and to ensure that repaired structure maintains the required performance over its intended life time.

1.2 OBJECTIVE AND SIGNIFICANCE

The main objectives of this research work were to investigate the behavior of interface between concrete and PCM, at material level and member level. Detailed objectives are listed as follows;

(i) Composite specimens are exposed to severe environmental conditions after proper curing of integrated specimens/structures. Environmental conditions which are responsible for the degradation in mechanical strength of composite specimens must be evaluated. So the first objective is to evaluate the properties of polymers in PCM under hygrothermal conditions to describe the mechanism of degradation of PCM.

(ii) The second objective is to understand the influence of moisture and temperature separately on bulk and composite specimens under tensile load in order to predict the interfacial tensile strength of composite specimens under both conditions of moisture and temperature.

(iii) Mostly composite specimens are exposed to tensile stress and shear stress at interface between old substrate concrete and PCM. So, the third objective is to understand interfacial strength viz, tension and shear strength, at elevated temperature in order to predict interfacial strengths at concerned temperature, which can be used in designing of structures strengthened by PCM overlay in given climatic condition.

(iv) The last objective is to understand the behavior of strengthened RC beam at elevated temperature, such as failure load, failure mode, load deflection relationships, flexural crack spacing and crack width in order to predict failure loads and crack widths, which can be applied

to the design of structures strengthened by PCM overlay.

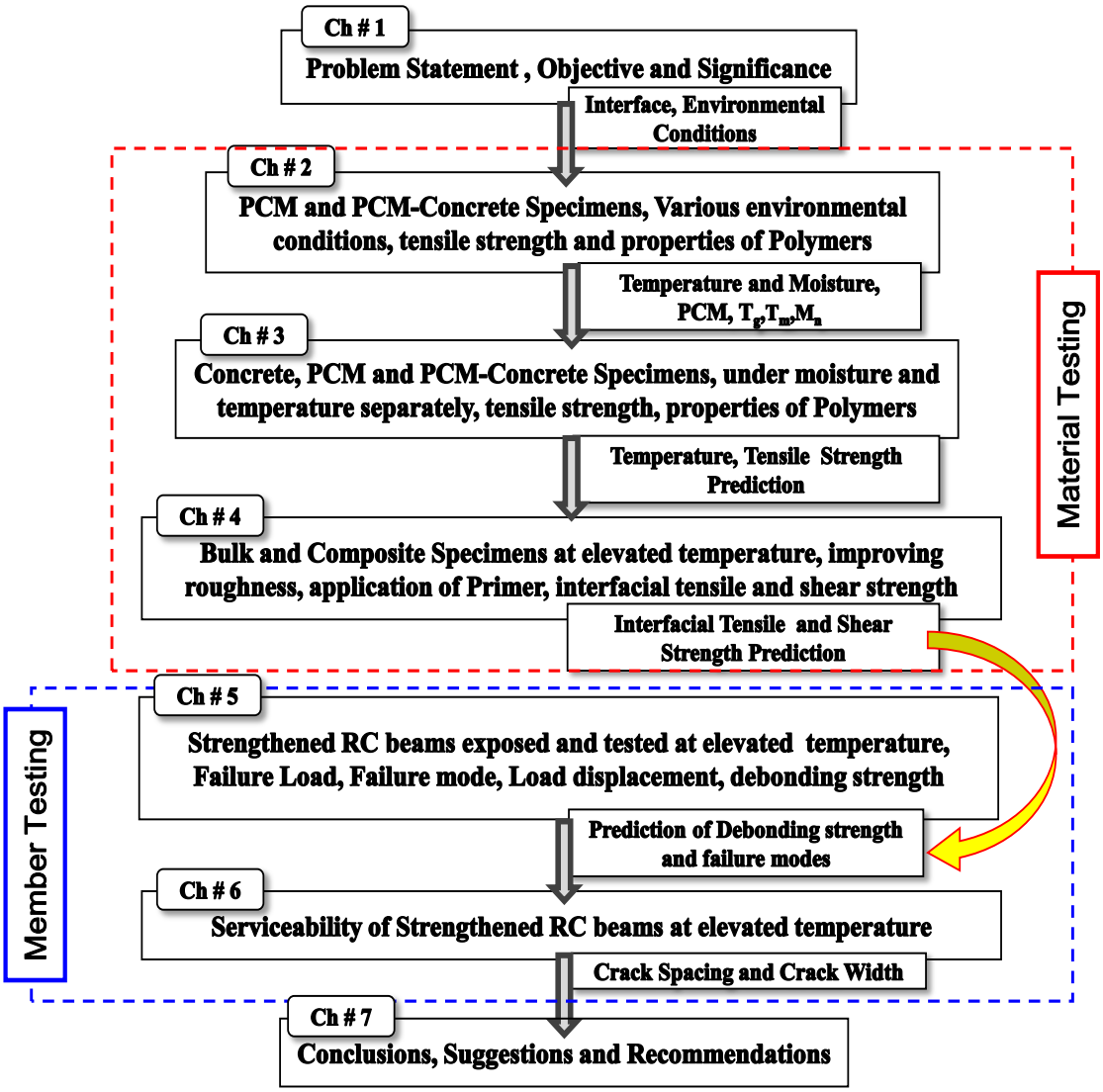

Fig. 1.2 Research flow and organization of dissertation.

In this detailed experimental and analytical study, large fluctuation of temperature was considered that covers most of the regions of the world. The outcomes of this work can be used by manufacturers of repairing materials and designers of retrofitting/rehabilitation work. And also open channels for other researchers and concrete technologists to consider the environmental condition along with the loading during testing and designing.

1.3 ORGANIZATION OF DISSERTATION

The dissertation is divided into seven chapters. Chapter 1 describes the background, problem statement, objective and significance of the present research. Chapter 2 to Chapter 4 describes the behavior of interface between concrete-PCM at material level under different environmental conditions. In Chapter 2, various testing and environmental conditions are considered and

concluded the severe effect of moisture and temperature on composite specimen. Physical properties of polymers are also investigated. In Chapter 3, detailed experimental and analytical study are conducted on tensile strength of concrete, PCM and concrete-PCM specimens under effect of moisture and temperature. Chapter 4 describes the further extension of Chapter 3 for the purpose of enhancement of interface of composite specimens by increasing roughness level of substrate concrete and also by incorporating primer at interface. Several tests are conducted at elevated temperature and evaluate the properties of composite and constituent material in tension and shear. In Chapter 5 and Chapter 6, behavior of interface at member level are discussed by strengthening of RC beams with PCM at elevated temperature. Failure mode, failure load and load deflection relationships are discussed in detail in Chapter 5. Shear load and failure modes of all beams were predicted by using truss analogy approach. Debonding strength are also proposed by incorporating interfacial tensile and shear strength that were analysed in Chapter 3 and Chapter 4. Serviceability of repaired structure at elevated temperature is discussed in Chapter 6. Flexural crack spacing and crack width at elevated temperature are explained in Chapter 6. Chapter 7 shows the broad conclusions of this detailed experimental and analytical work. Several conclusions are extracted from Chapter 2 to Chapter 6, which clarify the objective and significance of the study and also give outcomes very useful for manufacturers of repairing materials and designer. Some recommendations are also proposed in Chapter 7. Research flow and organization of dissertation is presented in Fig. 1.2.

REFERENCES

[1] Morgan DR. Compatibility of concrete repair materials and systems. Construction and Building Materials. 1996;10(1):57-67.

[2] Li G. A new way to increase the long-term bond strength of new-to-old concrete by the use of fly ash. Cement and Concrete Research. 2003;33(6):799-806.

[3] Li G, Xie H, Xiong G. Transition zone studies of new-to-old concrete with different binders. Cement and Concrete Composites. 2001;23(4–5):381-7.

[4] Ohama Y. Handbook of polymer-modified concrete and mortars-properties and process technology. New Jersy: Noyes Publications; 1995.

[5] Brien JV, Mahboub KC. Influence of polymer type on adhesion performance of a blended cement mortar. International Journal of Adhesion and Adhesives. 2013;43:7-13.

[6] Sakai ES, J. Composite mechanism of polymer modified cement. Cement and Concrete Research. 1995;25:127-35.

[7] Fowler DW. Polymers in concrete: a vision for the 21st century. Cement and Concrete Composites. 1999;21(5–6):449-52.

[8] Al-Jabri KS, Hago AW, Al-Nuaimi AS, Al-Saidy AH. Concrete blocks for thermal insulation in hot climate. Cement and Concrete Research. 2005;35(8):1472-9.

[9] Al-Gahtani AS R, AI-Mussallam AA. erformance of repair materials exposed to fluctuation of temperature. Journal of Materials in Civil Engineering. 1995;7:9-18.

Chapter 2

BOND STRENGTH OF CONCRETE-PCM UNDER ENVIRONMENTAL CONDITIONS

2.1 INTRODUCTION

The application of polymers in concrete has significantly progressed in last four decades and were used in various amounts and ways in concrete to form; (1) polymer concrete (2) polymer modified concrete (3) polymer impregnated concrete. All types have superior properties than ordinary Portland cement concrete and were widely used as either precast members such as bridge decks, pipes, floor tiles etc., or repairing and rehabilitation works in construction industry [1]. For repairing purpose, the deteriorated part of concrete is removed and reinstated with the polymer cement mortar (PCM). Durability of an integrated structure may be described as ability of the system to maintain designed performance strength and behavior over harsh and changing environmental conditions. The adverse conditions that may affect the durability of concrete and PCMs can be hypothesized to be: freeze thaw cycles, alkali silica reaction, chloride attacks, carbonation, chemical attacks, repeated loading and elevated temperature conditions. These conditions may change the microstructure and morphology of constituent materials due to physical and chemical aging. Thus, durability of polymeric materials deals with the assessment of design strength of the repaired structure that may be lost due to physical-chemical attacks during service life.

The condition of the substrate surface is of major significance in structural rehabilitation of existing concrete structures. The behavior of concrete to repair material interface is highly influenced by many parameters like strength, stiffness, moisture condition and micro-cracking of substrate concrete etc. In order to ensure full structural interaction within concrete and polymer cement mortar (PCM) it is necessary to have good bond between them. It is usual to increase surface roughness with the purpose of improving the bond strength between concrete and repairing material [2]. Several methods have been introduced to prepare the rough surface of concrete such as chipping, wire brushing, water jetting and sand blasting, etc. Among all, sand blasting is one of the best surface preparation method which insignificantly damages or causes micro-cracks in the substrate surface. Roughness was measured qualitatively and quantitatively by many researchers and several methods were adopted to measure it [3].

All concrete structures such as buildings, bridge decks, pavements and runways, etc. are exposed to high environmental temperature which rises up to 60 ℃ in some regions of hot and arid climate [4]. In other regions temperature also rises due to rapid industrialization, global warming and non-sustainable development. Concrete as well as repair material must be durable under such environmental conditions. In severe condition mismatch properties between materials may be dominant and damage the adhesive bonding between them. Environmental factors such as

temperature and moisture affect the materials as well as adhesive bonding among constituent materials. These factors in our real environment is varying instead of constant temperature so all material must be durable under cyclic condition of temperature and wetting and drying.

The objective of this work was to obtain information on the utilization of commercially available repairing material for repairing of concrete structures located in hot regions. The compatibility of repairing mortar and degradation mechanism of mortar-repaired composites under high temperature underline the importance of proper choice of repairing material. In this work concrete surface was prepared by sand blasting and roughness measured quantitatively. PCM was casted over it to make composite specimens. Splitting tensile strength test was conducted on composite specimen under different severe environmental conditions. Molecular weight $(M_n)$of polymers were measured by using gel permeation chromatography (GPC). Properties of polymers such as glass transition temperature (T_g) and melting point (T_m) were also analysed by using differential scanning calorimetry (DSC) on extracted polymers after designed exposure conditions.

2.2 METHODOLOGY

2.2.1 Materials & Specimen Preparation

Two types of material used in this work and first one was concrete which was casted in laboratory and its mean cylindrical strength was 38.2 MPa. Second material was a commercially available PCM, only desired amount of clean water at 20 ℃ was required to prepare repairing mortar. Before casting of PCM, concrete surface was roughened by sandblasting. Aggregate in concrete was exposed and roughness was measured by using three dimensional shape measurement apparatus. Surface roughness (R_a) is the arithmetic average of values at randomly selected spots. An example of three dimensional view of roughness profile of substrate concrete is shown in Fig. 2.1. Before casting of PCM, all concrete specimens were submerged in water for saturation and then put in formwork with rough surface dried and PCM was casted on treated surface. PCM cured in wet environment for seven days then dry cure for 21 days to get appropriate strength. Strength of PCM highly depends upon curing condition and adopted curing condition was more suitable among other conditions [5].

2.2.2 Split Tensile Strength

Split tensile strength of concrete can be evaluated by split cylinder test and detail of this method was explained in ASTM standards [6]. Li used splitting prism method with cubical specimens for determining bond strength between old concrete and new material [7]. In this study, Splitting tensile prism test was conducted to evaluate tensile strength of concrete-PCM interface. For even distribution of load two wooden strips of 10 mm wide were used between loading plates and specimen as shown in Fig. 2.2. Splitting tensile strength can be evaluated by using eq. (1).

$$f_t = \frac{2P}{\pi A} \tag{1}$$

Where; f_t =Split tensile strength (MPa), $\boldsymbol{P}$ = Ultimate Load (N) and $\boldsymbol{A}$=area of interface connected (mm^2)

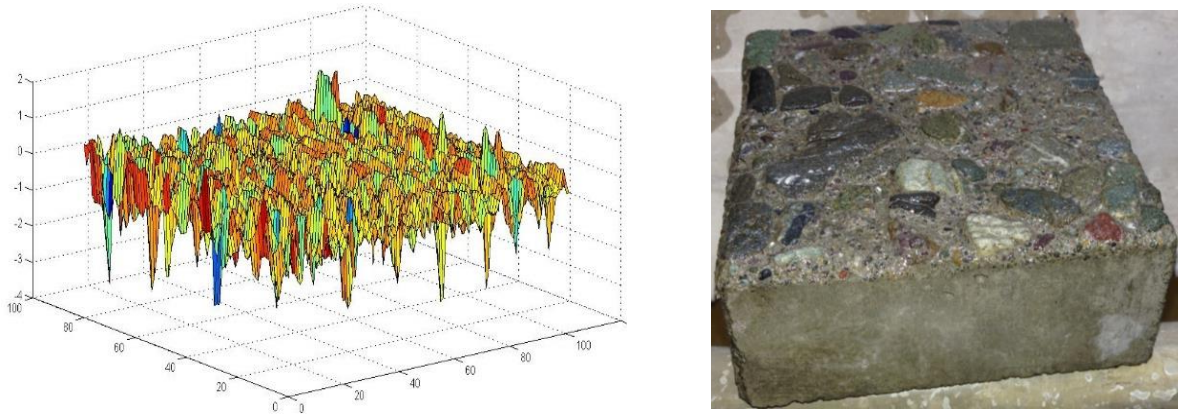

Fig. 2.1 3D-view of roughness of the substrate concrete.

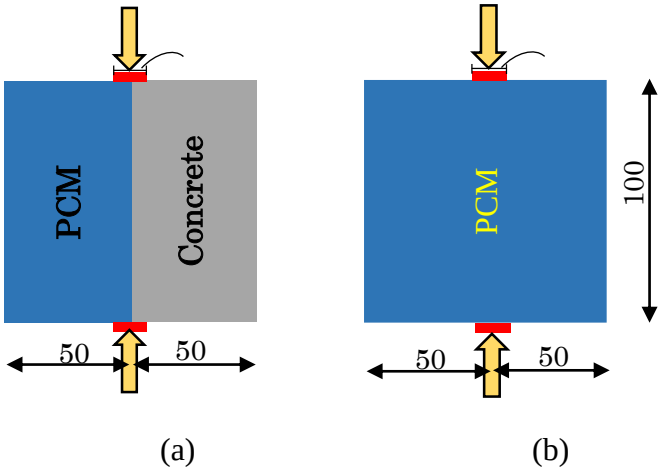

(a) (b)

Fig. 2.2 Schematic diagram for tensile test (a) composite specimen (b) bulk specimen (unit: mm).

2.2.3 Tests on Properties of Polymer

Different forms of polymers were used in the construction industry and the properties of the polymers such as glass transition temperature, melting point and molecular weight have significant importance and change in these properties may result in the change of the behavior of polymers. In PCM, small amount of polymers are present as compared to other constituents and to evaluate the properties of polymers they were extracted form PCM by using Tetrahydro furan (THF) as solvent. The extraction procedure adopted is presented in Fig. 2. PCM were pulverized after performing split tensile strength test into very fine powder that is able to pass 150 μm sieve (Fig. 2.3(a)). Some amount of THF was put into fine powder container and filtered after 24 hours (Fig. 2.3(b)) and then filtrate was evaporated to get only polymers (Fig. 2.3(c)). In this work glass transition temperature (T_g) and melting point (T_m) of polymers were analysed by using differential scanning calorimetry (DSC). DSC test was performed on extracted polymers by following ASTM E 1356 [8]. T_g was selected from the DSC curve as a midpoint of a tangent between the extrapolated baseline before and after transition and endo-thermal peak represents the T_m of polymers. Both, T_g and T_m were evaluated from temperature of -50 to 150 ℃ at heating rate of 10 ℃/min from second cycle of heating. Molecular weight (M_n) of polymers was measured by using gel permeation

chromatography (GPC), which is widely used technique for measuring molecular weight of polymers [9].

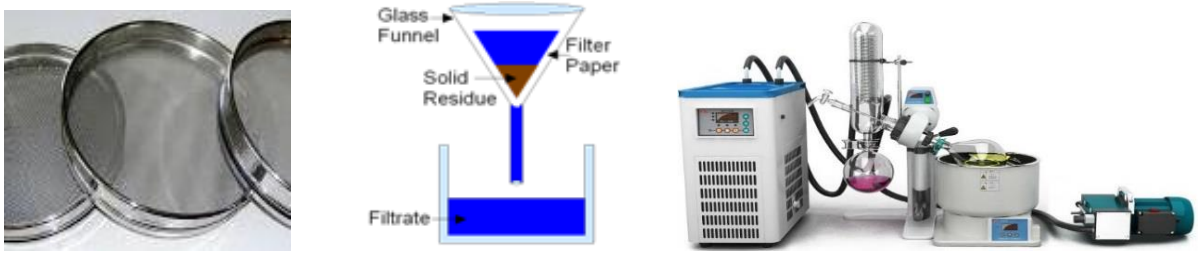

(a) Sieving (b) Filtration (c) Evaporation

Fig. 2.3 Procedure for extraction of polymers from PCM.

Table 2.1 Exposure and testing conditions for experimentation

Exposure Conditions	Notation	Testing Temperature℃		
(i) Temperature of 60 ℃ for 24 hours	T_u	20	60	---
(ii) Constant temperature of 60 ℃ for 30 days	T_{CO}	20	60	---
(iii) 12 hour at 60 ℃ and 12 hour at 30 ℃ (Thermal Cycle 1)	TC1	30	60	---
(iv) 24 hours at 60 ℃, 24 hour at 20 ℃ in water, 24 hours at 0 ℃ and finally at 25 ℃ ambient condition (Thermal Cycle 2)	TC2	25	60	Zero

2.2.3 Exposure Conditions

Durability of the repair material and its adhesive bonding to substrate concrete may be affected by the severe environmental conditions. Concrete repaired by PCM was exposed to temperature of 60 ℃. To investigate this affect in detail, first condition was the exposure of 60 ℃ to composite specimen for 12 hours and temperature while testing was monitored by thermocouples attached at interface before casting of PCM. This condition is abbreviated as "T_u" (Uniform Temperature). Long term exposure to constant temperature was also investigated and composite specimen was put in oven at 60 ℃ for one month and split tensile test were conducted, while specimens were hot. Split tensile test also performed after cool down the specimen at 20 ℃ and this condition abbreviated as "T_{co}" (Constant Temperature). Split tensile test was conducted under two types of cyclic conditions as well and adopted conditions in this work represent real environmental conditions. In first Thermal Cyclic (TC1) condition specimen was exposed at 60 ℃ for 12 hours and then at 30 ℃ for another 12 hours just to simulate day and night effect. Oven was used and this cyclic condition was programmed in it. One cycle completes in one day and specimen were tested after 30 cycles at 60 ℃ as well as 30 ℃. In second Thermal Cyclic (TC2) condition one season of a year was replaced by one day in laboratory. Composite specimens were exposed at 60 ℃ in oven for 24 hours to represent summer season, then these specimen was shifted to curing

tank and immersed in water for 24 hours at 20 ℃ to show rainy season, then specimens was put in chamber below zero degree centigrade for one day which represents winter season and finally specimen was put in ambient condition like 25 ℃ for another 24 hours to represent spring season. In this condition one cycle completed in 4 days and specimen tested after 10 cycles at different testing conditions. All environmental conditions were presented in Table 2.1. And testing temperature at which split tensile strength was obtained is mentioned in Table 2.2.

2.2.4 Definition of Failure Modes

Composite specimen can be considered as three zones, first zone consisted of concrete material and failure in this zone considered as cohesive failure in Concrete (C). Second zone is the PCM and failure in this zone termed as cohesive failure in PCM and failure abbreviated as "PCM". Last zone is the overlay transition zone (OTZ), which is the weakest zone in the composite specimen. The failure in this zone is the adhesive failure and abbreviated as "I" (Interface Failure) in this study. Interfacial transition zone in concrete is the weakest zone and in composite specimen OTZ considered as the weakest zone, So failure at this zone may be hybrid failure and it may be partially adhesive and partially cohesive on concrete side or PCM side and termed as "I-C" and "I-PCM" respectively. In (I-C) some amount of substrate concrete attached on the PCM side and in I-PCM failure most amount of PCM attached to the substrate concrete.

2.3 RESULTS AND DATA DISCUSSION

2.3.1 Uniform Temperature Condition

Compressive strength of constituent materials and interfacial split tensile strength of composite specimens were evaluated at control temperature of 20 ℃ and at 60 ℃. For uniform temperature within the specimens 12 hours exposure of heat was provided by an oven and also monitored by thermo couple while testing. Compressive strength of cylindrical specimen after 28 days of curing was 38.2 MPa and 42.9 MPa for concrete and PCM, respectively. After exposure of uniform temperature of 60 ℃ strength reduced to 32.1 MPa and 33.8 MPa for concrete and PCM respectively. Reduction in compressive strength of PCM was 21 % and in concrete it was about 16 %. Split tensile test of composite specimen was reduced to about 30 % when exposed to 60 ℃ temperature for short duration as mentioned in Table 2.2. Temperature affects concrete and other cementitious materials and reduces its tensile strength and compressive strength as reported by other researchers [10]. They have one common and general conclusion that temperature adversely affect the concrete and degradation in concrete was due to: damage in aggregate, weakening of the bond between cement paste and aggregate, also called interfacial transition zone (ITZ). Reduction in strength of cementitious material under high temperature was also due to increase in porosity and development of cracking. Internal microcracking in concrete was due to thermal incompatibility of hydrated cement paste and aggregate. Adhesive failure were observed for control specimen but when exposed to high temperature, failure shifted to PCM side and failure was partially adhesive and partially cohesive in PCM as shown in Fig. 2.4 and Table 2.2.

Table 2.2 Split tensile strength and failure modes under all exposure and testing conditions.

Condition	f_t (MPa)	Standard Deviation (MPa)	Failure modes	Failure mode percentage		
				Conc.[a]	Inter.[b]	PCM
C1@20	2.543	0.11	I	5	90	5
T_u@60	1.778	0.14	I-PCM	0	40	60
C2@20	3.556	0.27	I	4	90	6
T_{CO}@60	3.304	0.16	I-PCM	0	15	85
Tco@20	3.018	0.08	C	100	0	0
TC1@60	2.593	0.27	I-PCM	0	17	83
TC1@30	3.084	0.16	I	3	92	6
TC2@60	2.044	0.02	I-PCM	0	12	88
TC2@00	2.401	0.09	I-C	80	12	8
TC2@20	2.716	0.20	I	7	86	7

C1@20 ℃ (I) T_u@60 ℃ (I-PCM)

Fig. 2.4 Failure mode under uniform temperature exposure condition (T_u).

2.3.2 Constant Temperature Condition

Split tensile strength of composite specimen after one month exposure of constant temperature of 60 ℃was measured. Split tensile strength of composite specimen was evaluated at test condition of 60 ℃ and also after cool down the specimen at room temperature and tested at 20 ℃ temperature as mentioned in Table 2.2. Reduction in tensile strength of composite specimens were observed by an amount of about 7% and 15%, when tested at hot and after cool down the specimen respectively as showed in Fig. 2.5. The failure of the control specimen was adhesive at interface and hot specimen showed partially cohesive failure on PCM side and failure also measured quantitatively by mapping of failed surface as presented in Table 2.2. Failure after cool down the specimen were substrate concrete failure or cohesive failure of concrete as shown in Fig. 2.6. Similar trend was observed in the PCM bulk tested at 60 ℃ and the amount of reduction in strength was 25%. Strength of PCM improved after cool down the specimen by an amount of about 28% from the heated specimen but is still less than the control specimen by an amount of almost 4%, as showed in Fig. 2.5.

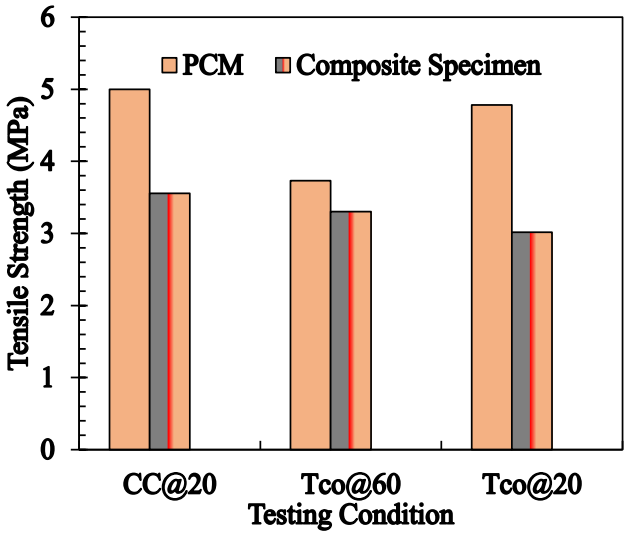

Fig. 2.5 Tensile strength under Constant Temperature condition.

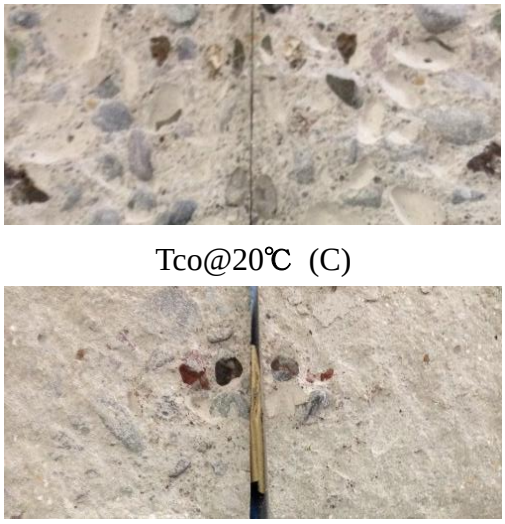

Tco@20℃ (C)

Tco@60℃(I-PCM)

Fig. 2.6 Failure modes under constant temperature condition.

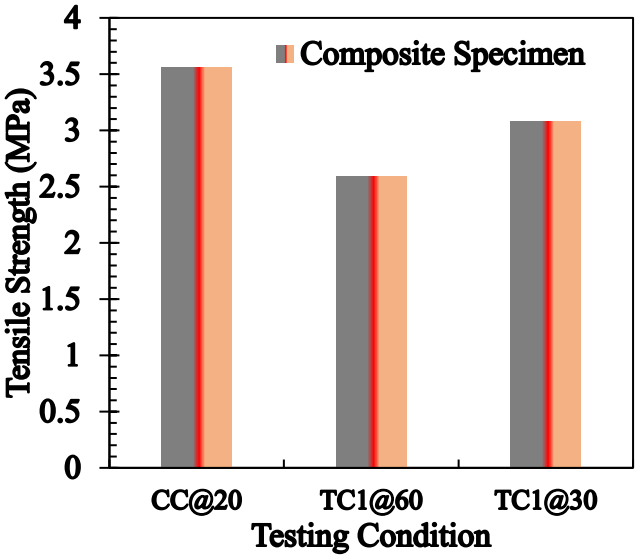

Fig. 2.7 Tensile strength under Thermal Cycle1(TC1) condition

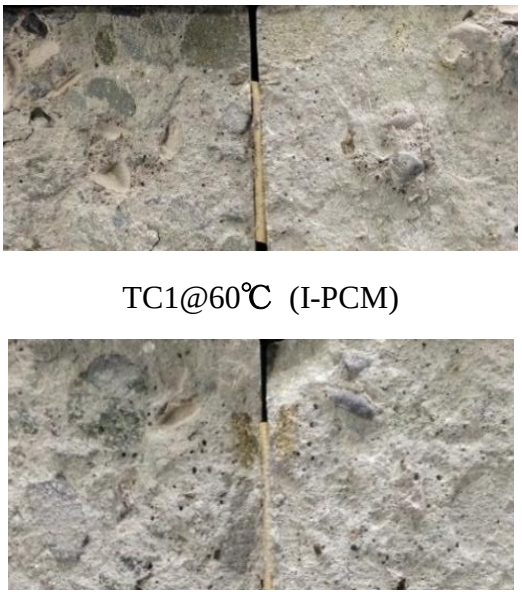

TC1@60℃ (I-PCM)

TC1@30℃ (I)

Fig. 2.8 Failure modes under Thermal Cycle1(TC1) condition

2.3.3 Thermal Cycle 1

For durability of repaired system, real environmental condition was assumed and provided in laboratory by programmed oven and giving cyclic condition of 60 ℃ and 30 ℃ to simulate day and night temperature in arid region. Tensile strength of composite specimen evaluated at 60 ℃ and at 30 ℃ after 30 cycles. Reduction in strength from control specimen was about 27% and 13%, at testing temperature of 60 ℃ and 30 ℃ respectively as shown in Fig. 2.7. The failure modes were observed after performing split tensile strength and more than 80% of PCM was attached to

the substrate concrete, when tested temperature was 60 ℃. Failure were shifted towards PCM cohesive side from adhesive interface as compared to the control specimen. Adhesive failure were also observed of failure surface of a composite specimen after testing at 30 ℃ as presented in Fig. 2.8. Due to cyclic loading there will be either a residual expansion or contraction after first heating-cooling cycle and further cycles increases the strains in the concrete. But amount reduces with further cycles so first few thermal cycles are most crucial for the behaviour of concrete [10].

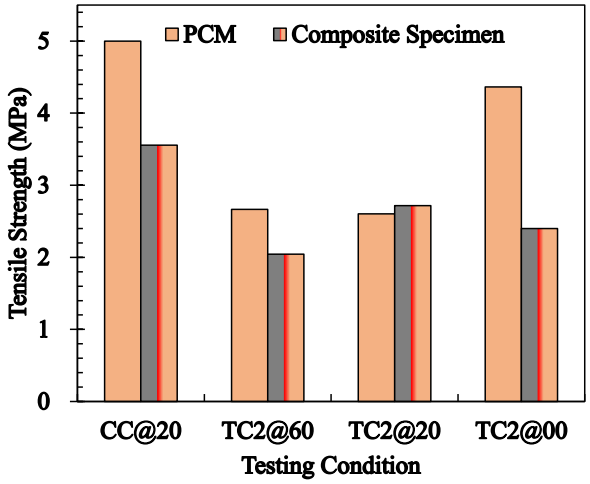

Fig. 2.9 Tensile strength under Thermal Cycle 2 (TC2) condition

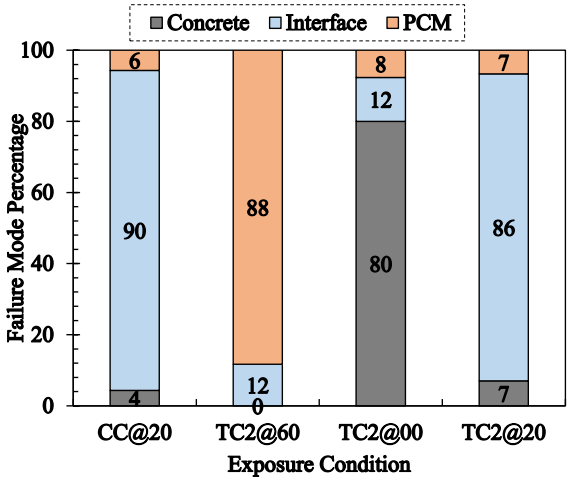

Fig. 2.10 Failure modes under Thermal Cycle 2 (TC2) condition

2.3.4 Thermal Cycle 2

In second cyclic condition, seasonal temperature variation was provided in laboratory by manually put in each specific environment for 24 hours. Split tensile strength of PCM as well as of composite specimen were evaluated after 10 cycles at 60 ℃, 20 ℃ and about zero 0 ℃. After 10^{th} cycle the reduction in strength were about 42% and 47% in composite specimen and in PCM respectively (Fig. 2.9). So much reduction in PCM also showed that this condition severely affects the PCM as well as bonding between concrete and PCM. Due to large amount of degradation the failure shifted towards PCM cohesive side and more than 85% amount of PCM attached to the substrate after failure as showed in Table 2.3 and graphically in Fig. 2.10. At 20 ℃ testing the tensile strength of composite specimen reduces to 24% as compared to the control specimen, but little improvement observed when compared to the specimen tested at 60 ℃, and the failure observed was adhesive failure at interface "I". When composite specimen tested at lower temperature (about 0^{o}C) that may be close to the glass transition temperature recovering in the strength were observed in the PCM as compared to the other testing condition that is clearly showed in Fig. 2.9. But composite specimen had still degraded after 10^{th} cycle and no improvement in strength was observed. The failure transferred to the concrete cohesive side from interface as shown in Fig. 2.10. Temperature and moisture both adversely affect the bonding as well as the constituent material as explained by Ohama & Bazant [5, 10].

2.3.5 Properties of Polymer

Properties of Polymers extracted from PCM after testing discussed under following two heads.

Molecular Weight

Higher the molecular weight gives the higher degree of polymerization and gives higher mechanical strength and vice versa [9, 11]. Degree of polymerization for impregnated concrete was investigated by Chen et al. [11], who observed the greater improvement in mechanical strength and reduction in porosity than ordinary concrete under higher degree of polymerization. Degree of polymerization in the impregnated concrete might be compare with the polymer film in the polymer modified concrete or mortar. The contribution to the property improvement of modified concrete is almost similar. In both cases, impregnated concrete and polymer modified concrete, polymer film fills the pores and surrounds the hydration products and gives the higher strength than ordinary concrete or mortar. In opposite way, decomposition in the polymer film by harsh environment may decrease the mechanical properties of PCM and also may degrade the properties of polymer used in PCM.

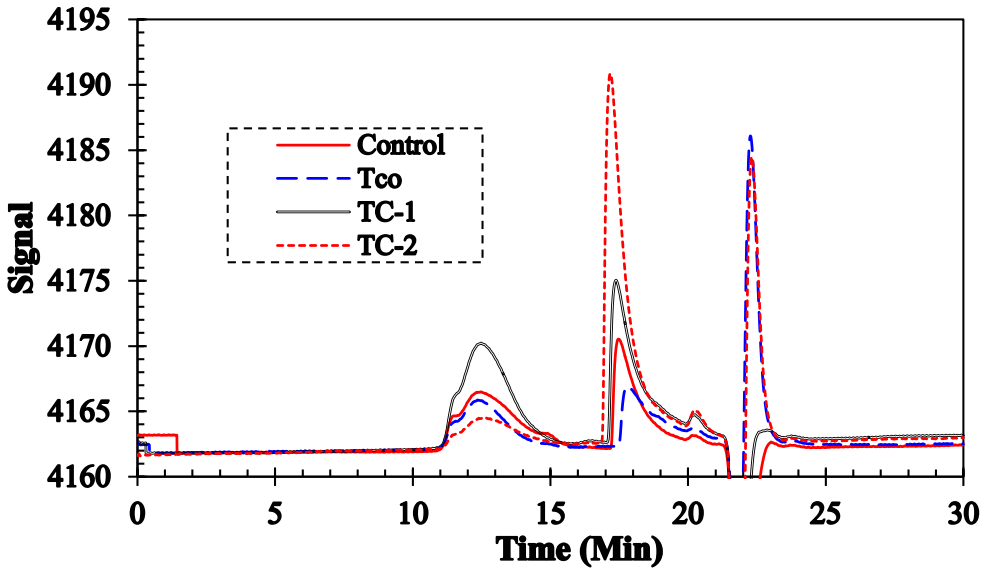

Fig. 2.11 GPC Analysis of extracted polymers under different environmental conditions.

Molecular weight (M_n) of polymers were investigated in this work by performing GPC test on extracted polymers. Polymers were extracted after conducting tensile strength test after designed environmental conditions. Molecular weight (M_n) was obtained by the distribution under the first peak of GPC curve and distribution under the second peak shows the amount of oligomers (Fig. 2.11). The molecular weight under all conditions remains same and its value was in the range of 70,000 to 90,000. Under given exposure conditions the amount of oligomer increases, which may be observed in the increase in second peak and the degradation in the first peak in Fig. 2.11. But this change is insignificant and did not affect so much. GPC test was performed at 40 ℃ but interfacial tensile strength of composite specimens were conducted at 60℃. Polymer properties

may recover due to lowing of temperature so experimentation is still needed to conform the relationship between molecular weight and strength.

Glass Transition Temperature and Melting Point

DSC test was performed to evaluate the glass transition temperature (T_g) and melting point (T_m) of the extracted polymers. Fig. 12 shows the DSC curves of extracted polymers after exposure to different environmental conditions. The T_g of all polymers was below 8 ℃ and slight variation in T_g was observed under the influence of exposure condition. Moisture and temperature can greatly influence the physical properties of polymers and its composites. Once polymers composites exposed to variation of temperature and moisture that may alter properties of the polymers either in irreversible manner (by hydrolyzation, cracking or crazing), or a reversible manner (plasticization). Ohama [5] shows that flexural and compressive strength of polymer modified cement mortar change with the T_g and reduced with the reduction in T_g. Polymer mortar shows exponential degradation in tensile strength after glass transition temperature [12]. Melting point T_m of polymers observed were less than 60 ℃ (Fig. 2.12) and slight reduction in T_m was also observed and significant reduction in tensile strength was observed above this temperature. Reduction in these temperatures may reduce the mechanical properties of the polymer cement mortars.

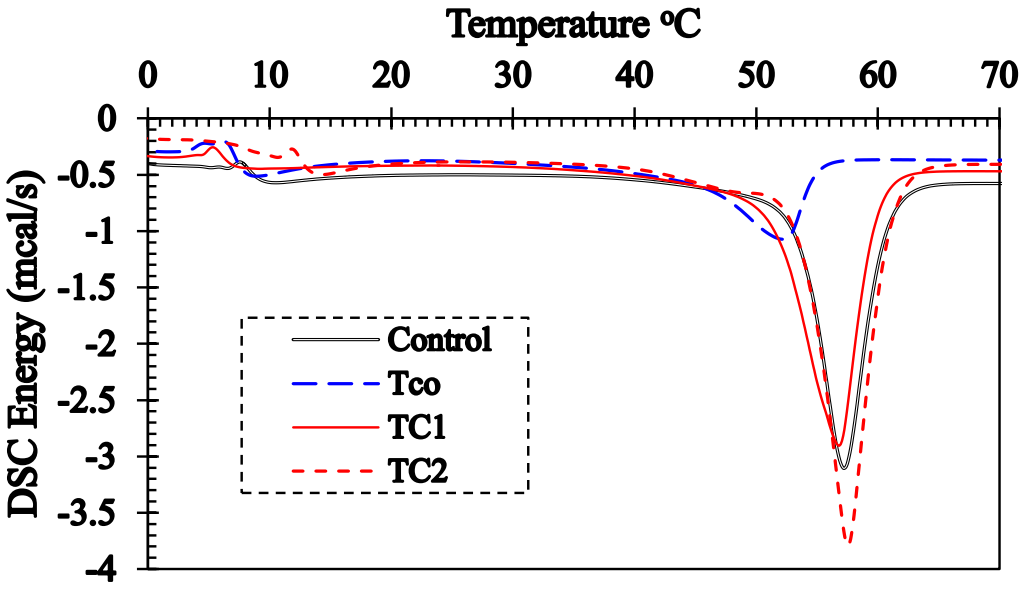

Fig. 2.12 DSC Analysis of extracted polymers under different environmental conditions.

2.4 CONCLUSIONS

Different environmental conditions, by considering fluctuation of temperature of arid regions, were assumed in this experimental work. Designed exposure conditions have very close resemblance with the real environmental conditions. Interfacial tensile strength of composite specimens, glass transition temperature (T_g), melting temperture (T_m) and molecular weight (M_n) of polymer were tested after such exposure condition and following conclusions were extracted;

1) After 24 hours exposure of 60 ℃ and at testing temperature of 60 ℃, reduction in split tensile strength of composite specimens was 30 %, whereas, after long exposure of 30 days at elevated temperature of 60 ℃ the reduction in strength was only 7% of control specimen tested at 20 ℃. Under long exposure, there may be further curing of polymers and reduction in porosity of cementitious materials. `
2) Polymers cement mortar (PCM) and composite specimens are more sensitive to temperature when exposed to short period and there was significant decrease in compressive and split tensile strength.
3) PCM is also sensitive to testing temperature. Under constant temperature condition "Tco" condition recovery in tensile strength of PCM was 28% tested at 20 ℃, and recovery was 67% tested close to zero ℃ of respective specimen tested at 60 ℃.
4) Under thermal cycle 1 (TC1) condition of composite specimens, recovery in tensile strength by an amount of 19 % was observed when tested by lowering the temperature to 30 ℃ instead of 60 ℃. However, tensile strength at both temperature level, 30 ℃and 60 ℃, is less than tensile strength of control specimen.
5) At high temperature of 60 ℃ after 24 hours exposure, after 30 days, after 30 cycles of TC1 condition and after 10 cycles of TC2 condition, failures of specimens shifted from adhesive interface to cohesive PCM side, indicating a more serious degradation of PCM cohesion than interfacial adhesion under above conditions.
6) Molecular weight (M_n) of polymers were evaluated after constant temperature condition (T_{co}), Thermal Cycle 1 (TC1) and Thermal Cycle 2 (TC2) condition and compared with the control specimen. Insignificant effect was observed in (M_n) of polymers.
7) Glass transition temperature (T_g) and melting point (T_m) of polymers were evaluated after constant temperature condition (T_{co}), Thermal Cycle 1 (TC1) and Thermal Cycle 2 (TC2) condition and compared with the control specimen. Insignificant effect on T_g and T_m values of polymers were observed under all exposure conditions.

REFERENCES

[1] Fowler DW. Polymers in concrete: a vision for the 21st century. Cement and Concrete Composites. 1999;21(5–6):449-52.

[2] Júlio ENBS, Branco FAB, Silva VtD. Concrete-to-concrete bond strength. Influence of the roughness of the substrate surface. Construction and Building Materials. 2004;18(9):675-81.

[3] Santos PMD, Júlio ENBS. A state-of-the-art review on roughness quantification methods for concrete surfaces. Construction and Building Materials. 2013;38:912-23.

[4] Al-Jabri KS, Hago AW, Al-Nuaimi AS, Al-Saidy AH. Concrete blocks for thermal insulation in hot climate. Cement and Concrete Research. 2005;35(8):1472-9.

[5] Ohama Y. Handbook of polymer-modified concrete and mortars-properties and process technology. New Jersy: Noyes Publications; 1995.

[6] International A. ASTM C-496. Standard Test Method for Splitting Tensile Strength of Cylindrical Concrete Specimens 2004.

[7] Li G, Xie H, Xiong G. Transition zone studies of new-to-old concrete with different binders. Cement and Concrete Composites. 2001;23(4–5):381-7.

[8] International A. ASTM E-1356-03. Test method for assignment of the glass transition temperatures by differential scanning calorimetry. West Conshohocken, PA.2004.

[9] Nair P, Ku DH, Lee CW, Park HY, Song HY, Lee SS, et al. Microstructural studies of PMMA impregnated mortars. Journal of Applied Polymer Science. 2010:3534-40.

[10] Bazant PK, FM. Concrete at high temperature-Material properties and mathematical methods,: Harlow:longman; 1996.

[11] Chen C-H, Huang R, Wu JK, Chen C-H. Influence of soaking and polymerization conditions on the properties of polymer concrete. Construction and Building Materials. 2006;20(9):706-12.

[12] Biswas M, Kelsey, R. G. Failure model of polymer mortar. Journal of Engineering Mechanics. 1991;117:1088-104.

Chapter 3

CONCRETE-PCM INTERFACE UNDER HYGROTHERMAL CONDITIONS

3.1 INTRODUCTION

Concrete is one of the most utilized materials in the world and is widely used in different structures that are exposed to continuous variation in temperature and moisture levels, combined with various loading impacts. The physical and mechanical properties of the concrete are impacted by these severe environmental and mechanical conditions and the service lives of the structures are reduced [1, 2] Enormous research was conducted on curing of concrete during extreme weather conditions and remedies was proposed and widely used to overcome these affects. But after standard curing concrete is again exposed to such conditions and deteriorated, which accelerates other damages such as frost damage, chloride ion penetration and corrosion of reinforcement, etc. To avoid further degradation, it is a common practice to remove the deteriorated part and reinstate with the repairing material which should be durable and compatible with the concrete [3].

Moisture and temperature influence the constituent properties of the both materials of composite specimens and also the weakest zone between them which may be called as overlay transition zone (OTZ). Additional stress is generated at OTZ due to drying shrinkage, which may lead to failure of interface, when exposed to hot dry environment. However PCM shows the better compatibility with concrete and shows insignificant effect of drying shrinkage [4]. Additional stress is also generated due to difference in volumetric changes owing to high temperature and moisture absorption between two constituent materials and produces tensile stresses at OTZ and creates a condition in which cracks readily develop [5, 6]. The interfacial strength also depends upon the intrinsic properties of the constituent material. The degradation in the properties of repairing material directly influenced interfacial tensile strength under severe conditions [7].

With such background, a series of experiments were conducted under different exposure conditions which cover almost all ranges of hot summer conditions of the world. The properties of concrete and PCM as well as composite specimens were evaluated under the fluctuation of temperature and moisture. The glass transition temperature, melting point and molecular weight of polymers in PCM were also investigated under such exposure conditions. Finally, to design a long lasting concrete structure, analytical model was presented based on properties of both constituent materials under standard condition. The model can estimate the interfacial tensile strength under various levels of temperatures, both in dry and wet conditions.

3.2 METHODOLOGY

3.2.1 Materials & Mix Proportion

In this study two types of commercially available PCMs were used, one having the styrene-

butadiene rubber (SBR) polymer and other having polyacrylic ester (PAE) polymer, and named as "SBR" and "PAE" PCM, respectively, whose information is provided by the manufacturers as seen in Tables 3.1 and 3.2. SBR PCM was casted in laboratory by mixing 1 bag of 25 kg of PCM with 1.1 kg of liquid polymer and 2.25 kg of water. The temperature of water was maintained at 20 ^{o}C and the properties of polymers are mentioned in Table 3.1. The PAE PCM was composed of three units. One is the emulsion, and other two units were composed of cement and silica sand. Mixing ratio of each constituent is presented in Table 3.2. Two types of concrete were casted in the laboratory by using ordinary Portland cement, river sand and gravel. Mixing proportion of each constituent is mentioned in Table 3.3. Concrete with higher water to cement ratio was termed as low strength "LS" and with lower water to cement ratio was referred as normal strength "NS" in this study.

Table 3.1 Properties of Polymer used in SBR PCM.

Property	Description
Main component	SBR Type gum latex
Solid component	45-46% (mass)
Apparent condition	White or pink color
Viscosity	500-1500 (mPa-s)
PH	8~9
Density	1.0 g/cm^3

Table 3.2 Compounding ratio of PAE-PCM material.

Constituent Material	Emulsion	Compound Type-I	Compound Type-II
Unit volume mass (kg/L)	1.02	2.74	2.70
Acrylic acid ester copolymer (%)	27.0	---	---
Water (%)	73.0	---	---
White cement (%)	---	40.0	33.0
Silica sand (%)	---	60.0	67.0

Table 3.3 Mix proportion of concrete for one cubic meter.

Material	LS	NS
Cement (kg/m^3)	275	413
Sand (kg/m^3)	912	859
Aggregate (kg/m^3)	1119	1054
Water (L)	165	165
W/C*	0.6	0.4

W/C*= water to cement ratio

3.2.2 Specimen Preparation

Bulk Specimen

Both types of concrete were casted to a cubical specimen of 100 mm side length. All concrete specimens were cured for 28 days in wet condition and then exposed to different conditions (explained in section 3.2.3). Both types of PCMs were made the same cubical size of 100 mm as shown in Fig. 3.1(a). After casting, all specimens were warped with plastic sheets and covered with wet rags. After 24 hours, the specimens were de-moulded and put into curing water tank for 6 days. Temperature of water was maintained at 20 ℃. After wet curing, all specimens of PCM were shifted to an open air for drying and temperature was maintained at 20 ℃ for further 21 days. The strength of PCM highly depends upon the curing method and the proposed curing method is considered as the best one by different researchers [8] and is suggested by the PCM manufacturers as well. For both types of materials, Concrete and PCM, cylinder of size 100 mm diameter with 200 mm in height was also prepared to measure the 28 days compressive strength and strengths at ages of test.

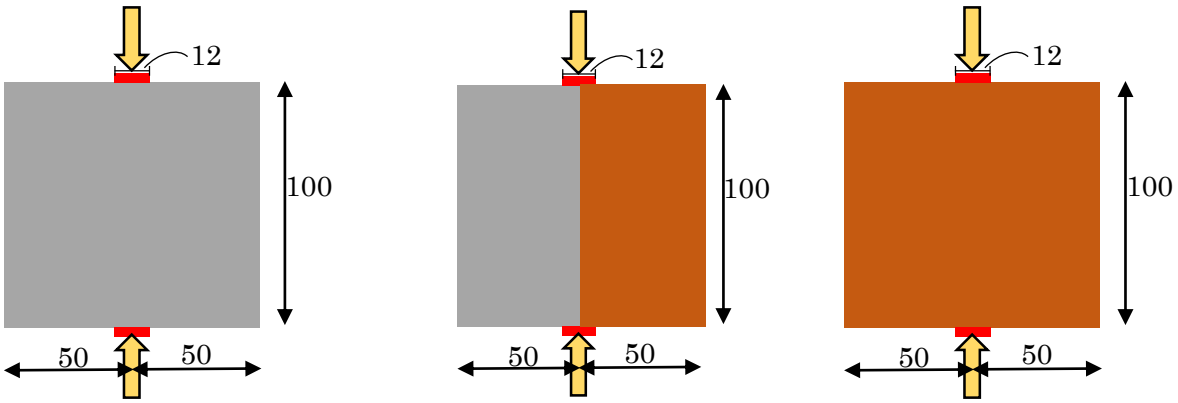

(a) Concrete (b) Composite Specimen (c) PCM

Fig. 3.1 Schematic diagram for split tensile strength test.

Composite Specimen

After 28 days moist curing of concrete, concrete specimens were cut into size of 100 x 100 x 50 mm. One surface of specimen having a size of 100 x 100 mm was roughened by sand blasting method, which is one of the most suitable methods for better interlocking and generating less micro-cracks in substrate [9]. The roughness of substrate concrete surface was measured quantitatively by using a three dimensional shape measurement apparatus. Roughness coefficient (R_a) is the arithmetic average of values at randomly selected spots and quantified by measuring the difference between the average height of the peak and average height of valley from an arbitrary baseline based on JIS B0610 [10]. R_a value of both NS and LS concrete was 0.30 mm and 0.36 mm respectively and three-dimensional profile of the rough surface was presented in previous chapter (Fig. 2.1) and also in conference [11]. Before casting of PCM, all substrate concrete specimens were immersed in water for 48 hours. Wet specimens were put in moulds and free water on the

rough surface was removed by towel just before casting of PCM to provide saturated concrete substrate with dry surface for adequate bonding [12]. PCM with PAE polymer was sprayed onto two types of concrete substrates while SBR PCM was casted by spreading with trowel, as suggested by the manufacturers. The total size of the composite specimens was 100 x 100 x 100 mm (Fig. 3.1(b)). Concrete in the composite specimens has been already cured and in hard state but PCM is in fresh state. Curing methodology of composite specimen was similar to the curing of PCM bulk specimens. All composite specimens were cured in moisture for 7 days and 21 days dry ambient condition. The age of concrete was 45 days more than age of PCM in all cases (composite and bulk specimens). Composite specimen was referred in this study by two words. First word presents the type of concrete and second word presents the type of PCM. For example NS-SBR means composite specimen consisting of normal strength concrete and SBR PCM.

3.2.3 Exposure Condition

All bulk and composites specimens were exposed to different conditions in laboratory which resemble with the real environmental conditions. The specimens were divided into two series with different temperature and moisture parameters.

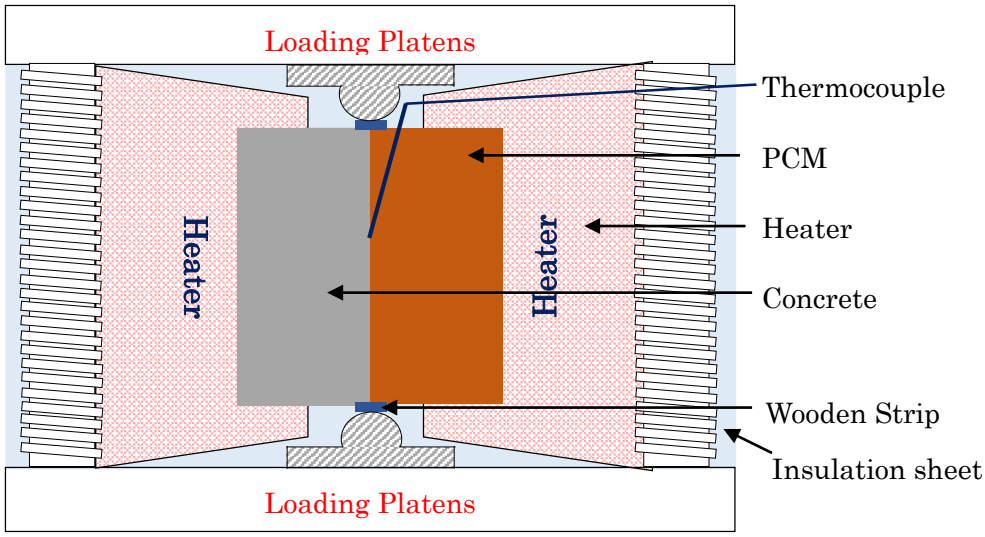

Fig. 3.2 Interfacial tensile strength test set-up under influence of temperature.

In the first series, the influence of temperature was incorporated. In many regions temperature fluctuates from ambient condition of 20 ℃ to extreme temperature of 60 ℃ [13]. To cover maximum regions of the world, three temperatures were selected in this study. After 28 days of standard curing of composite and PCM bulk specimens, all specimens were put in laboratory at 20 ℃ for another 28 days. One set of specimens were tested at 20 ℃. Other sets of specimens were put in oven at 40 and 60 ℃ for 12 to 16 hour. Test was also conducted in present of moisture and each set of specimens were submerged in water and temperature of water was maintained at 20, 40 and 60 ℃ for 12 to 16 hours. For wet exposure conditions, the specimens were taken out from hot water tank and tested immediately. The temperature while performing test was maintained same as the exposure temperature by using heater as shown in Fig. 3.2. The temperature distribution

within specimen while testing was monitored by thermocouple placed at the interface of composite specimens. The composite specimen with the instrumentation is shown in Fig. 3.2.

In the second series, influence of moisture was investigated by applying wetting and drying cycles (W/D cycles) and continuous immersion of specimens in water. In both categories, temperature was maintained at 20 ℃. For W/D cycles, all specimens were submerged in water at 20 ℃ for wetting and drying was conducted in ambient air exposure in the laboratory at 20 ℃. There is no standard test method available for the W/D cycles. Different researchers used different wetting and drying cycles [8]. In this study, after standard curing, 2 days dry and 2 days wet were used to represent one W/D cycle. Tests were conducted after exposure of 1, 3, 6 and 12 W/D cycles. The test was performed in wet state because of the sensitivity of PCM to the surrounding moisture [8]. For continuous wet condition, all specimens were submerged into a same curing tank where temperature was maintained at 20 ℃. The specimens were taken out of curing tank on testing day and test was conducted immediately in wet conditions. Test was performed after 4, 12, 24 and 48 days of continuous immersion in water. Moisture in specimens was also maintained during test by preparing special chamber around the testing instrument. The age of the specimen at test under both categories was same. Specimens without the temperature and moisture exposures, which is termed as control specimen, were also prepared for comparison purpose. Table 3.4 shows the summary of all exposure conditions and number of specimens designed in this work.

Table 3.4 Summary of exposure conditions, test performed and number of specimens.

Test Performed		Exposure condition															
		Temperature						Moisture									
		Dry Condition			Wet Condition			W/D Cycles					Continuous Immersion				
		℃			℃			No.					Day				
		20	40	60	20	40	60	0	1	3	6	12	0	4	12	24	48
Tensile Strength	NS	3	3	3	3	3	3	3	3	3	3	3	3	3	3	3	3
	LS	3	3	3	3	3	3	3	3	3	3	3	3	3	3	3	3
	SBR	3	3	3	3	3	3	3	3	3	3	3	3	3	3	3	3
	PAE	3	3	3	3	3	3	3	3	3	3	3	3	3	3	3	3
Bond Strength	NS-SBR	3	3	3	3	3	3	3	3	3	3	3	3	3	3	3	3
	NS-PAE	3	3	3	3	3	3	3	3	3	3	3	3	3	3	3	3
	LS-SBR	3	3	3	3	3	3	3	3	3	3	3	3	3	3	3	3
	LS-PAE	3	3	3	3	3	3	3	3	3	3	3	3	3	3	3	3
T_g and T_m	SBR	1	1	1	1	1	1	1	1	1	1	1	1	1	1	1	1
	PAE	1	1	1	1	1	1	1	1	1	1	1	1	1	1	1	1
M_n	SBR	1	1	1	1	1	1	1	1	1	1	1	1	1	1	1	1
	PAE	1	1	1	1	1	1	1	1	1	1	1	1	1	1	1	1

3.2.4 Testing Procedures

Cylinder compressive strength of both materials, concrete and PCM, was evaluated by conducting compressive strength test according to ASTM C 39 [14]. 28 days strength of LS and NS concrete was 26.7 and 43.4 MPa, respectively. Compressive strength of SBR and PAE PCM was tested after 28 days curing and found to be 54.3 and 55.9 MPa, respectively. Compressive strength of both constituent materials was also measured after 90 days of casting. No significant change in strength from the strengths at 28 days was observed.

Tensile strength test

The tensile strength of both constituent materials was evaluated by split tensile test according to ASTM C 496 [15]. In this work the specimens were cubes instead of cylinders and past studies showed the effect of geometry on tensile test [16, 17]. Li et al. [17] also proved that both the cylinder and square prism produced an essentially uniform tensile stress across most of the vertical splitting plane using the finite element method. The maximum tensile stress varied between the two types of specimens by less than 2%. Before testing, two strips were used at top and bottom of specimen as shown in Fig. 3.1, for even distribution of the load. The selection of the material and size of the strip affect the tensile strength of the specimen [16]. Wooden strip of 12 mm wide was used in this work and ratio of width of strip to depth of specimen was 0.12, which is within the limits mentioned in ASTM C 496 standard [15].

Bond strength was measured for all composite specimens after given exposure conditions, in a similar way of split tensile test. Extensive literatures are available, which verified this methodology to evaluate bond strength or interfacial tensile strength by using Eq. (1) [18-20].

$$f_t = \frac{2P_u}{\pi A} \tag{1}$$

where,

f_t = Interfacial tensile strength (MPa)

P_u = Ultimate load (N)

A = Area of interface (mm^2)

Tests on polymer properties

Glass transition temperature (T_g) and melting point (T_m) are two important properties of polymers and affect the strength of the PCM [8]. T_g and T_m were determined by using Differential Scanning Calorimetry (DSC) test. DSC test was performed following ASTM E 1356 [21] on the extracted polymers. T_g was chosen from the midpoint of the tangent between the extrapolated baseline before and after transition and endo-thermal peak represents the melting point of polymer. All values were evaluated from temperature of -50 to 150 ℃ at heating rate of 10 ℃/min from second cycle. Polymers, used in this test, were extracted after performing split tensile strength on PCMs and 200 gram of sieved PCM was used for the extraction of the polymers and tetrahydro furan was used as solvent [22]. More than 15 mg of polymers were extracted from which 5 mg was

used for the DSC analysis and 3 mg was used for gel permeation chromatography (GPC) test to evaluate the molecular weight *(M_n)* [23, 24]. Table 3.4 shows the number of specimens for measurement of T_g, T_m and M_n.

3.3 RESULTS AND DISCUSSION

The results of the 432 cubes of bulk and integrated specimens after different exposure conditions were discussed in the following sections.

3.3.1 Failure Mode Observed

The composite specimens are considered as three phases or three zones. The first one is the concrete zone in which the failure is considered as cohesion failure of concrete. The second zone is the PCM in which crack or fracture is considered as cohesion failure of PCM. The third one is the more sensitive and critical zone, that is interface between concrete and PCM and termed here as overlay transition zone (OTZ). This zone has resemblance with the interfacial transition zone in concrete and is the weakest zone in composite specimens. Failure in this zone is referred as adhesion failure or interface failure.

At macro scale all failure of composite specimen, under all exposure conditions, were adhesion failure, which verifies that OTZ is the weakest zone in the composite specimen. At meso scale these failures may be further categorized a hybrid or mixed failure. Some PCM was attached to the concrete substrate as shown in Fig. 3.3(a) and in some cases especially for low strength concrete (LS substrate), some aggregates were attached to the PCM side as shown in Fig. 3.3(b). The mixed failure is because the strength and stiffness of the PCM-aggregate adhesion was stronger than mortar-aggregate adhesion.

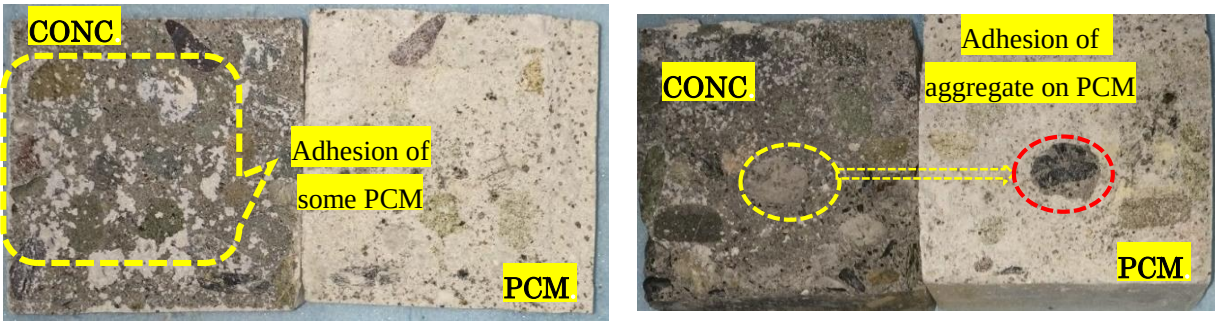

(a) Adhesion of some PCM (b) Adhesion of aggregate

Fig. 3.3 Sample failure surface of composite specimens.

3.3.2 Effect of Temperature

Dry Condition

The tensile strength of composite specimens with their respective constituent materials, under different testing temperatures is presented in Fig. 3.4. The tensile strength was taken as average of three specimens and standard deviation is indicated as error bar. Significant reduction was noticed in tensile strength of four types of constituent materials when compared to the specimens cured and

tested at 20 ℃, which was referred as control specimens. Concrete at 40 ℃ had about 8% reduction in strength. But at 60 ℃ temperature, tensile strength was reduced by 23% and 13% for normal strength concrete and low strength concrete, respectively. Bazant and Kaplan [25] summarized the work of different researchers and concluded that concrete with high cement to aggregate ratio showed more reduction in strength as compared to the low cement to aggregate ratio. Result presented in this work is also matched with their findings. The reduction in strength is due to the different rate of expansion of aggregate and cement paste at elevated temperature, which produces high internal stresses and generating micro-cracks in paste and interfacial transition zone and weakens the bond between aggregate and hydrated cement paste resulting in the deterioration of concrete. Other possible mechanism for the reduction in strength of concrete is the increase in porosity at elevated temperature [26]. It is believed that the stress related to surface tension of the receding water menisci collapses some of the fine pores, which results in an increase in volume of larger pores.

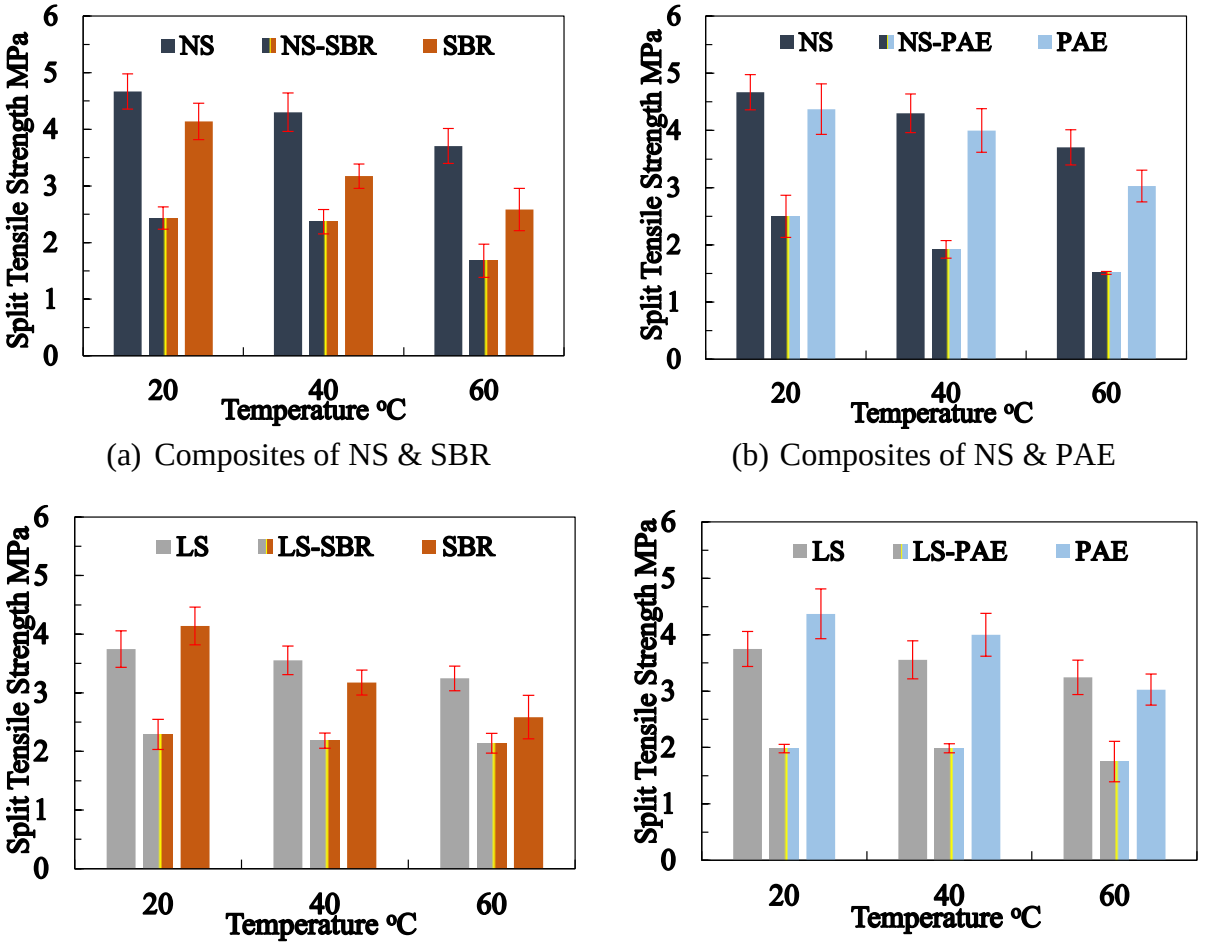

(a) Composites of NS & SBR

(b) Composites of NS & PAE

(c) Composites of LS & SBR

(d) Composites of LS & PAE

Fig. 3.4 Tensile strength of constituent and composite specimens under dry condition.

Significant reduction in tensile strength of both types of PCMs was also observed at elevated temperature. For SBR PCM, 23% and 37% reduction in tensile strength from control specimen

were noticed at temperature of 40 and 60 ℃, respectively. For PAE PCM, reduction observed was 30% at temperature of 60 ℃. PCM shows more reduction in the tensile strength at elevated temperature which may be due to following reasons: (1) PCM is cementitious material and having rich quantity of cement that may be responsible for more reduction in strength. (2) High temperature increases the porosity of cementitious material and in PCMs the polymer film which penetrates in pores may be disturbed by high temperature and contributes to strength reduction. (3) Polymers in PCM are sensitive to temperature and shows significant reduction in strength with temperature [27, 28]. Reis [27] conducted test on polymer mortars and noticed 91.6% reduction in flexural strength at temperature of 90 ℃. Biswas & Kelsey [28] has explained the failure model of the polymer mortar with temperature and observed the significant reduction in the tensile strength with increase in temperature.

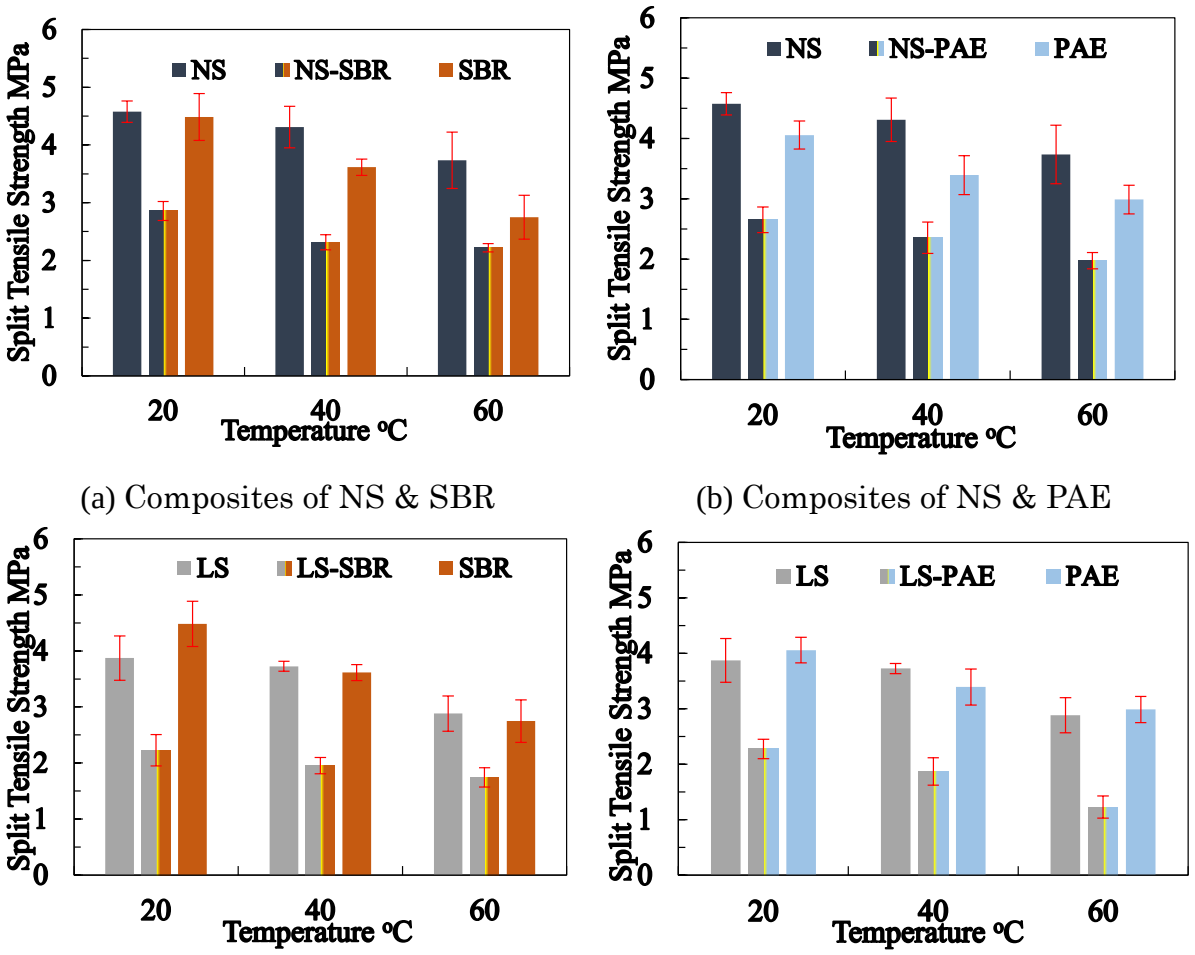

(a) Composites of NS & SBR

(b) Composites of NS & PAE

(c) Composites of LS & SBR

(d) Composites of LS & PAE

Fig. 3.5 Tensile strength of constituent and composite specimens under wet condition.

Fig. 3.4 also represents the influence of temperature on four types of composite specimens. At 20 ℃, the interfacial tensile strength was smaller as compared to that of the constituent materials. This verifies that OTZ is the weakest zone in composite specimens. Although among all, the best methodology was used to rough the substrate concrete and one of the best materials were used. But

interface is still very weak and observed interfacial strength is very low as compared to the strength of constituent materials. With the increase in temperature further reduction in interfacial strength was observed which may be due to degradation of constituent materials and deformation of interface. At 60 ℃, 31 and 40% reduction in interfacial strength was observed for NS-SBR and NS-PAE specimen respectively. It was observed 7 and 12% reduction in LS-SBR and LS-PAE specimen respectively at 60 ℃ temperature as compared to control specimen. As the average of all the specimens, interfacial tensile strength was the 54% of concrete tensile strength and 59% of PCM tensile strength under all temperature conditions, which implies that the interface strength is dependent on the strength of constituent materials.

Wet Condition

Another set of specimens of similar quantity were investigated under the effect of wet condition which was provided by heating water, all specimens were exposed to set temperature for duration of 16 hours. The average tensile strength of three specimens for each condition is presented in Fig. 3.5. Reduction in the strength was observed with increase in temperature, similar to the dry condition case. At 60 ℃ LS concrete was degraded by 26% and tensile strength of NS concrete was reduced by 18% from control specimens which were tested at 20 ℃. High temperature increases the porosity by rupturing fine pores. The pores were filled by the moisture which increases the moisture level in the concrete. LS concrete has less cement content and higher water to cement ratio than NS concrete. When exposed to high temperature, LS is more porous and of higher moisture level than NS concrete. Higher degree of saturation degrades the mechanical properties of concrete [29]. The reason for degradation in strength is due to pressure exerted by intensified pore water which results in generation of micro-cracks during application of external forces. Other mechanism of reduction in strength due to moisture and temperature is the activation energy of concrete, which highly depends upon the moisture content or degree of saturation as moisture lies in the very high disjoining pressures caused by layers of hindered adsorbed water within the finest pores of cement gel. Stresses due to load increased by these pressures, thus lowering the energy barrier for bond rupture [30]. The trend in the PCM strength was noticed similar to the dry temperature condition case. PCM is the water tight material, therefore 12 to 16 hours immersion resulted in almost the same effect as in dry temperature case. At 60 ℃ temperature SBR PCM was degraded by 39% of control specimen and reduction in PAE PCM strength was observed of an amount of 26%. Similar tendency was also observed in composite specimens. Similarly the strength of composite specimen at control condition was lower than the tensile strength of both constituent materials, the interfacial tensile strength was noticed as 55 and 61% of tensile strength of concrete and PCM respectively, under all temperature cases. With the increase in temperature reduction in interfacial strength was observed due to reduction in the strength of constituent materials and deformation of interface. In NS-SBR and NS-PAE composite specimens the reduction in the interfacial strength observed was about 22 and 26% respectively at 60 ℃. More than 22% reduction was also observed in composite specimens of low strength concrete at 60 ℃.

Comparison of heating effects under dry and wet conditions

As seen in Fig 3.4 & Fig 3.5 both conditions of heating have some influence on the tensile strength and comparisons of the tensile strength results under the same temperature are shown in Fig. 3.6. Up to 40 ℃ temperature the tensile strength of concrete decreases with temperature regardless of the heating method and insignificant effect of the heating method was observed. The difference in tensile strength was within 5% between wet and dry conditions. At 60 ℃ the reduction in the strength of LS concrete was more under wet condition than dry condition. This fact may be due to the higher level of moisture in it that fills all pores and during application of external forces water exert pressure from inside and increase the level of damage. Although reduction in tensile strength of PCM was observed with temperature increase, the effect of wet condition was ignorable. At 60 ℃ temperature the dry condition and wet condition tensile strength was within 8%. PCM is less permeable material because many pores occupied by polymer film so the effect of 16 hours immersion was insignificant to degrade it. Composite specimens with NS concrete have higher tensile strength in wet condition as compared to dry condition. All integrated specimens with LS concrete have lower tensile strength in wet condition due to the higher moisture level in concrete and high amount of moisture at interface.

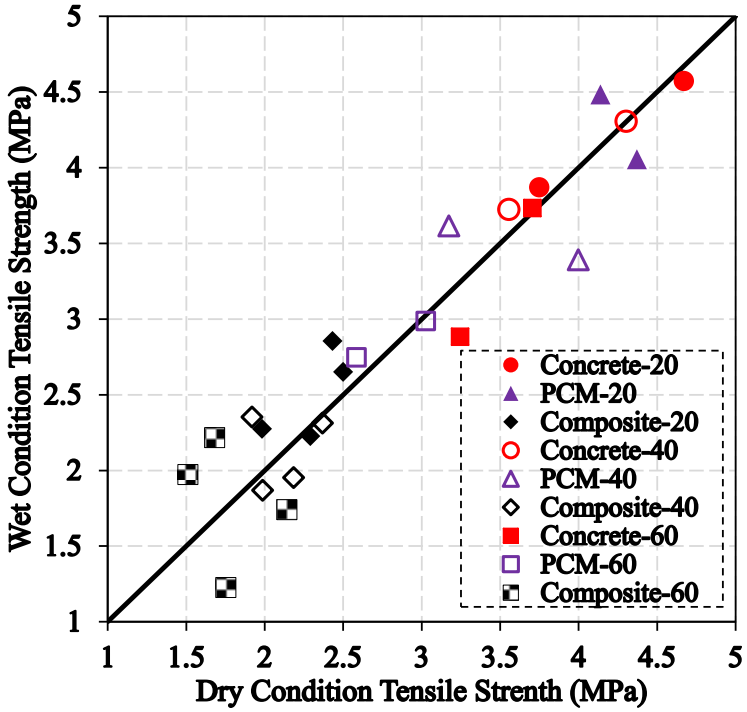

Fig. 3.6 Comparison of strength at various temperatures between wet and dry conditions.

3.3.3 Effect of Moisture

Wetting and drying cycles

The influence of W/D cycles on strength of bulk specimens and composite specimens is presented in Fig. 3.7. The tensile strength of concrete reduced as W/D cycles increased. Under first

cycle no significant effect was noticed but under 3rd, 6th and 12th cycle the reduction in strength were increased to 4, 11 and 19%, respectively for LS concrete. The reduction in strength of NS concrete was observed by an amount of 10 and 13% at 6th and 12th cycle, respectively. The strength of concrete highly depends upon the degree of saturation. With further increase of cycles the degree of saturation increases and the reduction in strength also increases significantly. At 12th cycle the reduction in the LS concrete was more than NS concrete, which may be due to higher moisture level than that of NS concrete. The strength reduction mechanism with different moisture level is also described in other study [29].

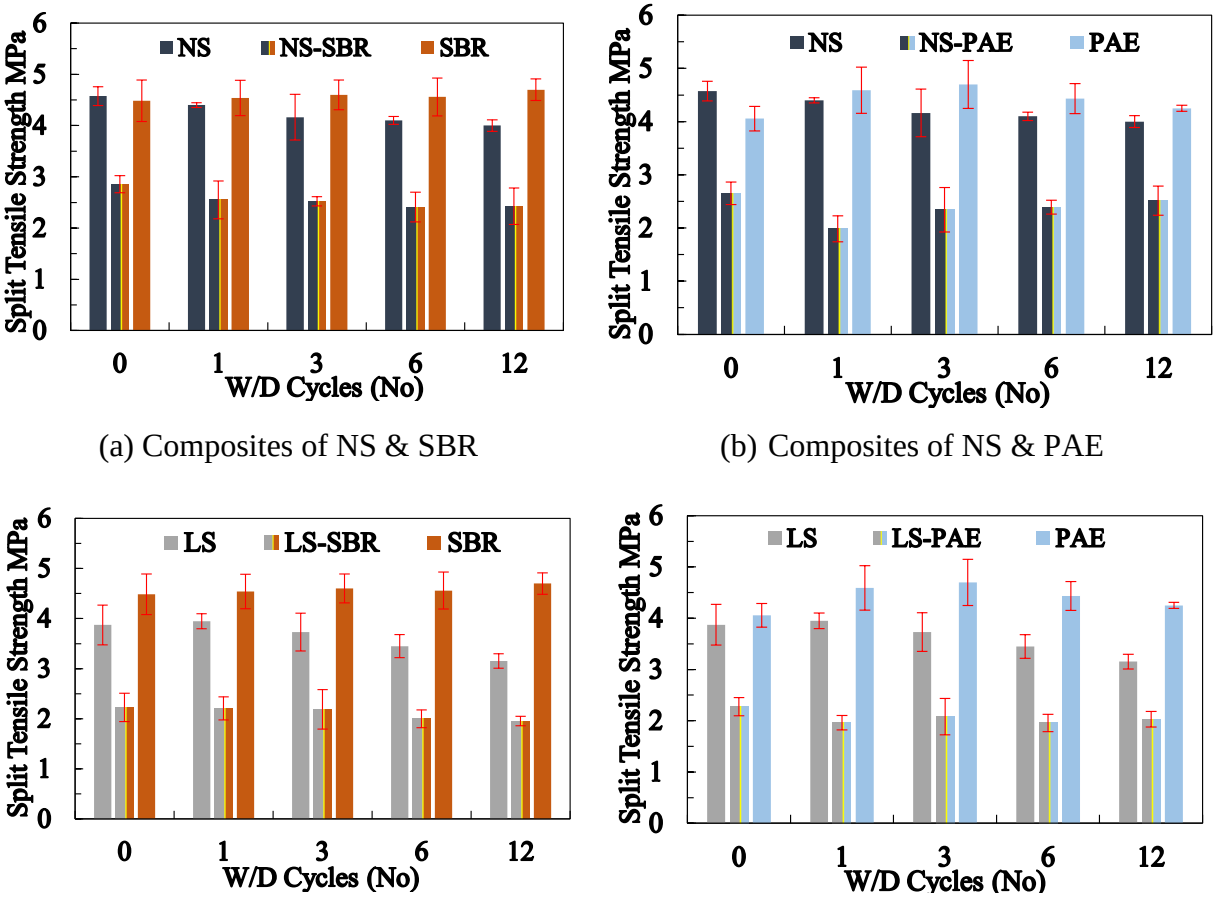

(a) Composites of NS & SBR

(b) Composites of NS & PAE

(c) Composites of LS & SBR

(d) Composites of LS & PAE

Fig. 3.7 Tensile strength of constituent and composite specimens under W/D cycles.

For PCM, no obvious loss in strength was observed after different W/D cycles. Little improvement in strength was noticed in both types of PCMs and PAE PCM shows more improvement with respect to SBR PCM. Strength of PCM highly depends upon types of polymer used and under various conditions different polymers behave in different ways. Some of them may react with water and lose their cohesion by swallowing and dissolving of polymer film, but some may react and make strong hydrogen bond to increase the strength [31, 32]. However, since the absorbed water in PCM is quite limited during W/D cycles and it is observed by Ramli et al. [33] and reported the water absorption was below 0.5% even after 550 days. In this study, its effect on

the PCM strength is marginal. For the composite specimens, interfacial strength highly depends upon the properties of the constituent materials and the behavior of interface under different W/D cycles. Reduction in concrete strength and increase in PCMs strength was observed under different W/D cycles but the reduction in composite strength was observed with the increase in the W/D cycles that may be due to presence of moisture at interface and significant reduction in the concrete strength. Reduction in strength was observed by an amount of 11% of NS-SBR specimen after 1st W/D cycle, and after 12th W/D cycle the amount in reduction increased to 15%. Whereas in the composite specimen PAE PCM, only 5 % reduction was observed after 12th cycle. For both types of composite specimens with low strength concrete the reduction in strength observed was 12 and 11% for LS-SBR and LS-PAE specimens.

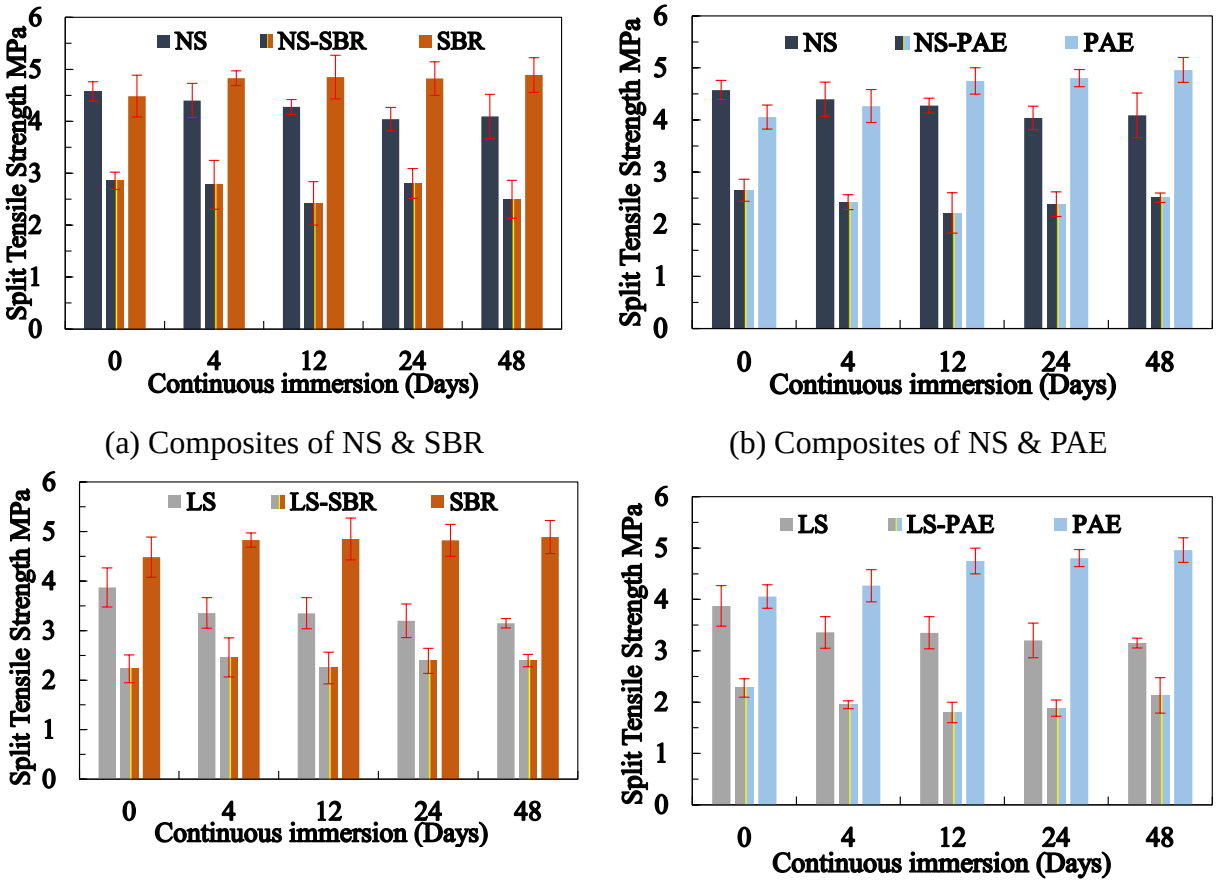

(a) Composites of NS & SBR

(b) Composites of NS & PAE

(c) Composites of LS & SBR

(d) Composites of LS & PAE

Fig. 3.8 Tensile strength of constituent and composite specimens under moisture.

Continuous immersion in water

The effect of age up to 48 days after 28 days curing was noticed insignificant on both composite and bulk specimens. Therefore, all specimens were compared with the 28 days curing (zero immersion day) control specimen. Fig. 3.8 shows the tensile strength of bulk specimen and composite specimens under different days of continuous immersion in water. The effect on tensile strength in continuous immersion in water was almost similar to the W/D cycle strengths at the

same age after the moisture exposure starts. In continuous wetting, the reduction in normal strength concrete and low strength concrete was noticed as 12 and 19% respectively, after 48 days immersion in water, when compared to the control specimen. About 9% improvement in strength was observed in SBR PCM and significant improvement in PAE PCM strength was observed and it increases by an amount of 5, 17, 18 and 22% after 4, 12, 24 and 48 days continuous immersion in water respectively. PAE PCM also shows slight improvement in strength under the exposure of W/D cycles. Continuous immersion in water provides suitable environment for the hydration and curing of the PAE PCM. For composite specimens, insignificant effect was observed on the interfacial tensile strength. Presence of moisture at interface hydrates the concrete and presence of hydroxyl group in cement paste/mortar makes hydrogen bond with the PCM and gives extra adhesion or anchorage to the composite specimen, which is presented in another study [37]. Almost in all composite specimens the interfacial strength observed was within 6% of the strength of control specimens, small variation was just due to some experimental errors or some scattering of data.

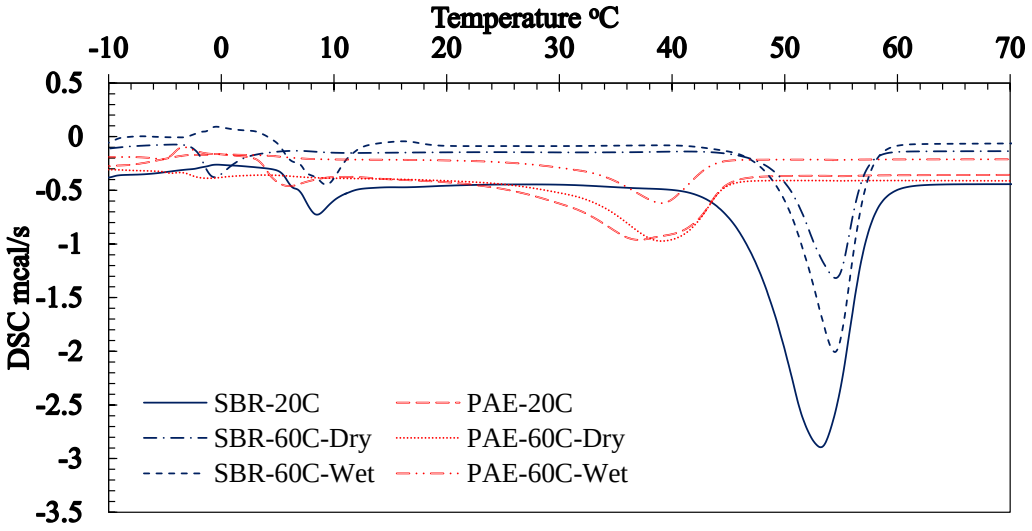

Fig. 3.9 Differential scanning calorimetry of both types of polymers under the influence of temperature.

3.3.4 Properties of Polymers in PCM under Different Conditions

Fig. 3.9 shows the result of differential scanning calorimetry (DSC) of both polymers under dry and wet condition. T_g values were observed as 7.6 and 4.3 ℃ for SBR and PAE polymers respectively. Insignificant effect was observed in the T_g value after various exposure conditions. Melting point (T_m) of SBR polymer was noticed as 53 ℃ and that of PAE was 37 ℃. Endothermic peak did not change after exposure conditions but only small change in DSC energy was observed. Temperature exposure under both dry and wet conditions did not change the T_g and T_m of polymers but both types of PCM shows significant reduction in tensile strength beyond T_m. The reduction in tensile strength before and after T_m is on same rate. Significant loss in strength due to crossing T_m value was not observed, but reduces linearly with the variation of temperature. In some literatures

abrupt change was observed in tensile strength of polymer mortar after T_g [28]. In this work the reduction was linear even after crossing T_m of polymers in PCMs. The effect of moisture on polymers was not significant and unable to change T_g and T_m of polymers and did not change the tensile strength significantly.

Fig. 3.10 shows the sample result of gel permeation chromatography (GPC) of both types of polymers. The average of measured number molecular weight (M_n) of polymer was 27700 and 80200 for SBR and PAE polymers respectively. Increase in molecular weight increases the degree of polymerization and strengthens polymer concrete or mortar against external environmental applications [22, 34]. Oppositely, reduction in molecular weight of polymers may reduce the strength of PCM. Insignificant effect was observed in molecular weight after different exposure conditions and it varies from 25000 to 37000 for SBR and 72000 to 92000 for PAE.

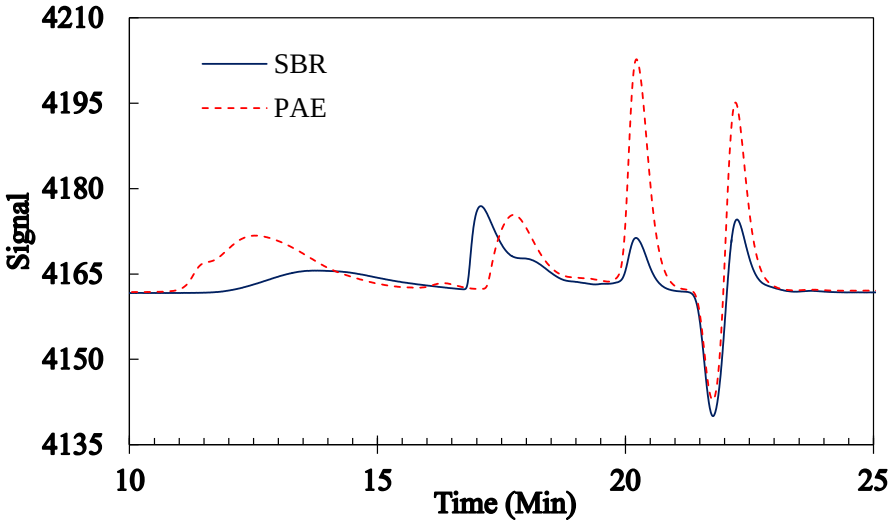

Fig. 3.10 Gel permeation chromatography of both polymers

3.4 PREDICTION FORMULA OF INTERFACIAL TENSILE STRENGTH

In all cases the fracture was observed at interface and the interfacial strength can be determined by using the following Eq. (2).

$$\frac{1}{f_{ITS}} = \frac{A}{f_{t.pcm}} + \frac{B}{f_{t.conc}} \tag{2}$$

Where,

f_{ITS} Interfacial tensile strength at concerned time (MPa)

$f_{t.pcm}$ Tensile strength of PCM at concerned time (MPa)

$$= 1.24 f_{to.pcm} exp(-0.01T) \tag{3}$$

$f_{t.conc}$ Tensile strength of concrete at concerned time (MPa)

$$= 1.14 f_{to,conc} exp(-0.005T) \tag{4}$$

$f_{to.pcm}$ Tensile strength of PCM after 28 days standard curing condition

$f_{to.conc}$ Tensile strength of concrete after 28 days standard curing condition

T Temperature (20 ℃ < T < 60 ℃)

A and B Experimental coefficients

Eq. (2) shows that interfacial strength is the function of the strength of the constituent materials and *A* and *B* are coefficients indicating the contribution weight of each constituent material, which depend upon many parameters such as interface roughness, moisture condition and properties of constituent materials, etc. Reduction in tensile strength was observed by the increase in temperature in both concrete and PCM specimens. By the way of normalizing with control condition (28 days standard curing condition) the tensile strength of PCM and concrete was obtained as Eqs. (3) and (4) respectively. From Eq. (2) finally the following Eq. (5) can be derived:

$$f_{ITS} = \frac{1.24(f_{to.pcm}f_{to.conc}\exp(-0.01T))}{(Af_{to.conc} + Bf_{to.pcm}\exp(-0.005T)} \quad (5)$$

Constituent material corresponding to the smaller of *A* and *B* contributes more to the bond strength according to Eq. (5). Values of *A* and *B* are shown in Table 3.5, which were determined based on the best fitting of test results. *B* in Eq. (5) is always smaller than *A*, which means that PCM contributes more to the bond strength than concrete due to the fact that concrete is already in hard form when the interface was created.

Table 3.5 Values of A & B under different exposure conditions.

Exposure conditions	A	B
Dry condition	1.00	0.85
Wet condition	1.00	0.85
W/D cycles	1.00	0.90
Continuous immersion in water	1.00	0.90

Eq. (5) is able to predict the interfacial tensile strength of composite specimen by giving any temperature from 20 ℃ to 60 ℃ and tensile strength of PCM and concrete after 28 days standard curing. Here, temperature ranges were above the glass transition temperature and melting point of polymers, so Eq. (5) might be used for higher environmental temperatures. But further experimentation is still required to verify it. Meanwhile, since values of *A* and *B* were regressed based on the test results in this study, which were all adhesive failure at interface, the applicability of proposed equation to the other failure modes needs to be verified with more experimentations.

To verify Eq. (5), a comparison was made between experimental and predicted values in Fig. 3.11 shows the interfacial tensile strength under the effect of temperature. In Fig. 3.11(a), Composite specimens with NS concrete showed very close results and verified the applicability of

Eq. (5), almost all data lies within ±10% limit. Fig. 3.11(b) presents the interfacial tensile strength under the exposure of temperature under the wet condition and all data was observed within the range of ±8% of the experimental work but still some values lies beyond ±10% that was happened mostly in the case of LS concrete.

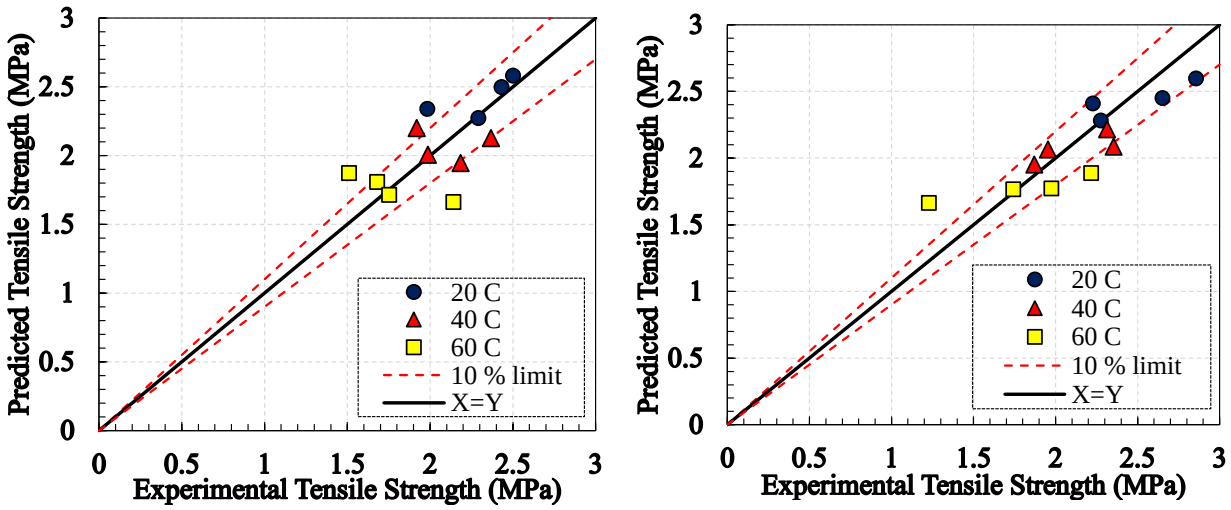

(a) dry conditions (b) wet conditions

Fig. 3.11 Experimental and predicted values of interfacial tensile strength under temperature

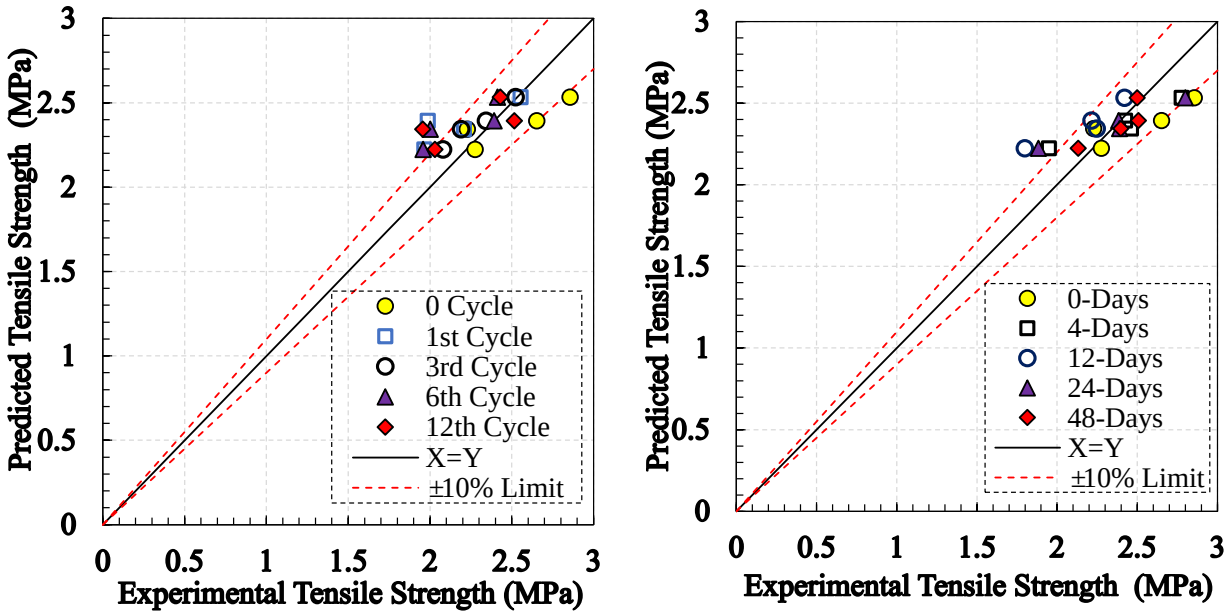

(a) W/D cycles. (b) continuous immersion

Fig. 3.12 Experimental and predicted values of interfacial tensile strength under moisture.

Insignificant effect of moisture was noticed on interfacial tensile strength of composite specimens. Therefore Eq. (5) was also used to predict the bond strength under exposure of continuous immersion in water at various days and under different W/D cycles. Fig. 12 shows the comparison between predicted and observed bond strength under moisture condition, W/D cycles

and continuous immersion. Almost all predicted values were within the range of ±10% of experimental observations in case of W/D cycles (Fig. 3.12(a). And slight variation may be due to experimental scatter. Similarly, Fig. (Fig. 3.12(b) shows the comparison between the experimental values obtained after different continuous immersion in water by using Eq. (5). All data lies within ±10% limits and some data deviate slightly from this range.

3.5. CONCLUSIONS

The experimental study was conducted on the interface behavior between two types of concrete (normal and low strength concrete) and two types of commercially used polymer cement mortars (SBR and PAE PCMs). The influence of temperature and moisture on the strength of constituent materials and composite specimen was investigated and the following conclusions were drawn.

1) Overlay transition zone (OTZ) is the weakest zone in the composite specimens and fracture occurred in this zone so that failure was adhesive failure at macro level, regardless of the temperature and moisture condition in which specimens were exposed.
2) Concrete and PCM both degraded with the increase in temperature. Reduction in the tensile strength of PCM was more than concrete. Reduction of interfacial tensile strength of composite specimens was observed with the increase in temperature, which was more than 20% at temperature of 60 ^{o}C. Almost similar effect on tensile strength of bulk and composite specimen was observed between heating under dry and wet conditions, except for low strength (LS) concrete which shows more reduction in wet condition.
3) Reduction in the tensile strength of concrete was observed under both W/D cycles and continuous immersion, but insignificant effect was observed on PCM strength. In contrast, slight improvement in strength was observed in PAE PCM. Insignificant variation in interfacial tensile strength was observed under the influence of moisture by wetting/drying and continuous immersion.
4) Insignificant effect of temperature and moisture was observed on glass transition temperature, melting point temperature and molecular weight of the extracted polymers.
5) Prediction formula of interfacial tensile strength was proposed and showed close agreement with the experimental results under all exposure conditions. The proposed formula covers temperature range including the glass transition point, T_g and the melting point, T_m of polymers.

REFERENCES

[1] Neville AM. Properties of concrete. 4th and Final ed. Harlow:: Pearson Prentice Hall; 2004.

[2] Mehta P, Monteiro PJM. . Concrete: microstructure, properties, and materials. 3rd ed. New York: The McGraw Hill Companies; 2006.

[3] Morgan DR. Compatibility of concrete repair materials and systems. Construction and Building Materials. 1996;10(1):57-67.

[4] Hassan KE, Brooks JJ, Al-Alawi L. Compatibility of repair mortars with concrete in a hot-dry environment. Cement and Concrete Composites. 2001;23(1):93-101.

[5] Park D, Ahn J, Oh S, Song H, Noguchi T. Drying effect of polymer-modified cement for patch-repaired mortar on constraint stress. Construction and Building Materials. 2009;23(1):434-47.

[6] Park D, Park S, Seo Y, Noguchi T. Water absorption and constraint stress analysis of polymer-modified cement mortar used as a patch repair material. Construction and Building Materials. 2012. 819-30

[7] Hassan KE, Robery PC, Al-Alawi L. Effect of hot-dry curing environment on the intrinsic properties of repair materials. Cement and Concrete Composites. 2000;22(6):453-8.

[8] Ohama Y. Handbook of polymer-modified concrete and mortars-properties and process technology. New Jersy: Noyes Publications; 1995.

[9] Santos PMD, Júlio ENBS. A state-of-the-art review on roughness quantification methods for concrete surfaces. Construction and Building Materials. 2013;38:912-23.

[10] JIS. JIS B 0601. Geometrical Product Specifications (GPS)-Surface texture: Profile method-Terms, Definitions and surface texture parameters 2001.

[11] Rashid K, . Ueda, T., Zhang, D., Fujima, S.,. Tensile strength and failure modes of concrete repaired by polymer cement mortar in hot region. In: ACF, editor. 6th International Conference of Asian Concrete Federation. Seoul, Korea2014. p. 1338-45.

[12] Zhang D, Ueda, T., Furuuchi, H., . Fracture mechanisms of polymer cement mortar: concrete interfaces. Journal of Engineering Mechanics. 2013;139:167-76.

[13] Al-Jabri KS, Hago AW, Al-Nuaimi AS, Al-Saidy AH. Concrete blocks for thermal insulation in hot climate. Cement and Concrete Research. 2005;35(8):1472-9.

[14] International A. ASTM C 39-03. Standard test method for compressive strength of cylindrical concrete specimens. USA 2003.

[15] International A. ASTM C-496. Standard Test Method for Splitting Tensile Strength of Cylindrical Concrete Specimens 2004.

[16] Rocco C, Guinea GV, Planas J, Elices M. Size effect and boundary conditions in the brazilian test: theoretical analysis. Mat Struct. 1999;32(6):437-44.

[17] Li S, Geissert, DG., Frantz, GC., Stephens, JE.,. Durability and bond of high performance concrete and repaired Portland cement concrete. Joint Highway Research Advisory Council: University of Connecticut, Storrs-Mansield, CT, 06269; 1997.

[18] Momayez A, Ehsani MR, Ramezanianpour AA, Rajaie H. Comparison of methods for

evaluating bond strength between concrete substrate and repair materials. Cement and Concrete Research. 2005;35(4):748-57.

[19] Li G. A new way to increase the long-term bond strength of new-to-old concrete by the use of fly ash. Cement and Concrete Research. 2003;33(6):799-806.

[20] Li G, Xie H, Xiong G. Transition zone studies of new-to-old concrete with different binders. Cement and Concrete Composites. 2001;23(4–5):381-7.

[21] International A. ASTM E-1356-03. Test method for assignment of the glass transition temperatures by differential scanning calorimetry. West Conshohocken, PA.2004.

[22] Nair P, Ku DH, Lee CW, Park HY, Song HY, Lee SS, et al. Microstructural studies of PMMA impregnated mortars. Journal of Applied Polymer Science. 2010: 3534-40.

[23] Van Kreveld ME, Van Den Hoed N. Mechanism of gel permeation chromatography: distribution coefficient. Journal of Chromatography A. 1973;83:111-24.

[24] Mulder JL, Buytenhuys FA. A system for preparative separation of a wide range of small molecules by gel permeation chromatography in organic liquids. Journal of Chromatography A. 1970;51:459-77.

[25] Bazant PK, FM. Concrete at high temperature-Material properties and mathematical methods,: Harlow:longman; 1996.

[26] Gallé C. Effect of drying on cement-based materials pore structure as identified by mercury intrusion porosimetry: A comparative study between oven-, vacuum-, and freeze-drying. Cement and Concrete Research. 2001;31(10):1467-77.

[27] Reis JMLd. Effect of temperature on the mechanical properties of polymer mortars. Materials Research. 2012;15(4):645-9.

[28] Biswas M, Kelsey, R. G. Failure model of polymer mortar. Journal of Engineering Mechanics. 1991;117:1088-104.

[29] Shoukry SN, William GW, Downie B, Riad MY. Effect of moisture and temperature on the mechanical properties of concrete. Construction and Building Materials. 2011;25(2):688-96.

[30] Bazant P, Kaplan, FM.,. Effect of Temperature and Hunudity on fracture Energy of Concrete. ACI Material Journal. 1988:262-71.

[31] Mansur AAP, Nascimento OLd, Mansur HS. Physico-chemical characterization of EVA-modified mortar and porcelain tiles interfaces. Cement and Concrete Research. 2009;39(12):1199-208.

[32] Knapen E, Gemert DV. Effect of under water storage on bridge formation by water-soluble polymers in cement mortars. Construction and Building Materials. 2009;23(11):3420-5.

[33] Ramli M, Tabassi AA, Hoe KW. Porosity, pore structure and water absorption of polymer-modified mortars: An experimental study under different curing conditions. Composites Part B: Engineering. 2013;55:221-33.

[34] Chen C-H, Huang R, Wu JK, Chen C-H. Influence of soaking and polymerization conditions on the properties of polymer concrete. Construction and Building Materials. 2006;20(9):706-12.

Chapter 4

INTERFACIAL TENSILE AND SHEAR STRENGTH BETWEEN CONCRETE-PCM AT ELEVATED TEMPERATURE

4.1 INTRODUCTION

It was concluded form previous two chapters that temperature significantly degrade Polymer cement mortar (PCM) and composite specimens in tension. And overlay transition zone (OTZ) is the weakest zone and at all temperature levels fracture was observed at interface. To improve interfacial tensile strength or OTZ, new work was designed and presented in following sections. In which, roughness level was improved by introducing new laboratory method. And to further increase adhesion, primer was used at interface. Concrete of lower strength than previous work was used and also type of PCM was changed. Along with the interfacial tensile strength, interfacial shear strength test was also conducted. So many examples can be observed in which interfacial shear stress was generated between concrete-PCM interfaces. For example; Interface between the substrate concrete of existing slabs and newly poured PCM is subject to a self-equilibrated state of tension combined with shear. In bridge retrofitting, while repairing of slender stems of box girder decks, interface between old and new material are under shear stress due to combined application of dead and live load which results in the variation in bending moment. Columns strengthened by means of PCM jackets have a transference zone along which the longitudinal forces are transferred through interface shear stresses from the old cross-section to the new cross-section [1].

With such background, detailed experiments were designed to evaluate the behavior of concrete-PCM and Concrete-PCM specimens, in tension and shear, under exposure condition of 20 ℃, 40 ℃ and 60 ℃. Selected temperature range may cover most of regions in the world during summer, which have abundant RC structures. Prediction formula was proposed of interfacial strength in shear and tension and checked the reliability under selected temperature range along with previous available data.

4.2 EXPERIMENTAL METHODOLOGY

4.2.1 Materials

In this experimental work, three types of materials were used. First one was the concrete which was ready mixed concrete of target cubical compressive strength of 30 MPa. It was placed in desired molds in the laboratory and tested after 28 days wet curing. Second type of the material was the polymer cement mortar (PCM). It may be prepared in the laboratory by adding different amount of polymers, in form of latexes, emulsions and re-dispersible powder, in ordinary mortar [2, 3]. In this work commercially available PCM were used and compounding ratio provided by manufacturers is shown in Table 4.1, PCM used in this experimentation is different from PCM used in previous chapters. Third material was the primer which was used at interface between PCM and

concrete for proper adhesion. Primer also consisted of polymers and resist penetration of moisture from PCM to substrate concrete. Physical and chemical properties of primer used are indicated in Table 4.2.

Table 4.1 Compounding ratio of PCM material.

Constituents with corresponding ratios	
Unit volume mass (kg/L)	2.90
Portland cement (%)	38.0
Silica sand (%)	62.0
Type of polymer	Copolymer of vinyl acetate and ethylene

Table 4.2 Physical and chemical properties of primer.

Property	Description
Main ingredient	Acrylic ester styrene Latex
pH	7.5-9
Melting Point	0.10 ℃
Density	1.04 g/cm^3
Miscible with water	Slightly soluble
Dynamic viscosity	3000 - 5000 mPa.s
Solids content (mass %)	47 - 49 %

4.2.2 Specimen Prepration

For casting of concrete and PCM, wooden molds were prepared of following sizes; 150 and 100 cubic mm (for compression test), 150 x 150 x 75 mm (for interfacial splitting test), 150 x 150 x 100 mm (for interfacial shear test). Some amount of retarder were mixed with water and spread inside bottom of molds, except of cubic mold. Ready mixed concrete was cast in all molds, compacted and covered with polythene sheet to avoid evaporation of moisture. After 36 hours of casting bottom layer of mold was removed and concrete surface was exposed to environment. Observed concrete surface was not fully hard due to presence of retarder. Steel brush was spread over the soft surface and remove all soft particles of cement paste and mortar, until coarse aggregates were exposed. This rough surface was cleaned by strong jet of water. After 48 hours of casting all molds were removed and concrete was cured for more than 2 weeks in wet condition.
Concrete specimens of size 150 x 150 x 75 and 150 x 150 x 100 mm were put into mold of 150 cubic mm. The rough surface was kept upside in the mold. Primer was sprayed on rough surface of substrate concrete before 3 hours of casting of PCM, as suggested by the manufacturer. PCM was sprayed over the treated surface of concrete and fill all the mold of 150 cubic mm. PCM was also sprayed in mold of 100 mm cubic which was used for measuring compressive strength under designed exposure conditions. Methodology of specimen preparation at material level testing is explained in Fig. 4.1. PCM was 7 days wet cured and 21 days dry cured which was the most suitable

method for curing of PCM [2]. In wet curing condition hydration took place, while in dry condition polymer film formed and filled the voids and makes PCM stronger [2].

(a) wooden molds

(b) casting of material

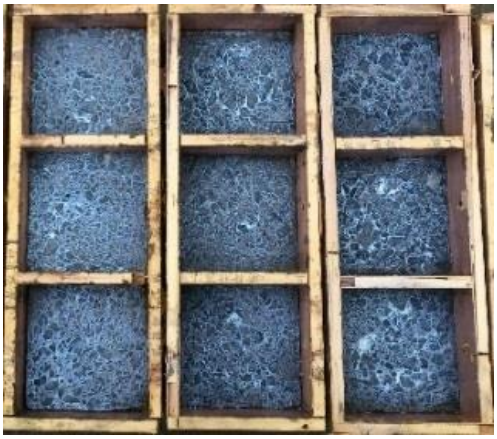

(c) rough surface with primer

(d) spraying of PCM

Fig. 4.1 Preparation of specimens for material level testing.

Table 4.3 Number of specimens and types of test performed at material level.

Test	Compressive strength			Tensile strength			Shear strength		
Temp.	20℃	40℃	60℃	20℃	40℃	60℃	20℃	40℃	60℃
Concrete	3	3	3	3	3	3	3	3	3
PCM	3	3	3	3	3	3	3	3	3
Comp-NP[a]	---	---	---	3	3	3	3	3	3
Comp-WP[b]	---	---	---	3	3	3	3	3	3

Comp-NP[a] = Composite specimens with No-Primer;
Comp-WP[b] = Composite specimens With Primer

4.2.3 Exposure Conditions & Testing Procedures

Temperature is the major parameter of the environment which severely affect the properties of PCM and composite specimens as observed and concluded in previous two chapters. In this extended experimentation various temperature levels were selected to cover the maximum range

of the regions of the world. Exposure condition and testing conditions was maintained at 20 ℃, 40 ℃ and 60 ℃ temperature while relative humidity was maintained at 60%. All specimens were exposed to design temperature level and relative humidity for 16 hours to 20 hours then tested under condition similar to the exposure condition.

Three types of testing was perfomed on concrete, PCM and composite specimens which is explained in following subsequent sections;

Compressive strength

Cubical specimens of size 150 mm for concrete and 100 mm for PCM were tested instead of cylindrical specimens to evaluate compressive strength. Cylindrical compressive strength which is mostly used in design may be obtained by using eq. (1) [4]. Average compressive strength of three specimens were recorded as a compressive strength at particular condition. Compressive strength tests were conducted at 20 ℃, 40 ℃ and 60 ℃ temperature. Corresponding modulus of elasticity can be calculated by using eq. (2) [5].

$$f_c' = 0.8 f_{cu} \tag{1}$$

$$E_c = 4730 \sqrt{f_c'} \tag{2}$$

Where;

f_c' = Cylindrical compressive strength ; f_{cu} = Cubcial compressive strength; E_c =Modulus of elasticity of concrete

Interfacial tensile strength

Interfacial tensile strength of composite specimens may be evaluated by simply conducting split tensile strength according to ASTM C 496 [6]. Specimen size and geometry is mentioned in Fig. 4.2, which were tested to obtain the split tensile strength as well as interfacial splitting tensile strength [7-10]. Interfacial tensile strength of composite specimens and split tensile strength of bulk specimens were reported as the average of three specimens results and evaluated by using eq. (3). Split tensile strength was also evaluated at 20 ℃, 40 ℃ and 60 ℃ temperature.

$$f_t = \frac{2P_u}{\pi A} \tag{3}$$

where,

f_t = Interfacial split tensile strength (MPa) ; P_u =Ultimate load (N); A =Area of interface (mm^2)

Interfacial shear strength

Interfacial shear strength may be evaluated by using Bi-Surface shear strength test which was explained in detail by Momayez et al. [10]. The methodology gives less variation in results and widely used for evaluation of interfacial shear strength. Three specimens at one condition were used for evaluation of shear strength at 20 ℃, 40 ℃ and 60 ℃ temperature. Geometry and types

of specimens tested for evaluation of Bi-Surface shear strength are shown in Fig. 4.3. Shear strength is evaluated by using following eq. (4).

$$\tau_v = \frac{P_u}{2A} \tag{4}$$

where,

$\tau_v =$ Interfacial shear strength (MPa) ; P_u =Ultimate load (N); A =Area of interface (mm^2)

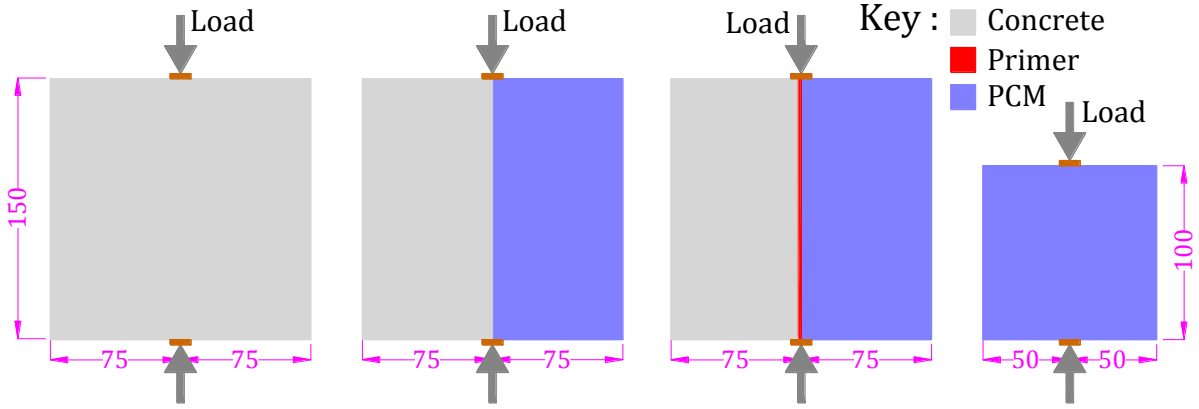

(a) Concrete (b) Comp-NP* (c) Comp-WP** (d) PCM

*Composite specimen without primer; **Composite specimen with primer

Fig. 4.2 Schematic diagram for tensile strength of bulk specimen and composite specimen (unit:mm)

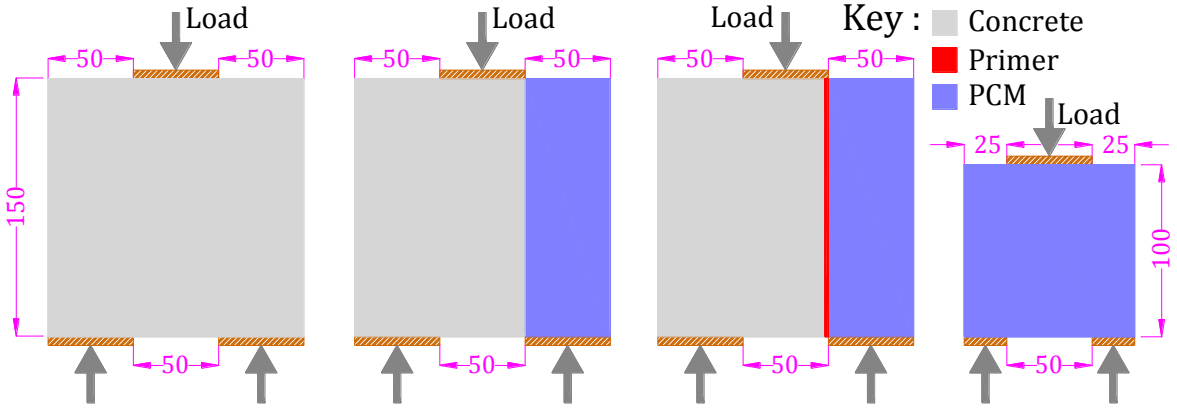

(a) Concrete (b) Comp-NP* (c) Comp-WP** (d) PCM

*Composite specimen without primer; **Composite specimen with primer

Fig. 4.3 Schematic diagram for Bi-Surface shear strength of bulk specimen and composite specimen (unit:mm)

Compressive strength, interfacial tensile strength and interfacial shear strength were obtained by the same testing machine. The testing machine was equipped with heaters near testing platens,

which maintain the desire temperature level and loading chamber was wrapped with insulation sheets. Specimens were put in oven for 24 hours at desired temperature level and were also wrapped with insulation sheet after getting off from oven and were transferred to the testing machine. Temperature in oven and inside loading chamber was maintained at same level and assuming similar exposure and testing condition during testing. Number of specimens and testing conditions of constituent materials and their respective composite specimens, which was referred as material level testing are provided in Table 4.3.

4.3. RESULTS & DISCUSSION

4.3.1 Compressive Strength

Compressive strength of both specimens, concrete and PCM, were evaluated on cubical specimens and presented in Table 4.4, where compressive strength was expressed as the average of three specimens and standard deviation is also shown in Table 4.4. The effect of temperature on the concrete compressive strength was observed to be insignificant, whereas large amount of reduction was observed in the compressive strength of PCM.

Table 4.4 Compressive strength of concrete and PCM.

Material	Cubical compressive strength (MPa)			Standadrd Deviation		
	20 ℃	40 ℃	60 ℃	20 ℃	40 ℃	60 ℃
Concrete	28.29	29.06	31.43	1.26	2.39	1.33
PCM	59.69	27.70	33.70	1.17	2.03	2.50

4.3.2 Tensile and Shear Strength

Similar trend was also observed in tensile strength and shear strength of concrete and PCM. Strength of PCM was reduced significantly with the increase in temperature. 26% reduction was observed in split tensile strength at 40 ℃ and with further increase in temperature more reduction in tensile strength was observed (Fig. 4.4(a)). And finally it was reduced by 30% at 60 ℃ as compared to the control specimens which were tested at 20 ℃. Shear strength was reduced by 30% at 40 ℃ and 70% at 60 ℃ as compared to specimens tested at 20 ℃ (Fig. 4.4 (b)). Several reasons are reported in literatures which describe the mechanism of reduction in strength as follows; (1) PCM is very rich in cement and very less amount of water is added in it as compared to ordinary Portland cement mortar of similar strength. Therefore higher amount of cement is one of the reasons of reduction in mechanical strength [11]. (2) PCM has various types of polymers and polymers are very sensitive to temperature [2, 12]. (3) Other causing the reduction in strength is the increase in porosity with increase in temperature. In ordinary cement mortar, fine pores collapse by receding water menisci that causes increase in volume of larger pores. (4) In PCM, pores are filled by polymer films during curing of PCM and high temperature may degrade the polymer film that increases the volume of large pores. PCM strength reduction under high temperature was also observed in other studies [2, 7, 12, 13].

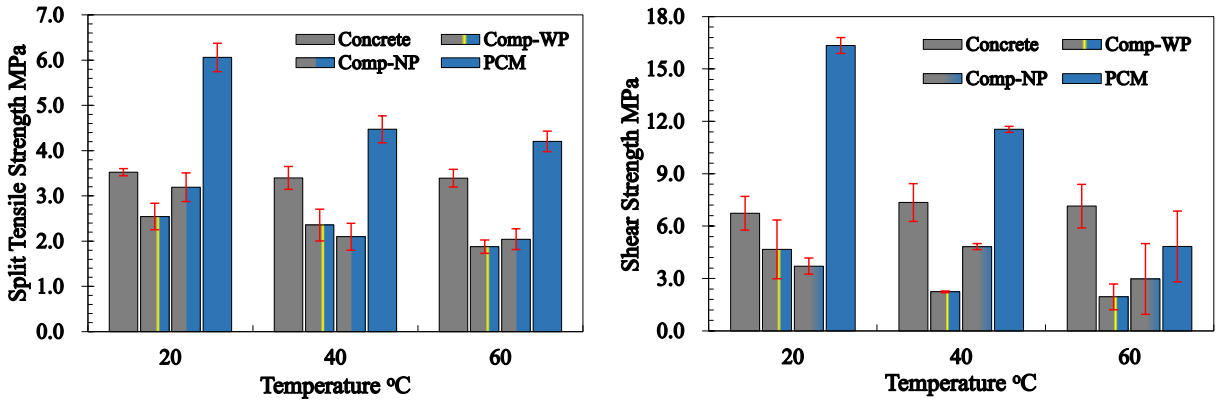

(a) Split tensile strength (b) Bi-Surface shear strength

Fig. 4.4 Strength of bulk and composite specimens at different temperature level.

4.3.3 Interfacial Strength

Fig. 4.4 also presents the interfacial tensile and interfacial shear strength of composite specimens at different temperature level, along with their constituents. Three specimens were tested at one condition and average value was recorded as strength at that particular condition. Standard deviation is presented by error bar in Fig. 4.4. Interfacial strength highly depends upon the roughness level of substrate concrete and type of virgin material attached to substrate concrete. It can be improved by increasing roughness level and by using PCM material [10, 14]. Interfacial split tensile strength was explored by the authors in another work, and it was observed that interfacial strength was about 0.60 of the strength of concrete ((Chapter 3) & [7]). Coefficient of roughness "R_a" was improved from 0.36 in that work to 0.72 in this study, which was measured by three dimensional shape measuring apparatus. Interfacial tensile strength was observed as 0.91 and 0.72, of the concrete strength at 20 ℃, without primer and with primer, respectively. At elevated temperature of 60 ℃ the ratios reduced to 0.60 and 0.55 for without primer and with primer case, respectively. Similar tendency was observed in interfacial shear strength. Bi-Surface shear strength observed was less than the shear strength of both constituents under all temperature condition. At 20 ℃ temperature, observed interfacial shear strength was 0.69 of the concrete shear strength and was reduced to 0.27 at 60 ℃. Specimens without primer have less ratio than the specimens with primer. It was observed 0.55 at 20℃ and reduced to 0.42 at 60 ℃. At higher temperature composite specimens with primer showed more reduction, which may be due to presence of higher polymer content at interface and failure mode of specimen was still the same as interface adhesive failure. Specimens without primer shows hybrid type of failure, in which failure was adhesive interface along with some amount of PCM attached to the concrete side. Effect of temperature on interface may have same analogy with behavior of interfacial transition zone of concrete at high temperature, as reduction in strength is due to the different rate of expansion of aggregate and cement paste which generate micro-cracks at interfacial transition zone. Reduction in interfacial strength is may be due to different coefficient of thermal expansion of concrete and PCM, which generates high internal stresses and micro-cracks and weakens the bond between two materials.

4.4 PREDICTION FORMULA OF INTERFACIAL STRENGTH

4.4.1 Interfacial Tensile Strength

Interfacial tensile strength of composite specimens at any concerned temperature can be predicted by using eq. (5). This equation has already been proposed in previous chapter to predict the interfacial tensile strength and the failure mode was observed in previous and current work was the adhesive interface failure.

$$\frac{1}{f_{ITS}} = \frac{A_t}{f_{t.pcm}} + \frac{B_t}{f_{t.conc}} \tag{5}$$

where,

f_{ITS} Interfacial tensile strength at concerned temperature (MPa)

$f_{t.pcm}$ Tensile strength of PCM at concerned temperature (MPa)
$= 1.2 f_{to.pcm} exp(-0.0095T)$ (6)

$f_{t.conc}$ Tensile strength of concrete at concerned temperature (MPa)
$= 1.07 f_{to,conc} exp(-0.004T)$ (7)

$f_{to.pcm}$ Tensile strength of PCM after 28 days standard curing condition

$f_{to.conc}$ Tensile strength of concrete after 28 days standard curing condition

T Temperature (20 ℃ $< T <$ 60 ℃)

A_t *and* B_t Experimental coefficients in tension

Interfacial tensile strength is the function of the tensile strength of both constituent materials. And always less than the tensile strength of respective constituent materials. A_t and B_t are the experimental coefficients which were explained in detail in previous chapter and author pub;lished work [7]. Same values of coefficients was used in this work and presented in Table 4.5. Eq. (6) and eq. (7) were obtained by normalizing with the tensile strength of respective material at control condition of temperature 20 ℃. PCM strength in current work was more and concrete strength was less than the work presented in previous chapter (Chapter 3). So large range of strength was used for normalization and that may be used in future for other researchers. Strength of PCM and concrete at concerned temperature can easily be obtained by using eq. (6) and eq. (7), respectively. Finally by using eq. (6) and eq. (7) in eq. (5) following eq. (8) was derived.

$$f_{ITS} = \frac{1.2(f_{to.pcm} f_{to.conc} \exp(-0.009T))}{A_t f_{to.conc} + B_t f_{to.pcm} \exp(-0.0055T)} \tag{8}$$

Table 4.5 Experimental coefficient values for prediction of interfacial strengths.

Strength	A	B
Interfacial tensile strength	1	0.85
Interfacial shear strength	1.65	2

Interfacial tensile strength can be predicted by using eq. (8). Boundary condition for temperature in eq. (8) was from 20 to 60 ℃. Which is large range and covers almost most regions of the world in summer. The failure of composite specimens was adhesive failure, so eq. (8) is applicable for adhesive failure. Eq. (8) was verified by using current and previous experimental results and compared with the predicted values and presented in Fig. 4.5. Influence of primer was observed to be insignificant and did not contribute to the improvement of interfacial strength. Most of the data lies with ±10% limits which verified the applicability of predicted equation (eq. 8). The average of all data at three temperature level (20, 40 and 60 ℃) was also draw in Fig 4.4 and which was observed almost equal to the predicted values and all data point lies on X=Y line (Fig. 4.5).

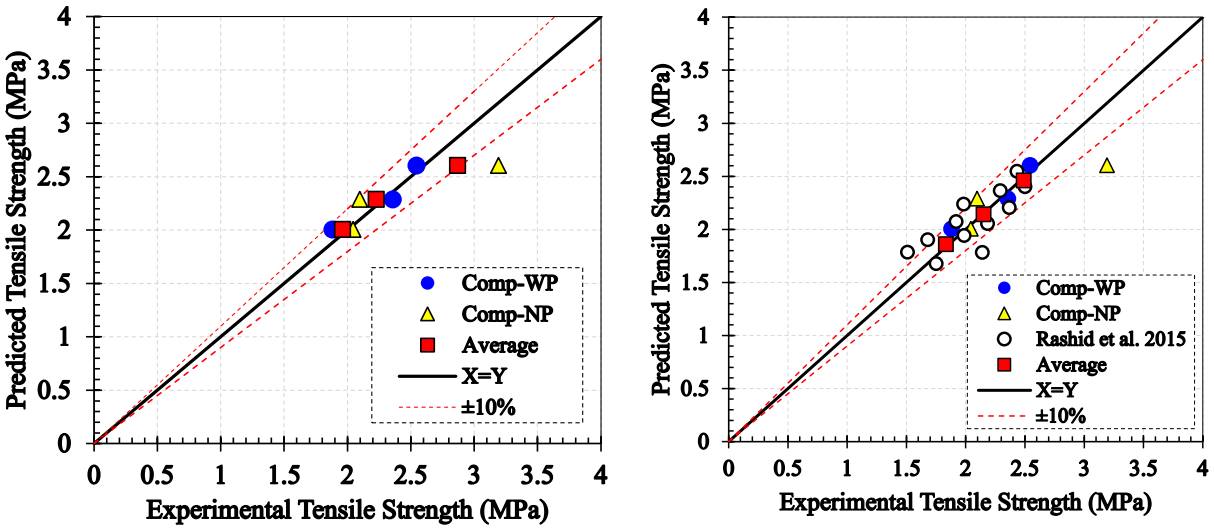

(a) Current experimentation (b) Incorporated with previous work.

Fig. 4.5. Interfacial tensile strength: experimental verses predicted values.

4.4.2 Interfacial Shear Strength

Eq. (5) was modified by replacing tensile strength by shear strength of respective specimen and eq. (9) was obtained. Eq. (10) and eq. (11) was also obtained similarly by normalizing shear strength with the control specimen shear strength which was cured for 28 days and tested at 20 ℃. Contribution weight of each constituent material was presented by coefficients A_v and B_v. These coefficients depends upon roughness, moisture condition and properties of constituent materials [7]. So material with smaller values of coefficients contributes more to the interfacial tensile strength and interfacial shear strength according to eq. (5) and eq. (9), respectively. Table 4.5 presents the values of coefficients in both shear and tension. In tension PCM contributed more towards bond strength due to already hard state of concrete substrate. And in shear concrete paid major role in contribution of the shear strength that was mostly due to surface roughness of concrete substrate [14].

$$\frac{1}{\tau_{ISS}} = \frac{A_v}{\tau_{v.pcm}} + \frac{B_v}{\tau_{v.conc}} \tag{9}$$

where,

τ_{ISS} Interfacial shear strength at concerned temperature (MPa)

$\tau_{v.pcm}$ Shear strength of PCM at concerned temperature (MPa)

$$= 2\tau_{vo.pcm} exp(-0.03T) \quad (10)$$

$\tau_{v.conc}$ Shear strength of concrete at concerned temperature (MPa)

$$= 0.99\tau_{vo,conc} exp(0.0015T) \quad (11)$$

$\tau_{v.pcm}$ Shear strength of PCM after 28 days standard curing condition

$\tau_{v.conc}$ Shear strength of concrete after 28 days standard curing condition

T Temperature (20 ^{o}C < T < 60 ^{o}C)

A_v & B_v Experimental coefficients in shear

$$\tau_{ISS} = \frac{2(\tau_{vo.pcm}\tau_{vo.conc}\exp(-0.03T))}{A\tau_{vo.conc} + B\tau_{vo.pcm}\exp(-0.0285T)} \quad (12)$$

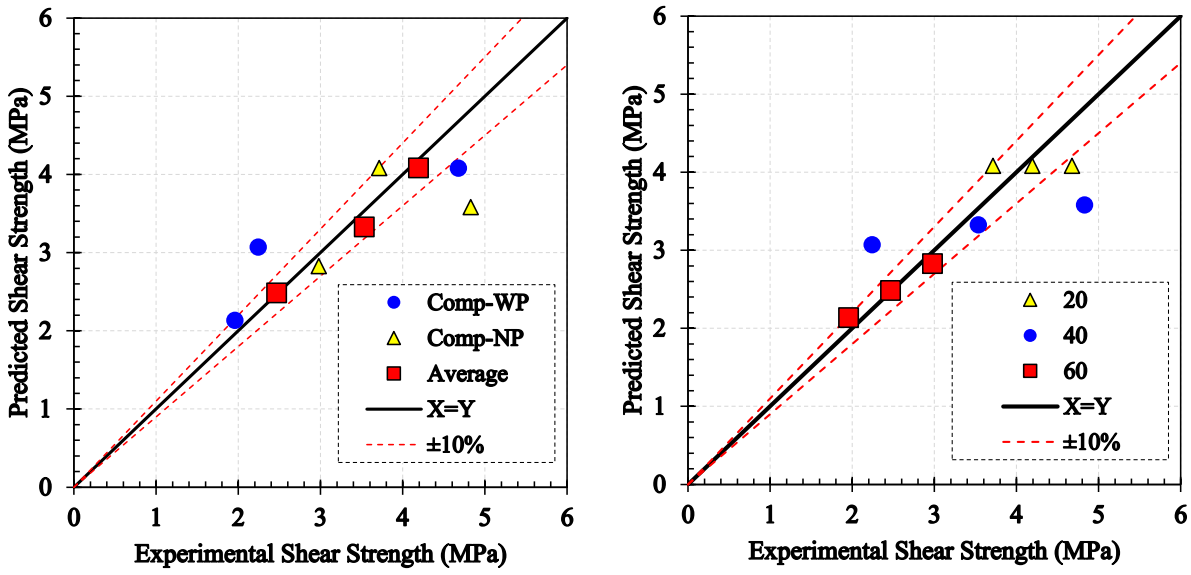

(a) Influence of Primer (b) Influence of Temperature

Fig. 4.6 Interfacial shear strength: experimental verses predicted values.

Eq. (12) was obtained by using eq. (10) and eq. (11) in eq. (9). Which was able to predict the interfacial shear strength and again the failure mode was the adhesive failure mode and still more experimentation is required for other failure modes. Eq. (12) was verified by comparing the experimental results with predicted values at different temperature levels. Eq. 12 can also predict the interfacial strength for both types of composite specimens, primer and without primer case. (Fig. 4.6(a)). Due to small range of data little scattering was observed, although three specimens were used at each temperature level. But still only one type of concrete and PCM was used in this experimentation. The average values of all data, with primer and without primer at each temperature level was also calculated and showed in Fig. 4.6. The prediction values of average data of experimental results have very close resemblance with the predicted values, which verified the utility of eq. (12). It is clearly observed form Fig. 4.6(b) that interfacial shear strength decrease

with the increase in temperature. Most of the data lies within the range of ±10 % limit.

4.5. CONCLUSIONS

The experimental and analytical study was conducted on the composite specimens of Concrete-PCM. Interfacial strength, tension and shear, was observed at different temperature level. Roughness level was improved from the previous work and primer was also used at interface for the purpose of enhancing interfacial behavior. Following conclusions were extracted;

1) Overlay transition zone (OTZ) is the weakest zone in both types of composite specimens, which were tested in tension and shear. Observed failure was just separation of concrete and PCM in tension and shear, regardless of the temperature condition in which specimens were exposed.
2) Interfacial tensile strength was improved by improving properties of PCM and substrate roughness condition. Tensile strength of PCM contributes more for improvement of interfacial strength.
3) Significant degradation in strength of polymer cement mortar (PCM) were observed with the increase in temperature. Compressive strength, tensile strength and shear strength significantly reduced with temperature as compared to bulk concrete specimens.
4) At macro and meso scale, insignificant effect or primer was observed. Primer did not contribute to adhesion of PCM with concrete as compared to specimens which were prepared without primer
5) Prediction formula of interfacial tensile and shear strength were proposed and showed close agreement with the experimental results under all exposure conditions. Interfacial tensile strength of composite specimens that were observed in Ch. 3, were also verified by using current prediction formula for interfacial tensile strength.

REFERENCES

[1] Espeche AD, León J. Estimation of bond strength envelopes for old-to-new concrete interfaces based on a cylinder splitting test. Construction and Building Materials. 2011;25(3):1222-35.

[2] Ohama Y. Handbook of polymer-modified concrete and mortars-properties and process technology. New Jersy: Noyes Publications; 1995.

[3] Ramli M, Tabassi AA, Hoe KW. Porosity, pore structure and water absorption of polymer-modified mortars: An experimental study under different curing conditions. Composites Part B: Engineering. 2013;55:221-33.

[4] Teng JG, Yao J. Plate end debonding in FRP-plated RC beams—II: Strength model. Engineering Structures. 2007;29(10):2472-86.

[5] ACI 318-02 ; Building code requirements for structural concrete (318-02) and commentary (318R-02). USA: American Concrete Institute (ACI) 2002.

[6] International A. ASTM C-496. Standard Test Method for Splitting Tensile Strength of Cylindrical Concrete Specimens 2004.

[7] Rashid K, Ueda T, Zhang D, Miyaguchi K, Nakai H. Experimental and analytical investigations on the behavior of interface between concrete and polymer cement mortar under hygrothermal conditions. Construction and Building Materials. 2015;94:414-25.

[8] Rocco C, Guinea GV, Planas J, Elices M. Size effect and boundary conditions in the brazilian test: theoretical analysis. Mat Struct. 1999;32(6):437-44.

[9] Li G, Xie H, Xiong G. Transition zone studies of new-to-old concrete with different binders. Cement and Concrete Composites. 2001;23(4–5):381-7.

[10] Momayez A, Ehsani MR, Ramezanianpour AA, Rajaie H. Comparison of methods for evaluating bond strength between concrete substrate and repair materials. Cement and Concrete Research. 2005;35(4):748-57.

[11] Bazant PK, FM. Concrete at high temperature-Material properties and mathematical methods,: Harlow:longman; 1996.

[12] Biswas M, Kelsey, R. G. Failure model of polymer mortar. Journal of Engineering Mechanics. 1991;117:1088-104.

[13] Reis JMLd. Effect of temperature on the mechanical properties of polymer mortars. Materials Research. 2012;15(4):645-9.

[14] Zhang D, Ueda, T., Furuuchi, H., . Fracture mechanisms of polymer cement mortar: concrete interfaces. Journal of Engineering Mechanics. 2013;139:167-76.

Chapter 5

STRENGTH OF BEAMS STRENGTHENED WITH PCM OVERLAY AT ELEVATED TEMPERATURE

5.1 INTRODUCTION

Along with repairing, strengthening or up-gradation of RC structures is another task of current scenario. Both purposes can be achieved by overlaying. In this methodology, deteriorated part was removed and reinstated with the overlaying material. At member level, performance of structural elements like RC beams strengthened at tension face by PCM were investigated [1, 2]. Increases in performance level and also durability by protection of flexural reinforcement were observed. However ductility and ultimate deflection reduced with the increase in strengthening reinforcement [3]. Debonding failure modes are also one of the commonly reported failure modes for overlay strengthened beams [1, 2, 4, 5]. Various models were presented in literature used to predict debonding in flexural zone, shear zone and flexural shear zone. All types of debonding mode were investigated analytically and experimentally [1, 2, 6, 7]. Some model also based on interfacial stresses between concrete and steel plate/FRP and peeling stress observed was the function of both normal and shear stress [8].

Growth in construction industry is considered as an indicator of the growth or development of country. Rapid growth in construction of infrastructure and skyscraper is observed in various regions and especially in Gulf States from last two decades. All RC structures have to expose daily high fluctuation of temperature, which may rise up to 60 ℃ in peak summer. Such temperature variation was also observed in some part of North America. In some regions of Subcontinent, temperature rises annually due to rapid industrialization, increases traffic load and non-sustainable development and may reach 60 ℃ after few years [9, 10]. Such hot climate may accelerate the deterioration of RC structures [9, 11]. Compatibility and durability of repaired materials and repaired structures must be checked under such exposure conditions. It must be ensured that repaired structure would maintain the required performance over intended service life, both at material level and member level.

High temperature affects the bond strength of steel to concrete in RC beams and bond failure of rebar lap splices was observed by Khan [12]. Temperature influences the interfacial strength both at bonding of material and bonding of member. Degradation in the interfacial strength at material level may cause debonding of overlay at high temperature that was one of the objective of this current work. Temperature may influence the behavior of overlay strengthened beams significantly due to sensitivity of PCM with temperature.

With such background, detailed experiments were designed to evaluate the behavior of RC beam and strengthened RC beams under exposure condition of 20 ℃, 40 ℃ and 60 ℃. Selected temperature range may cover most of regions in the world during summer, which have abundant

RC structures. Outcomes of this study will help to establish guidelines for designing of repair of RC structure in that specific region. In experimentation, large number of beams were casted and then strengthened by adding various amount of reinforcement at soffit of beams and covered by spraying with PCM. The performance of strengthened beams were compared with performance of unstrengthened RC beams as well as with the performance of strengthened beams at 40 ℃ and 60 ℃ temperature under different heads, viz. Failure modes, load deflection relationship, first crack and failure load. Along with experimentation, analytical work were also conducted to verify experimental observations and for applicability in practical design. Truss analogy approach were used for strengthened beams and ultimate shear load and failure modes were predicted and well matched with experimental observation at all temperature levels.

5.2 EXPERIMENTAL METHODOLOGY

5.2.1 Materials

Current experimental work was designed along with the experimentation at material level testing (Chapter 4). So, concrete, PCM and primer have similar properties and reported in detail in Chapter 4 (Table 4.1 and 4.2). Steel rebar were used as reinforcement, two types of bars were used, plane bars and deformed bars. Deformed bars have a diameter of 10 mm while the diameter of plane bar was 6 mm. plane bars were used as longitudinal as well as shear reinforcement. Properties of both types of rebars are presented in Table 5.1.

Table 5.1 Properties of reinforcement.

Diameter (mm)	Area of rebar (mm^2)	Yield Strength "f_y" (MPa)	Ultimate Strength "f_u" (MPa)	Elongation (%)	Modulus of Elasticity "E_s" (GPa)
10	70.75	470	614	25	203
6	28.05	430	617	35	200

5.2.2 Specimen Prepration

For testing of structural member reinforced concrete beams were prepared. Wooden mold of size of 200 x 150 x 1800 mm were prepared. Some amount of retarder were mixed with water and spread inside bottom of molds before placing of steel and concrete (Fig. 5.1(a)). Steel cage of 2 rebar at top and 2 rebar at bottom of size 10 mm diameter was put in mold size of 200 x 150 x 1800 mm and spacing from bottom was maintained by providing two spacers of height of 25 mm. Ready mixed concrete was placed in molds and covered with polythene sheet to avoid evaporation of moisture (Fig. 5.1(b)). Roughness at bottom surface of beam was achieved by removing bottom plank of mold and rubbed strongly with steel wire brush, until the aggregate was exposed. And then cement paste and mortar particle were removed by strong jet of water. After 72 hours of casting all molds removed and RC beams were cured for two weeks in moist condition.

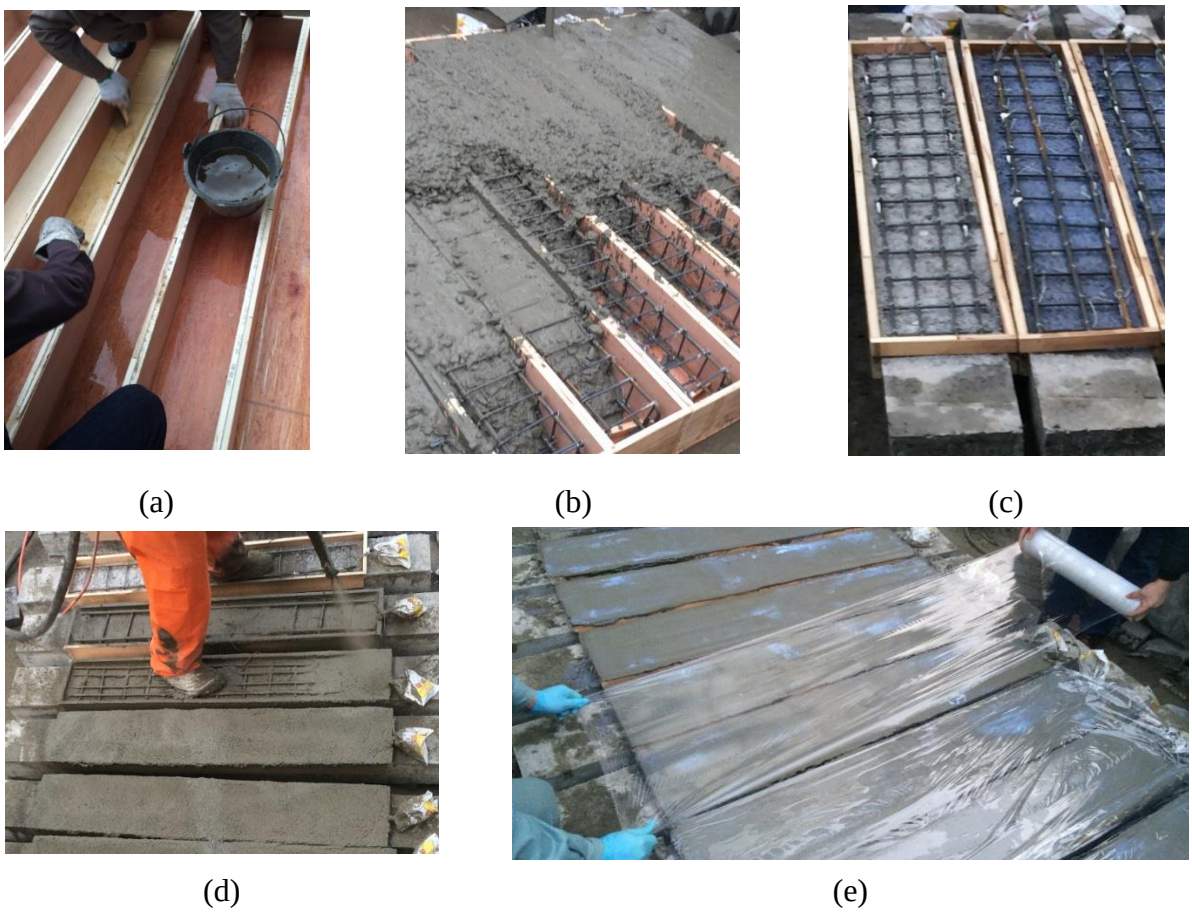

Fig. 5.1 Preparation of specimens for member level testing; (a) wooden molds with retarder at bottom (b) placing of steel and concrete (c) rough surface with mold and reinforcement for overlay and also with and without primer (d) spraying of PCM (e) spraying of primer and wrapping with polythene sheet.

Rough surface was exposed and mold of 200 x 25 x 1280 mm were placed over rough surface of RC beam. Primer were sprayed on treated surface of RC beam and after 3 hours curing of primer steel reinforcement, thermocouple was placed and PCM was sprayed over it (Fig. 5.1 (c) and (d)). Primer was again sprayed on top of PCM layer to avoid evaporation of moisture and wrap tightly with polythene sheets (Fig. 5.1 (e)). Detailed methodology for preparation of specimens for member level testing is presented in Fig. 5. PCM were cured for 7 days in dry condition and 21 day wet condition.

5.2.2 Exposure Conditions & Testing Procedures

In this extended experimentation various temperature levels were selected to cover the maximum range of the regions of the world. Exposure condition and testing conditions was maintained at 20 ℃, 40 ℃ and 60 ℃ temperature while relative humidity was maintained at 60%. All specimens were exposed to design temperature level and relative humidity for 16 hours to 20 hours then tested under condition similar to the exposure condition.

All beams were tested in four point bending test over the span of 1380 mm. The position of the loading points were set as to maintain shear span of 460 mm. Support was set at distance of

210 mm from ends of RC beam. The distance of support to the overlay end was 50 mm. All other dimensions are indicated in Fig. 5.2(a). Middle span deflection was also measured during loading by using four linear variable displacement transducers (LVDTs). Two of them were aligned with supports and remaining two were placed at center of beam. All LVDTs and load cell were attached to the data logger which is connected to computer to record all values. Thermocouple which was implanted at the interface during PCM casting, was attached to the temperature measuring device and temperature was continuously noticed during exposure time and at testing time. Front side of all beams were white washed and grid of spacing 50 mm was also drawn on constant moment zone and one shear span. Summary of all beam specimens which was referred as member level testing is presented in Table 5.2. Cross sectional area of strengthened beams is presented in Fig. 5.2(b).

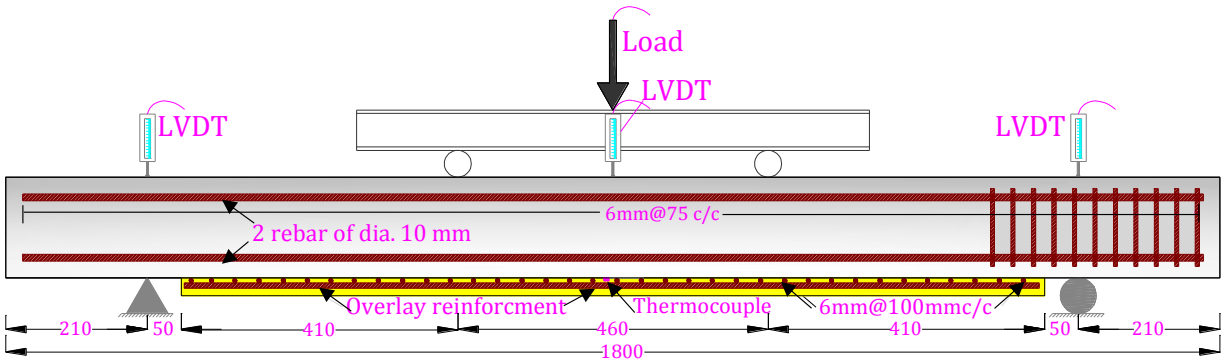

(a) Testing arrangement of four-point loading test

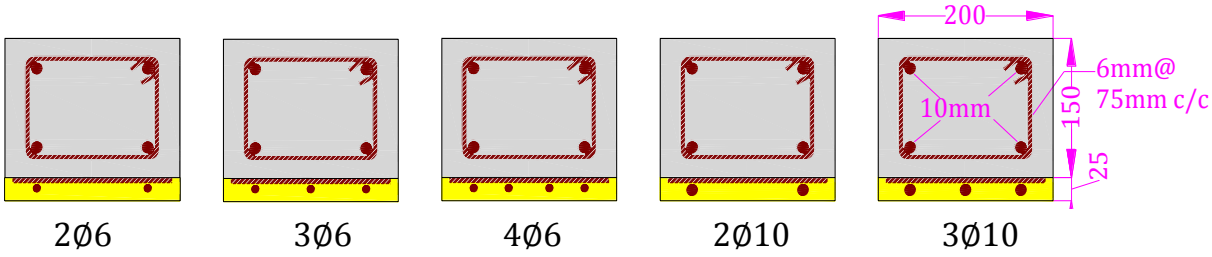

(b) cross sectional area of strengthened beams with different reinforcement in overlay

Fig. 5.2 Detail of overlay strengthened beams with loading set-up (unit: mm)

RC beam in subsequent sections is presented by two notations. First one is presented by "Con", which means control and second shows temperature of exposure and testing condition. e.g. "Con-40" means RC beam without overlay exposed and tested at 40 ℃ temperature. Overlay strengthened beam is presented by three notations. First notation shows number and diameter of rebar in overlay, second notation shows temperature of exposure and testing condition and last part shows the primer applied at interface between concrete and PCM or not. Presence of primer presented by "WP" and beams without primer abbreviated as "NP". e.g. 3Ø6-40-WP means overlay strengthened beam reinforced with three rebar of 6 mm diameter in overlay part and exposed and tested at 40 ℃. Primer was also applied at interface between PCM and concrete.

Table 5.2 Summary of specimens and testing conditions at memberlevel testing.

Specimen	$(n)_{OL}$	Diameter (mm)	$(A_s)_{OL}$ $(mm)^2$	Testing and Exposure Temperature					
				20 ℃		40 ℃		60 ℃	
				WP	NP	WP	NP	WP	NP
Overlay Beams	2	6	56.10	1	1	1	1	1	1
	3	6	84.15	1	1	1	1	1	1
	4	6	112.20	1	1	1	1	1	---
	2	10	141.50	1	1	1	1	1	1
	3	10	212.25	---	1	---	---	---	1
RC Beam	---	---	----	1		1		1	

$(n)_{OL}$ = number of rebar in overlay; $(A_s)_{OL}$ =Area of steel in overlay; WP = With Primer; NP = No Primer

5.3. RESULTS & DISCUSSION

5.3.1 Load Carrying Capacity

Debonding is the most common failure mode in the strengthened beams. Debonding occurs before the designed flexural strength of retrofitted/repaired beams. And influence of temperature on failure modes and failure load is still unexplored and detailed discussion is provided in the following subsections.

Failure modes and failure loads

In overlaying, the most common failure is the debonding failure before the flexural capacity is achieved, which is preferably prevented due to its brittleness. Conventional failure modes viz., flexural failure, shear failure, flexural shear failure and debonding failure are presented in Fig. 5.3. At 20 ℃ temperature, the failure mode of strengthened beams up to reinforcement area of 112.20 mm^2 (4Ø6), was flexural failure like in the control specimen. Beams with and without primer show similar failure modes. Strengthened beams "2Ø10" (141.50 mm^2) with and without primer show flexural-shear failure and the beams "3Ø10" (212.25 mm^2) show shear failure. No debonding was observed at 20 ℃ temperature, so strengthened member can be designed by conventional methods for RC members. Current results were compared with the results of Satoh and Kodama [5]. In their work, PCM strengthened beams were tested at different shear span in four point bending test. Although there are some variation in loading span and properties of steel, concrete and PCM, results were compared with similar shear span and similar amount of reinforcement in RC and overlay part. Current results have similarity with the work of the Satoh and Kodama up to 112.20 mm^2 area of reinforcement in overlay part. While debonding was observed in 2Ø10 and 3Ø10 beams in the study by Satoh and Kodama [5] that was not observed in this work due to following reason; Tension face of RC beam was treated to high roughness value whereas in Satoh and Kodama work, specimens were prepared by disk sander which gives rather smooth surface and results in lower bond strength. It may be concluded that the roughness or bond strength highly

influences the failure modes and must be considered in design guidelines of repairing structures.

Table 5.3 Failure modes of all beams at different temperature level.

Specimens	Notation	Failure modes								
		20 ℃			40 ℃			60 ℃		
		Exp.		Ana.	Exp.		Ana.	Exp.		Ana.
		WP	NP		WP	NP		WP	NP	
Overlay Beams	2Ø6	F	F	F	F	F	F	F	F	F
	3Ø6	F	F	F	F	F	F	F	F	F
	4Ø6	F	F	F	F	F	F	F	---	F
	2Ø10	F+S	F+S	F	DB	DB	DB	DB	DB	DB
	3Ø10	---	S	DB	---	---	DB	---	S	DB
RC Beam	Con.	F		F	F		F	F		F

F=flexural failure; S = Shear Failure; F+S = Flexural + Shear Failure;DB= Debonding Failure; Exp. = experimental; Ana. = analytical

(a) Flexural Failure

(b) Flexural + Shear Failure

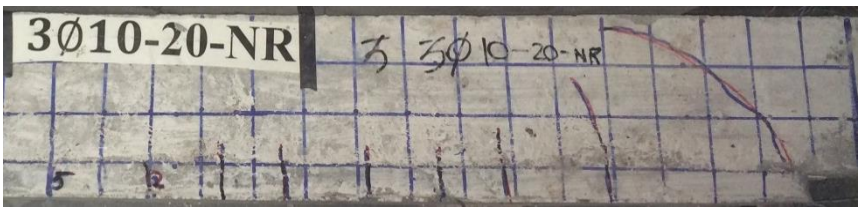

(c) Shear Failure

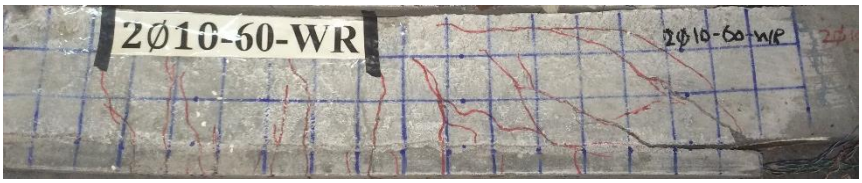

(d) Debonding Failure

Fig. 5.3 Observed failure modes of strengthened beams

The observed failure mode is presented in Table 5.3 for each beam and graphically presented in Fig. 5.3. Up to 4Ø6, the failure mode observed was flexural failure, similar to the failure modes of beam tested at 20 ℃. Debonding failure was observed in strengthened beams of 2Ø10 at 40℃ and 60℃. Debonding failure has been categorized in several types, and failure mode observed here was the overlaying delamination failure [1, 2, 5-8]. Debonding strength highly depends upon the interfacial normal and shear strength and crack distributions. Crack first initiated in tension zone of the constant moment zone and then propagated toward compression zone with further loading. Cracks also appear in flexural-shear zone and propagated in inclined direction. And this crack widened with further increase in load and propagated towards interface between concrete and PCM and finally resulted in separation of concrete and PCM at overlay end (Fig. 5.3(d)). This type of debonding mechanism was explained in detailed by other researchers [6-8].

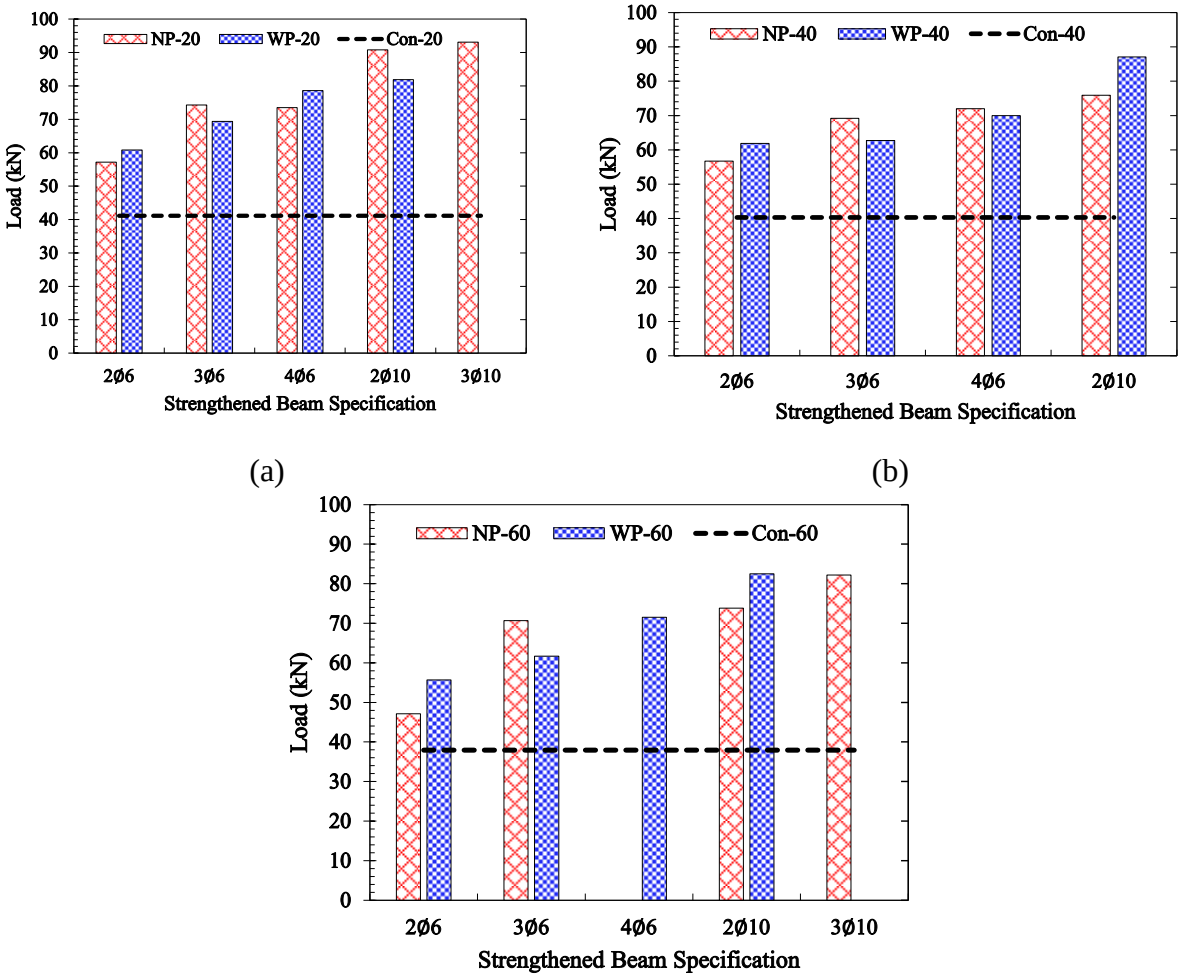

Fig. 5.4 Failure load of all beams at (a) 20 ℃, (b) 40 ℃ and (c) 60 ℃.

Fig. 5.4 presents the failure load of all beams including control and strengthened beams. It is clearly shown that the failure load of strengthened beams is more than the failure load of control specimens. Failure load increases with the increase in area of reinforcement of strengthening bars if flexure failure governs. At 20℃ temperature (Fig. 5.4(a)), the load carrying capacity was

increased by more than 100% from the control specimen if there were sufficient tension reinforcements in the overlay, e.g. 2Ø10 and 3Ø10. The confirmation of enhancing load carrying capacity was one of primary goals of this work. Fig. 5.4(b) and 5.4(c) presents the failure load of control and strengthened beams at 40℃ and 60℃, respectively. Slight degradation in the failure load was observed with the increase in temperature, as compared to respective specimen at 20 ℃. This point is explained in detail in subsequent section. The failure loads are still more than those of the control specimens at all temperature conditions. Load carrying capacity was improved by more than 100% from the control specimens.

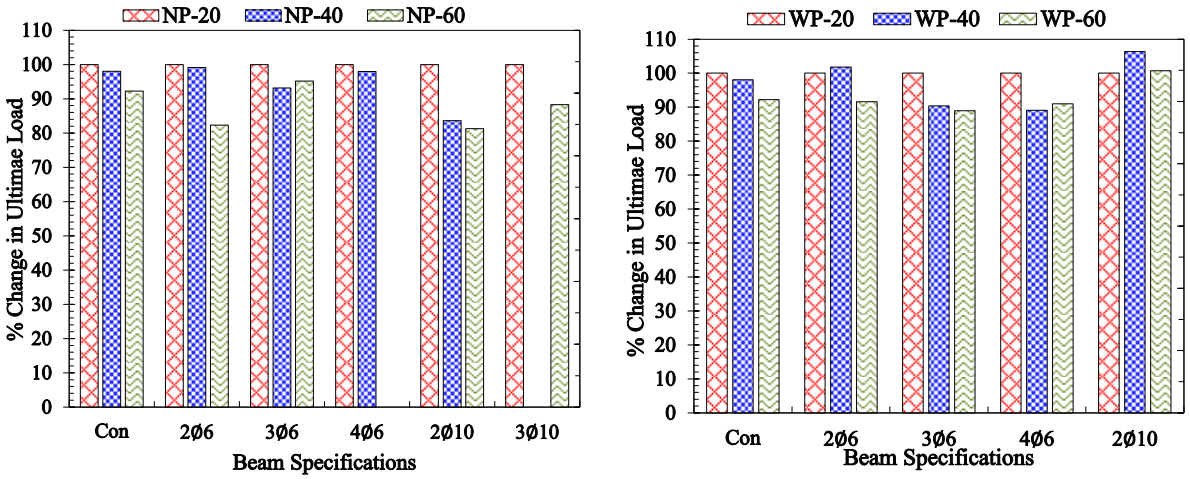

(a) No-Primer at concrete-PCM interface (b) With primer at concrete-PCM interface

Fig. 5.5 Effect of temperature on ultimate load of control and strengthened beams

Influence of temperature

Influence of temperature is evaluated by normalizing the ultimate load of all beams by that of the corresponding beams tested at 20 ℃ and presented in Fig. 5.5. For control specimens, without overlay, 8% reduction in failure load was observed at 60 ℃. And similar behavior was also observed in the strengthened beams. Most of the reduction was within 10% of specimen failure loads tested at 20 ℃, for both cases with and without primer. Bonding is the physical interaction of both materials as far as the stress and strain transferred is concerned. But both materials behave differently at high temperature and may result in loss in physical bonding. This mechanism was explained experimentally by Khan [12]. For strengthened beams, reduction in failure load was observed with the increase in temperature and may be due to following reasons; (1) Degradation in the properties of concrete and PCM with the increase in temperature [11]. (2) Degradation in the interfacial shear and normal strength.(3) Slippage of rebar in the RC beam and rebar in overlay [12]. (4) Reduction in bond strength between concrete and reinforcement at high temperature [13]. Bazant and Kaplan summaries the work of many researcher and reported that reduction in bond strength is more as compared to the compressive and tensile strength of concrete at elevated temperature [14]. In Fig. 5.5 reduction of about 10% was observed at high temperature as compared to the respective specimens at 20 ℃. While in Fig. 5.5(a), significant reduction was observed in

the 2Ø10 beam at 60 ℃. High reduction was due to premature debonding failure before achieving the full flexural capacity. Whereas, improvement in failure load was observed at high temperature of 2Ø10 beam with primer case (Fig. 5.5(b)). This may be due to experimental error in the testing of the beam at 20 ℃ temperature, and large variation in failure load is also observed from the beam tested without primer case.

5.3.2 Load Deflection Relationships

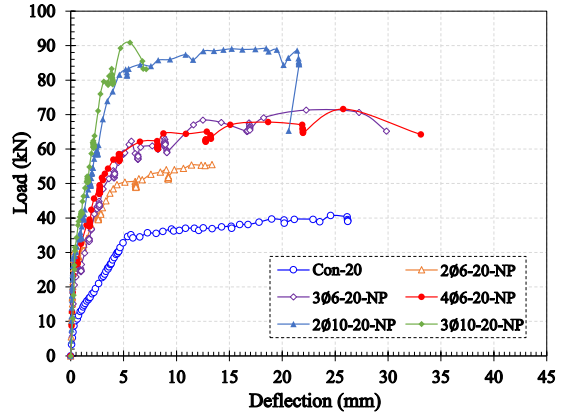

(a) At 20℃ with No-Primer

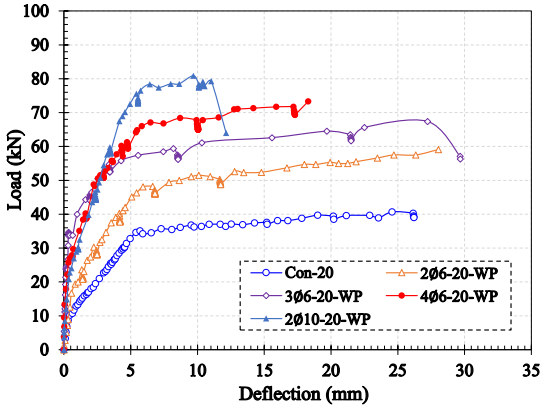

(b) At 20℃ with Primer

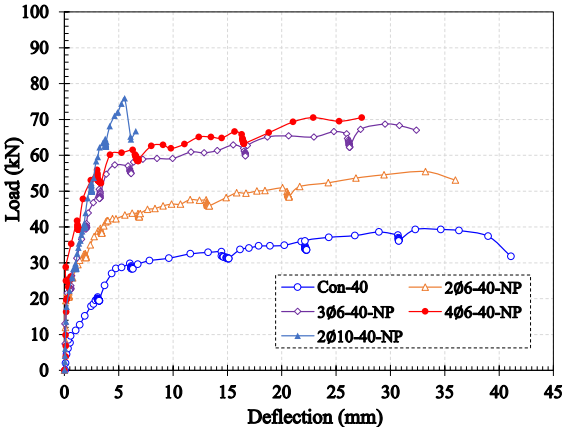

(c) At 40℃ with No-Primer

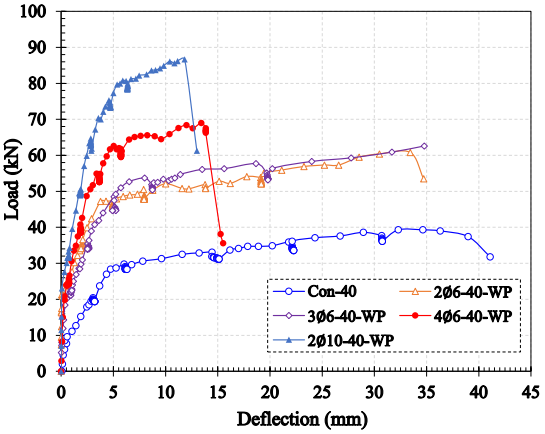

(d) At 40℃ with Primer

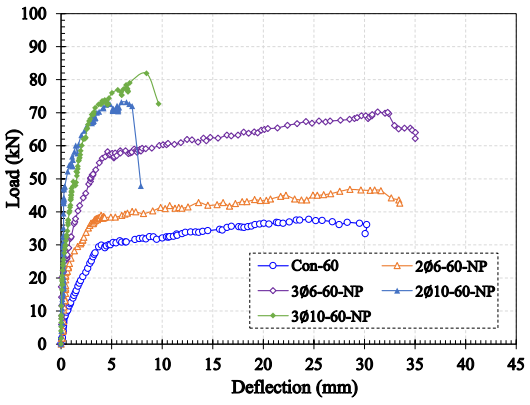

(e) At 60℃ with No-Primer

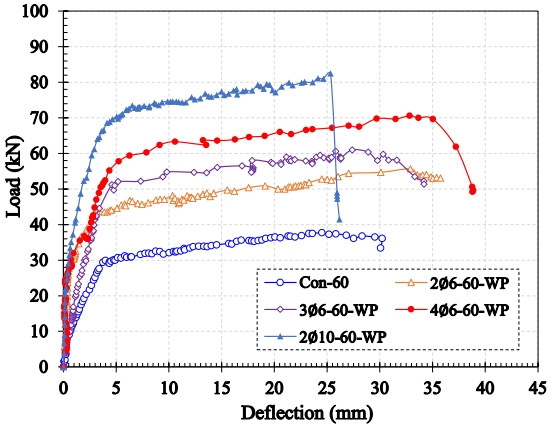

(f) At 60℃ with Primer

Fig. 5.6 Load deflection relationships under various temperature level of RC and RC strengthened beams.

Fig. 5.6 shows the load deflection relationships of all strengthened and unstrengthened beams at various temperature levels. No significant differences were observed between primer and no-primer beams. But some differences were observed at different temperature levels. Control specimen shows ductile behavior at 20, 40 and 60 ℃temperature. Ductility level decreased with increase in strengthening reinforcement area. Stiffness of all strengthened beams was observed more than unstrengthened beam and was observed directly proportional to strengthening reinforcement area. Similar trend was also observed in other studies, in which beams were strengthened by various repairing material at 20 ℃ temperature level [3, 5, 15]. In Fig. 5.6(a) & (b), beams of "2Ø10" specification show very less ductility and the failure observed was Flexure + Shear (Table 5.3). Whereas, brittle and shear failure was observed for beam of "3Ø10". In Fig. 5.6, strengthened beams of reinforcement area up to 112.20 mm^2 (4Ø6) showed ductile behavior at all temperature levels. Failure mode observed was flexural failure, similar to the control specimens. Fig. 5.6(c) and (d) shows the load-deflection relationships at 40 ℃. Some difference in terms of ductility, first crack load, yield load and ultimate load was observed. Strengthened beams up to the reinforcement area of 112.20 mm^2, flexural mode of failure was observed as similar to specimen tested at 20 ℃. But for beam specification of 2Ø10 shows sudden drop after yield load and failure mode also shifted from flexural + shear to debonding failure. Fig. 5.6(d) and (f) shows the load-deflection relationships of strengthened and unstrengthened beams at 60 ℃. Further reduction in first crack load and ultimate load was observed as compared to specimens tested at 20 ℃ and 40 ℃.

Debonding mode of failure was observed for 2Ø10 beams as similar to beams tested at 40 ℃ but different for beams tested at 20 ºC. Less deflection was due to delamination of overlay (Table 5.3), which was observed just at yielding of the flexural reinforcement, causing the brittle behavior. Beams of "3Ø10" show less deflection among all beams, and failure mode observed was the shear failure. Initial stiffness of all strengthened beams remains unchanged until onset of cracking. Load at crack initiation and ultimate load, are noticed from the load deflection curves and the detail is presented in the subsequent section.

5.3.3 First Crack Load and Ultimate Load

In this section, performance of strengthened beams are discussed under two heads viz., first crack load and ultimate load. The load at first crack signifies the start of flexural cracking and provides the information to evaluate initial stiffness. Whereas ultimate load describes the capacity of a structural member along with failure behavior.

Fig. 5.7 presents percentage increase in the first crack load of strengthened beams from control beam, at different temperature levels. First crack load increased with the increase in the reinforcement at tension face of beam. It was also observed by load-deflection curves (Fig. 5.6) that initial stiffness increases with the increase in reinforcement area. First crack load was increased up to 250% of beam with three rebar of 10 mm diameter in overlaying part, at 20 ℃(Fig. 5.7). First crack load increased more than 150%, even by using only 2 rebar of diameter 6 mm in overlaying part, at control condition (20 ℃), for both sets of beams, with and without primer, average was

taken and presented in Fig. 5.7 and error bar presents standard deviation between two types of beams. Large variation in standard deviation was observed in some cases which was only due to initial loading speed because it was controlled manually. Fig. 5.7 clearly shows that the performance of beam have increased by strengthening. Temperature affected the crack initiation load in such a way that reduction was observed with the increase in temperature. In all strengthened beams, significant reduction was observed in crack initiation load. And all cracks initiated from the bottom of PCM or extreme tensile surface of overlay. In past studies crack initiate at concrete side and propagated towards PCM and also towards compression zone [16]. The reduction in first crack load may be due to the significant reduction in the tensile strength of PCM at elevated temperature. The reduction in load may be also due to slippage of reinforcement bars in concrete as well as in PCM [12].

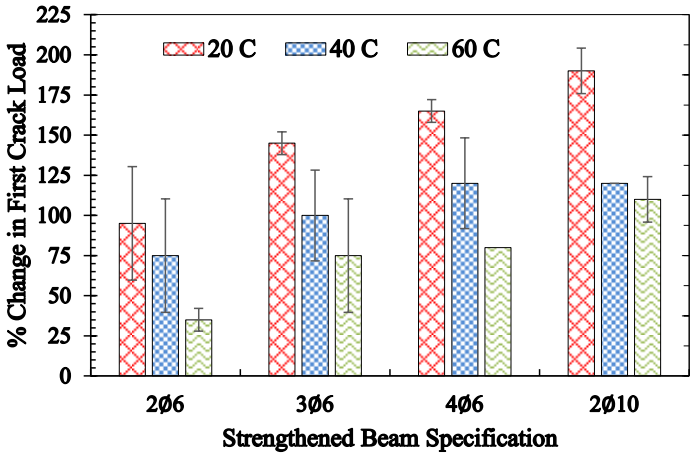

Fig. 5.7 Change in first crack load as compared to virgin RC beam at different temperature level.

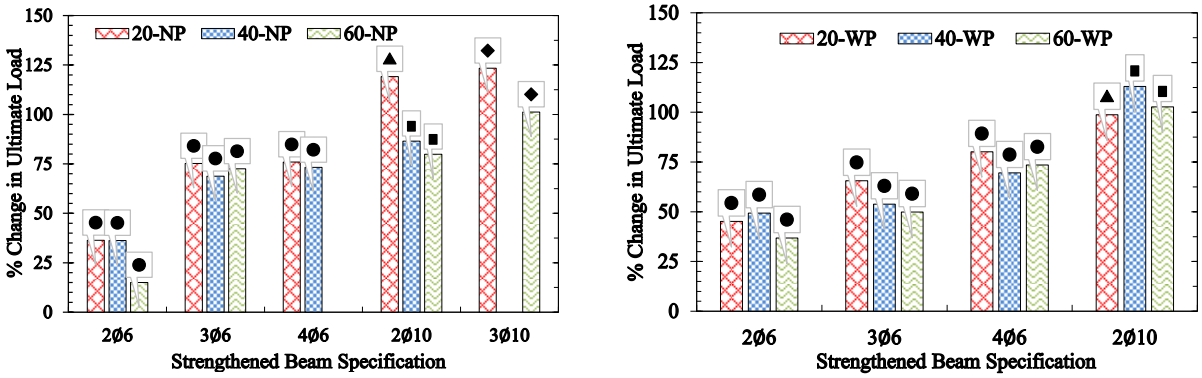

(a) with No-Primer (b) with Primer

● = Flexural failure; ◆ = Shear failure; ▲ = Flexural+Shear failure; ■ = Debonding failure

Fig. 5.8 Change in ultimate load as compared to virgin RC beam at different temperature level.

Fig. 5.8 shows percentage increase in ultimate load from control specimen (without overlay), which was tested at 20 ℃ along with the failure modes. Ultimate load of all strengthened beams, with and without primer, were observed to be greater than the ultimate load of control specimen. Ultimate load increased with the increase in strengthening reinforcement in overlay part. Increase

in ultimate load observed was more than 100 % from control specimen. At elevated temperature, 40 ℃ and 60 ℃, reduction in ultimate load was observed as compared to the corresponding beams tested at 20 ℃. The mechanism of reduction in ultimate load is assumed to be due to slippage of reinforcement in RC part and overlay part. Experimental verification of slippage of reinforcement with temperature is reported by Khan [12]. Significant reduction in ultimate load was observed of beam of "2ø10" without primer at 40 ℃ and 60℃, as compared to 20 ℃ temperature (Fig. 5.8(a)). The significant reduction observed was due to debonding failure at high temperatures. Whereas opposite behavior was observed for the beam with primer case (Fig. 5.8(b)). This was probably due to experimental error which is mentioned in previous section.

5.4 PROPOSED MODEL: TRUSS ANALOGY APPROACH

Proposed model is based on truss analogy approach which was proposed by conventional RC beam [17]. Same model was modified and used for plated RC beams [18, 19] and debonding was also predicted by using such model. Truss model also have several other advantages e.g.; Elastoplastic behavior of materials were incorporated instead of linear-elastic model. Load transfer by bond was incorporated in modified version, which was used for plated beams. Free body diagram of truss analogy approach is presented in Fig. 5.9, top chord presents compression concrete and bottom chord presents tensile reinforcement in RC beam and overlay part. Web elements were presented by diagonal concrete struts and transverse steel stirrups. Following assumptions were made;

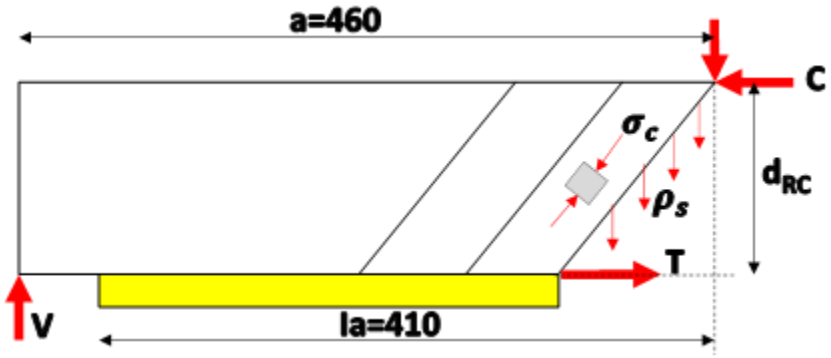

Fig. 5.9 Free-Body diagram for Truss model concept.

1. Perfectly plastic behavior of materials was assumed. Concrete crushing strength was modified by multiplying with effectiveness factor "v" and it can be measured by using simple and well known empirical formula (eq. (1)) [17]. And mostly effectiveness factor was assumed to be 0.7 and same value was used in this work.

$$v = 0.8 - \frac{f_c'}{200} \qquad (1)$$

Where;

v = effectiveness factor ; f_c'= cylindrical compressive strength

2. Beam shear reinforcement was provided by stirrups and force per unit length and can be shown by $\rho_s = A_t f_{ty}/s$; where "A_t" is the area of stirrup, "f_{ty}" is yield strength of stirrups and"s" is spacing between stirrups.

3. Perfect bond between concrete and overlay (PCM) was assumed. And the bonding force "*U*" is assumed to represent the plane stress flow at concrete-PCM interface. Uniform distribution of bonding force is assumed at ultimate stage.

4. The diagonal compressive zone is assumed to be zero near supports and loading points (Stress-free regions). Web of concrete is under uni-axial compression, being the compressive stress σ_c is inclined to an angle θ to the longitudinal axis of beam.

The detailed derivations for the predictions of load with respect to the failure mode is presented in literature [17-19]. Here only summary of equations was provided and all equation by truss model was converted to non-dimensional form by introducing some parameters and presented in eq. (2). Some of notations were explained in Fig. 5.9 and rest of notations was explained with equations.

$$\tau = \frac{V}{bd};\ \psi = \frac{p_y}{bf_c};\eta = \frac{T_y}{bdf_c} \tag{2}$$

Where; $T_y = \left(A_s f_y\right)_{OL} + \left(A_s f_y\right)_{RC}$

Shear Failure Mode. Eq. (3) to Eq. (5) is taken from literature which presents the failure load, when beam was failed in crushing of concrete web and/or yielding of stirrups. Eq. (3) was obtained from the truss model approach [18, 19].

$$\frac{\tau}{f_c} = \frac{1}{2}\left[\sqrt{1+\alpha^2} - \alpha\right] + \psi\alpha,\ \text{for } 0 \le \psi \le \psi_0 = \frac{\sqrt{1+\alpha^2}-\alpha}{2\sqrt{1+\alpha^2}} \tag{3a}$$

$$\frac{\tau}{f_c} = \sqrt{\psi(1-\psi)}\ \text{ for }\ \psi_0 \le \psi \le 0.5 \tag{3b}$$

$$\frac{\tau}{f_c} = \frac{1}{2}\ \text{for}\ \psi > 0.5 \tag{3c}$$

where; $\alpha = a/d_{OL}$ and ψ is taken from eq. (2).

Shear + Flexure Failure. Failure load corresponding to Shear and flexural failure was also obtained by truss model for convention RC beam and also valid for overlay strengthened RC beams as well. Eq. (4) used for getting failure load under failure mode of Shear + Flexural mode [18, 19].

$$\frac{\tau}{f_c} = \psi\left[\sqrt{\frac{2\eta}{\psi} + \alpha^2} - \alpha\right] \tag{4}$$

Flexure Failure. Overlay strengthen beam was designed in similar way as conventional RC beam as far as mode of failure is flexure, so Eq. (5) is applicable for the failure load of beams, which were failed in flexure [1, 19]. Effect of temperature was observed on ultimate load of control and strengthen beams (Section 5.3.1). It is fundamental assumption for designing of conventional RC beam that cross section is plane before loading remains plane under load. This assumption was under control condition of 20 ℃, but at higher temperature, the assumption of plane section and of a perfect steel-concrete bond may not be applicable. By using experimental values of all data and by simple regression analysis ultimate moment at any temperature can be obtained by using Eq. (6).

$$\frac{\tau}{f_c} = \frac{M_{uT}}{abdf_c} \tag{5}$$

$$\frac{M_{uT}}{M_{20}} = 1.04\exp(-0.0025T) \tag{6}$$

Where;

M_{uT}= Ultimate moment at concerned temperature from 20 to 60 ℃; M_{20} =Ultimate moment at 20 ℃; T= 20 to 60℃

Debonding Failure. Prediction of failure load corresponding to debonding mode of failure have the key importance, while designing repairing/retrofitting of RC beams. From a kinematic point of view, failure associated with the slippage of concrete-PCM interface in shear span, together with the diagonal crack. Bond stress resultant along the concrete-PCM interface reaches ultimate bond strength "U_y". Details about the calculation of U_y is presented in next section 5.4.1. Finally, debonding failure load can be calculated by using Eq. (7) [18, 19].

$$\frac{\tau_u}{f_c} = \psi[\phi + \alpha - \sqrt{(\phi + \alpha)^2 - 2\phi\beta}, \ \psi > 0 \tag{7}$$

where;

$\phi = \frac{U_y}{p_y} =$ Debonding strength to stirrup strength; $\beta = \frac{I_a}{d_{OL}}$ =Overlay shear span to overlay depth ratio

5.4.1 Limiting bond strength

Debonding strength was predicted according to the failure pattern of debonding. Strut and tie model was used by Clotti *et al.* and bond strength was predicted for plated RC beam [19]. For overlay strengthened RC beam concrete tooth model has been used by Zhang *et al*. and predicts the ultimate bond strength for the failure mode of concrete cover separation [1]. Vast range of debonding strength models are available in literature, which are based on shear capacity and were reviewed and summarized by Smith and Teng [8]. In which, Jansze proposed a model and modified

shear span to predict ultimate shear load. Modified shear span was also used by Ahmed's model [8,19]. Modified shear span (B_{mod}) is also used in this work and interfacial shear strength (τ_{iss}) was obtained by using Eq. (12) (Section 4.4.2). Eq. (8) presents the debonding strength from the overlay end. Modified shear span "B_{mod}" is obtained by using Eq. (9). Some terms, used in this equation are explained in Fig. 15.

$$U_{y1} = \tau_{iss} B_{mod} \tag{8}$$

$$B_{mod} = \sqrt[4]{\frac{\left(1-\sqrt{\rho_s}\right)^2}{\rho_s} d_{RC}(\mathrm{a}-\mathrm{I_a})^3} \tag{9}$$

where;

d_{RC} =Effective depth of RC beam = 120 mm; $\rho_s = \frac{A_s}{b.d_{RC}}$;

5.4.2 Validation of model

To verify the model presented in previous section (5.4.1), comparison were made between experimental and analytical shear strengths of overlay strengthened RC beams. For shear failure, eq. (3) were used to predict the ultimate shear load and presented in Table 5.4 under head of "S". Ultimate shear load of RC strengthened beams was obtained by using eq. (4) and eq. (5), corresponding to the failure mode of Flexure + Shear and flexural, respectively, and presented in Table 5.4, under head of "F+S" and "F", respectively. Finally, debonding strength was predicted by using eq. (7). Final shear load of RC beam strengthened beam was obtained by minimum of four strength presented in column 2 to column 5 of Table 5.4 and presented in column 6 and narrated as "V_{mod}". The obtained shear load and failure modes compared with the experimental observations for reliability of model. Average of both, with primer and without primer was taken to present the average experimental shear load and presented in Table 5.4 under the head of "V_{exp}". The variation in load of V_{exp}/V_{mod} is form 0.93 to 1.26, but average is 1.024 with the coefficient of variation of 8.53%. Graphically comparison between experimental shear load and model shear load also made and presented in Fig. 5.9. Comparison was also made with different temperature level and check the reliability of the predicted values with the experimental data (Fig. 5.10). All values lies within ±10% of the experimental values and verifies the utility of temperature at high temperature up to level of 60 ℃. Reduction in shear load was observed with the increase in temperature. Failure mode was also predicted by using proposed model and compared with observed failure modes in tabular form in Table 5.3 and Table 5.4. Close resemblance was observed with the experimental observation. Flexure failure and debonding failure were predicted well, however, shear failure in the case of 3Ø10-20 was not predicted by the model, having large difference in ultimate shear load between the experimental and predicted. Large difference was also observed in other works [18,19], where shear span and yielding of stirrups influence significantly on the ultimate shear strength. More than 100% variation was observed in ultimate shear load under the head of shear failure.

Table 5.4. Ultimate shear load and failure modes by Truss model approach.

Specimen	V (kN)				V_{mod}	V_{exp}	V_{exp}/V_{mod}	Failure	
	S	F+S	F	DB				Ana	Exp.
2Ø6-20	147.60	34.37	28.74	49.32	28.74	28.65	1.00	F	F
3Ø6-20	147.60	37.66	35.17	48.33	35.17	34.68	0.99	F	F
4Ø6-20	147.60	40.90	38.73	47.45	38.73	36.22	0.94	F	F
2Ø10-20	147.60	46.46	44.91	47.06	44.91	42.52	0.95	F	F+S
3Ø10-20	147.60	54.94	59.11	45.35	45.35	45.45	1.00	DB	S
2Ø6-40	149.82	34.37	27.04	43.80	27.04	29.05	1.00	F	F
3Ø6-40	149.82	37.66	33.09	42.81	33.09	32.88	0.99	F	F
4Ø6-40	149.82	40.90	36.45	41.94	36.45	34.88	0.94	F	F
2Ø10-40	151.70	46.46	42.26	41.54	41.54	40.65	0.95	DB	DB
3Ø10-40	151.70	54.94	55.62	39.87	39.87	-----	-----	DB	-----
2Ø6-60	156.40	34.37	25.72	36.09	25.72	25.62	1.00	F	F
3Ø6-60	156.40	37.66	31.48	35.17	31.48	32.8	1.04	F	F
4Ø6-60	156.40	40.90	34.67	34.36	34.36	35.30	1.03	DB	F
2Ø10-60	156.40	46.46	40.20	33.98	33.98	35.95	1.15	DB	DB
3Ø10-60	156.40	54.94	52.91	32.44	32.44	35.95	1.26	DB	DB
						V_{exp}/V_{mod}	1.02		

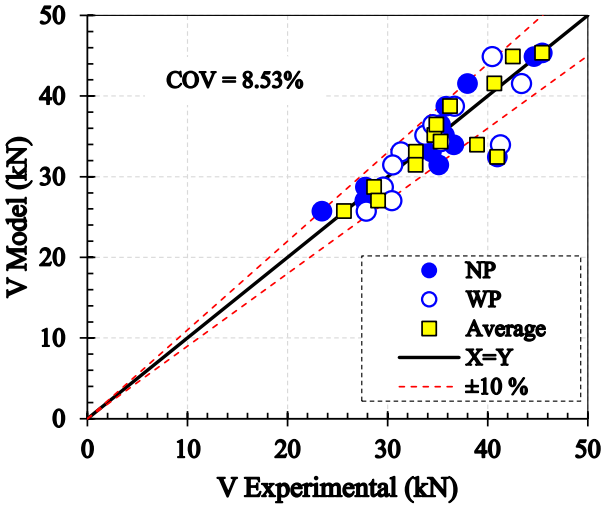

Fig. 5.10 Experimental and predicted ultimate shear load of overlay strengthened beams.

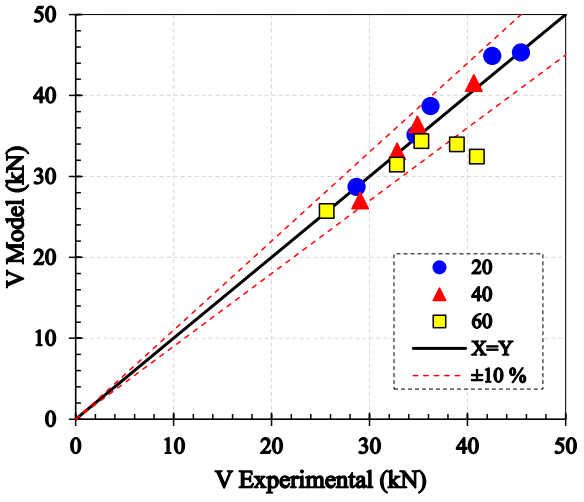

Fig. 5.11. Experimental and predicted ultimate shear load of overlay strengthened beams at different temperature level.

5.5 CONCLUSIONS

In the present study, influence of temperature was investigated for material bonding and member bonding. Selected temperature ranges have close resemblance with the real environmental condition and cover most of the regions having abundant RC structures. Three sets of beams were

prepared and tested in four points bending at 20 ℃, 40 ℃ and 60 ℃ temperatures. In each set of beam, one unstrengthened RC beam and 10 strengthened (5 with primer case and five without primer) beams were investigated and several conclusions can be drawn out as follows:

1) Ultimate load was increased with the increase in strengthening reinforcement area and failure load of all strengthened beams were observed higher than unstrengthened beams at all temperature levels. Reduction in failure load was observed at high temperatures as compared to specimen which were tested at 20 ℃.
2) Failure modes at 20℃ of strengthened beams were similar to conventional RC beams viz, flexural, flexural+shear and shear. But at high temperatures, deboning mode of failure was observed instead of flexural+shear.
3) Reduction in ductility of strengthened beams were observed with the increase in temperature and with the increase in strengthening reinforcement area.
4) First crack loads increased with the increase in strengthening reinforcement area, which verifies the effectiveness of strengthening. With the increase in temperature reduction in first crack was observed but was still higher than that of control specimens.
5) Formulas for ultimate debonding strength was proposed by incorporating shear interfacial strength and verified by predicting debonding shear load.
6) Ultimate shear load and failure modes was analytically calculated by using Truss model approach, and was proven to be sufficiently accurate for the current experimental results at all designed temperature levels.

Large amount of experimental and analytical results are presented in this work, which can be used by structural designers and researchers for further investigations, numerical verifications and to produce guidelines for repairing of structure in the specific regions.

REFERENCES

[1] Zhang D, Ueda T, Furuuchi H. Concrete cover separation failure of overlay-strengthened reinforced concrete beams. Construction and Building Materials. 2012;26(1):735-45.

[2] Zhang D, Ueda T, Furuuchi H. Intermediate Crack Debonding of Polymer Cement Mortar Overlay-Strengthened RC Beam. Journal of Materials in Civil Engineering. 2011;23(6):857-65.

[3] Benjeddou O, Ouezdou MB, Bedday A. Damaged RC beams repaired by bonding of CFRP laminates. Construction and Building Materials. 2007;21(6):1301-10.

[4] Zhang D, Ueda T, Furuuchi H. A Design Proposal for Concrete Cover Separation in Beams Strengthened by Various Externally Bonded Tension Reinforcements. Journal of Advanced Concrete Technology. 2012;10(9):285-300.

[5] Satoh K, Kodama K. Central peeling failure behavior of polymer cement mortar retrofitting of reinforced concrete beams. Journal of materials in civil engineering. 2005;17(2):126-36.

[6] Teng JG, Yao J. Plate end debonding in FRP-plated RC beams—II: Strength model. Engineering Structures. 2007;29(10):2472-86.

[7] Yao J, Teng JG. Plate end debonding in FRP-plated RC beams—I: Experiments. Engineering Structures. 2007;29(10):2457-71.

[8] Smith ST, Teng J. Interfacial stresses in plated beams. Engineering structures. 2001;23(7):857-71.

[9] Al-Gahtani AS R, AI-Mussallam AA. erformance of repair materials exposed to fluctuation of temperature. Journal of Materials in Civil Engineering. 1995;7:9-18.

[10] Al-Jabri KS, Hago AW, Al-Nuaimi AS, Al-Saidy AH. Concrete blocks for thermal insulation in hot climate. Cement and Concrete Research. 2005;35(8):1472-9.

[11] Rashid K, Ueda T, Zhang D, Miyaguchi K, Nakai H. Experimental and analytical investigations on the behavior of interface between concrete and polymer cement mortar under hygrothermal conditions. Construction and Building Materials. 2015;94:414-25.

[12] Khan MS, Prasad J, Abbas H. Bond strength of RC beams subjected to cyclic thermal loading. Construction and Building Materials. 2013;38:644-57.

[13] Chiang C-H, Tsai C-L. Time–temperature analysis of bond strength of a rebar after fire exposure. Cement and Concrete Research. 2003;33(10):1651-4.

[14] Bazant PK, FM. Concrete at high temperature-Material properties and mathematical methods,: Harlow:longman; 1996.

[15] Ramana V, Kant T, Morton S, Dutta P, Mukherjee A, Desai Y. Behavior of CFRPC strengthened reinforced concrete beams with varying degrees of strengthening. Composites Part B: Engineering. 2000;31(6):461-70.

[16] Zhang D, Ueda T, Furuuchi H. Average crack spacing of overlay-strengthened RC beams. Journal of Materials in Civil Engineering. 2011;23(10):1460-72.

[17] Hoang L, Nielsen MP. Plasticity approach to shear design. Cement and Concrete Composites. 1998;20(6):437-53.

[18] Colotti V, Spadea G. Shear strength of RC beams strengthened with bonded steel or FRP plates. Journal of Structural Engineering. 2001;127(4):367-73.

[19] Colotti V, Spadea G, Swamy RN. Structural model to predict the failure behavior of plated reinforced concrete beams. Journal of Composites for Construction. 2004;8(2):104-22.

Chapter 6

FLEXURAL CRACK SPACING AND CRACK WIDTH AT ELEVATED TEMPERATURE

6.1 INTRODUCTION

Retrofitting and strengthening of reinforced concrete structure is one of the most suitable and viable solution for deteriorated structures. Several materials have been introduced in construction industry for repairing and most common materials are the polymer cement mortar (PCM), fiber reinforced polymer (FRP), ultra high strength fiber reinforced concrete (UFC) panels etc. PCM is the cementitious material, having better adhesion strength and resistance to aggressive environment than concrete.

Overlaying with PCM is used to strengthen structural elements like; bridges, slabs and columns etc. Overlay-strengthened RC beams were investigated in various studies and increase in flexural capacity was observed [1-3]. Increase in load-carrying capacity by overlaying with PCM is not accompanied by a proportional increase in system rigidity, either in terms of deformation or in terms of transfer of stresses at concrete-PCM interface.

In this context, crack spacing plays a vital role in overlay strengthened RC structures, especially, in transferring shear stress along interface between overlay and substrate concrete. And in mitigating normal stress generated in the substrate concrete when debonding failure occur [3]. Different structural codes and researchers present model to predict crack spacing by considering various approaches, like; concrete-steel slippage, concrete cover, rebar spacing, effective reinforcement ratio etc. Zhang et al. [4] summarizes the crack spacing by considering various codes and concluded that codes are incapable for predicting crack spacing of overlay-strengthened RC beams. And proposed a new model by considering equilibrium and compatibility equations and verify it with the large data base. Application of overlaying substantially change the cracking scenario of the element due to additional tension stiffening. In RC element strengthened with PCM, crack width of strengthened element is generally less than for unstrengthened beams due to additional tension stiffness, which is provided by reinforcement in overlay and reduces the crack spacing.

Overlaying or patching with PCM is mostly used for bridges, highways, runways, etc. And such structure exposed to severe environmental condition that may influence the performance of repaired structure. Temperature is the one of environmental factors and fluctuation of temperature, which can be more than 60 ℃, may affect the durability of the repaired structure and considered as responsible for reduction of intended service life. High temperature degrades the mechanical properties of concrete, PCM and concrete-steel bond [5-7]. In this context, serviceability-related performance of the repaired structure should be checked at elevated temperature. The required performance level should be ensured over intended service life.

With such background, large number of RC beams were prepared and strengthened by overlaying with PCM at soffit of beam. Various amounts of reinforcement were used in the overlay part. Both types of strengthened and unstrengthened beams were exposed and tested in four point bending test at 20, 40 and 60 ℃. Flexural crack spacing and crack width were measured at tested temperatures. Observed flexural crack spacing was increased with increase in temperature and it was verified analytically. Crack width is the function of crack spacing and increase in crack width was also observed with increase in temperature. Crack width was also predicted by incorporating flexural crack spacing and very close agreement was observed between experimental crack width and observed crack width at respective temperature level.

6.2 EXPERIMENTAL PROGRAMME

6.2.1 Materials and Specimen Preparation

Concrete was the first material, which was used in this experimental work. Ready mixed ordinary concrete with target compressive strength of 30 MPa was used. Two types and sizes of reinforcement bars were used; First one was the deformed bar of 10 mm diameter and second one was plain bar of 6 mm in diameter. Polymer cement mortar (PCM) was used as repairing material for overlaying. Primer was used to improve chemical and physical interaction of concrete-PCM interface. Primer also resists against penetration of moisture from PCM to concrete side. Retarder was used to delay the hardening process of concrete.

Cubes casted in wooden molds were used to evaluate the compressive strength and split tensile strength of concrete and PCM at concerned testing condition. 150 mm and 100 mm cube were used for concrete and PCM to evaluate respective strengths. Wooden molds with size of 1800 x 200 x 150 mm were used to prepare reinforced concrete (RC) beams. Frist of all, retarder was mixed with suitable amount of water and spread at bottom of mold. Then, steel cage with two deformed bars at top and two at bottom was placed inside the mold. Stirrups of plain bar were used as shear reinforcement and spaced at 75 mm c/c through the entire span of beam. 25 mm clear concrete cover was maintained along four sides of longitudinal reinforcement. After steel cage placement, ready mixed concrete was poured into the molds to prepare final product as RC beam. At 36 hours after casting, bottom plank of wooden mold was removed to expose bottom side to environment. It was still soft as compared to top surface due to presence of retarder at bottom. All soft particles, cement paste and mortar were removed by steel brush and strong water jet, until aggregates were exposed. After treating substrate concrete surface, all RC beams were cured in moist condition for further two weeks. Wooden molds with size of 1280 x 200 x 25 mm were prepared and placed over the treated surfaces of RC beams. Primer was sprayed on the treated surface in some cases and steel reinforcement of various amounts were placed in the mold. Thermo-couple was also implanted at interface to monitor temperature during temperature exposure and loading test of specimens. PCM was sprayed in the mold and again primer was sprayed on top of PCM to avoid evaporation of moisture from PCM. Overlaid part of beam is covered by polythene sheets to avoid evaporation of moisture with time. Methodology for specimen preparation is explained pictorially in Fig. 6.1. The

overlaid beams and PCM cubes were cured under 7 days wet condition for hydration of cement and 21 days dry condition for polymerization of polymers [8]. Detail of reinforcement in overlay part is indicated in Fig. 6.2.

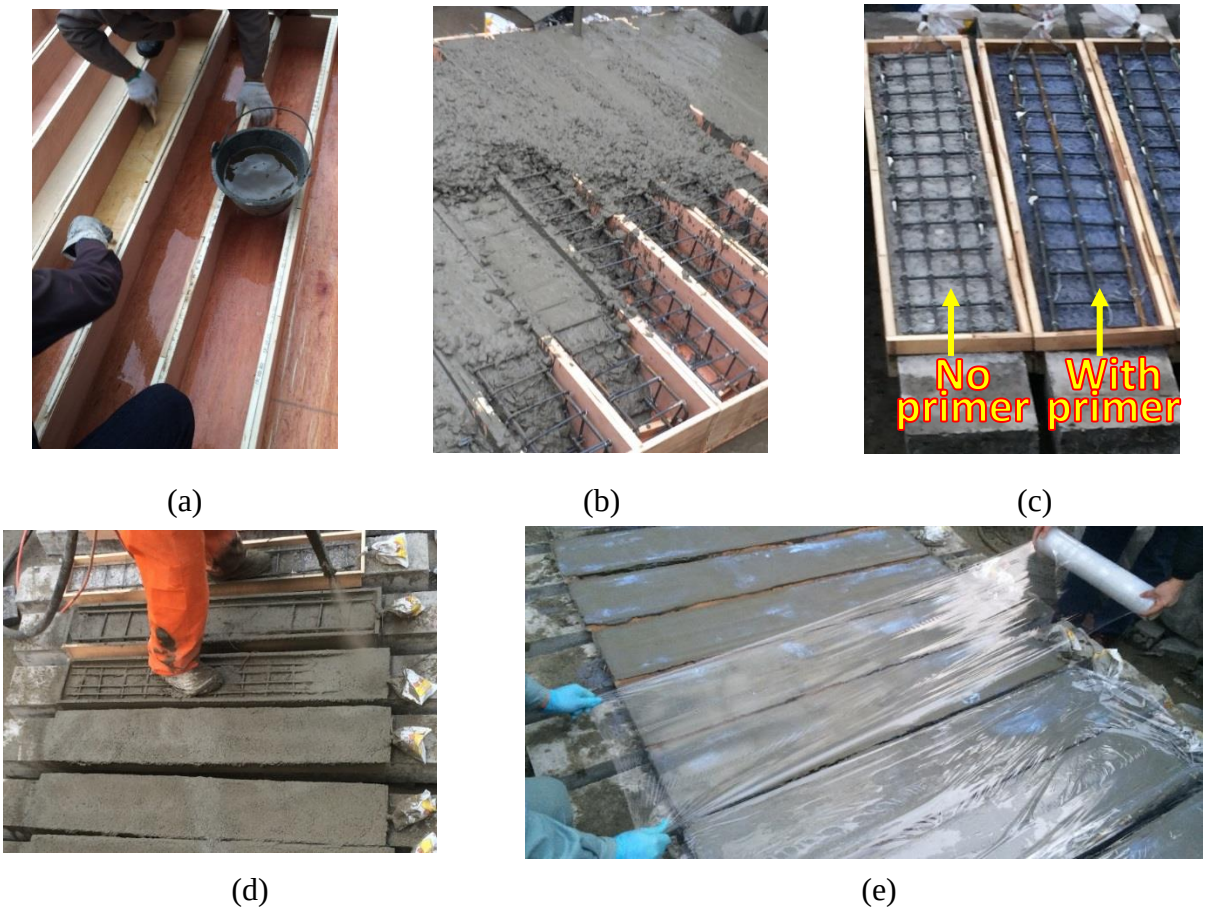

Fig. 6.1 Methodology for preparing overlaid beams (a) wooden molds with retarder at bottom (b) placing of steel and concrete (c) treated surface, placement of mold and reinforcement for overlay (d) spraying of PCM (e) spraying of primer and wrapping with polythene sheets.

6.2.2 Testing and Exposure Conditions

Three temperature levels were selected for investigating the performance of overlay-strengthened RC beams under elevated temperature. All specimens, cubes and beams, were exposed to 20, 40 or 60 ℃ temperature level for 16 hours before testing, while the relative humidity was fixed at 60% for all temperature conditions. Cubes were placed in oven and then wrapped with insulation sheet before being transferred to testing machine. Testing machine was also equipped with heaters and insulation sheets for testing cubes. For beams, desired temperature level and relative humidity was obtained by specially designed environmental chamber, which is capable of maintaining temperature up to 100 ℃. Loading set-up was established inside the chamber. So, all beams were exposed to designed exposure condition for 16 hours and then tested by maintaining similar exposure conditions.

The cubes were tested for evaluating compressive strength and split tensile strength. In many

design procedures cylindrical compressive strength was used instead of cubical compressive strength. So, tested cube strengths were converted to the cylinder strength by using Eq. (1) [9]. Split tensile strength was evaluated by using Eq. (2) [5]. Compressive and tensile strengths were measured at 20, 40 and 60 ℃. Averages of three specimens were used to evaluate respective strength at concerned temperature level.

$$f_c' = 0.8 f_{cu} \quad (1)$$

$$f_t = \frac{2P_u}{\pi A} \quad (2)$$

where;

$f_c^{'}$ = Cylindrical compressive strength (MPa) ; f_{cu} = Cubcial compressive strength (MPa);

f_t = Split tensile strength (MPa); P_u =Ultimate load (N); A =Area (height x depth) (mm^2)

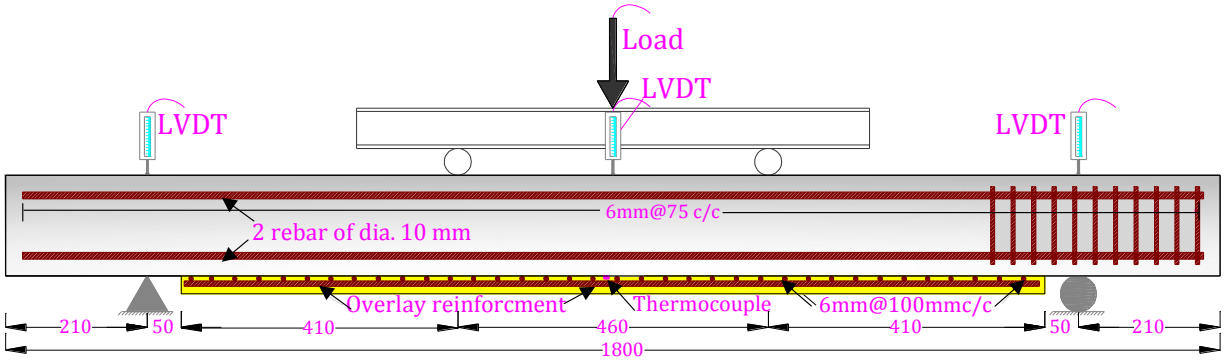

(a) Test setup of four-point loading test

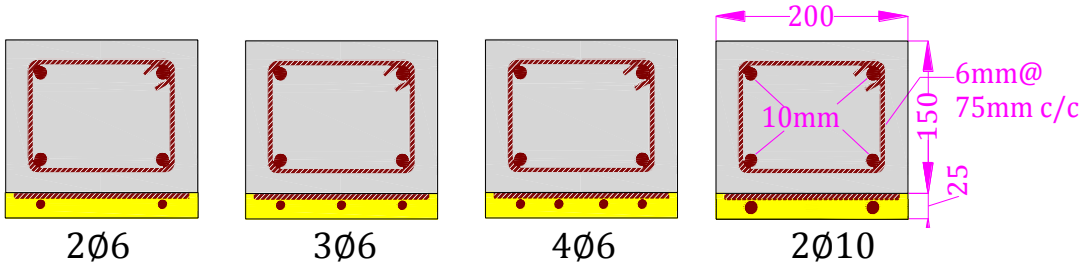

(b) cross sectional area of strengthened beams with different reinforcement in overlay

Fig. 6.2 Longitudinal and cross section of overlaid beams

All beams were tested in four-point loading test. Loading set-up along with the respective dimensions is presented in Fig. 6.2(a). Unstrengthened beams, without overlay, is referred as control beams and named as "Con" in this work. Control beams and overlaid beams were tested at 20, 40 and 60 ℃. Exposure and testing at 20 ℃ is referred as control condition. Overlaid beams were abbreviated in this work according to amount of reinforcement in overlay part and testing condition. e.g. "3Ø6-40" means that overlaid beams having three rebars of diameter 6 mm, exposed and tested at 40 ℃. Fig. 6.2(b) shows the detail of reinforcement in overlay part. Front side of all

beams were whitewashed and grid of spacing 50 mm was made on it to monitor crack length and spacing during loading. Cracks lengths were marked at various loading points during testing at 20 and 40 ℃. At 60 ℃, crack spacing was marked after finishing of test and reducing temperature to control condition. Flexural crack spacing (S_{cr}) for each beam was obtained by using Eq. 3 and detail is provided in Fig. 6.3.

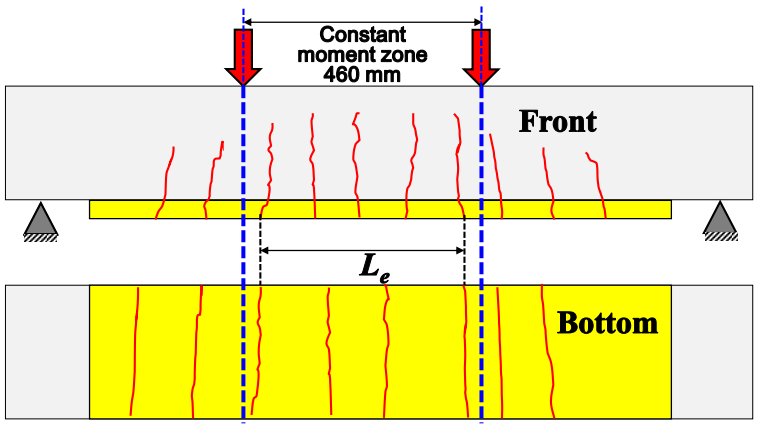

Fig. 6.3 Experimental crack pattern to evaluation flexural crack spacing at stabilized cracking condition.

$$S_{cr,exp} = \frac{1}{2}\left[\frac{L_e}{(n_{c,F}-1)} + \frac{L_e}{(n_{c,B}-1)}\right] \quad (3)$$

where;

$\boldsymbol{L_e}$ = Effective span for number of flexural cracks (mm); $\boldsymbol{F}$ = Front; $\boldsymbol{B}$ = Bottom; $\boldsymbol{n_c}$ = number of flexural cracks; $\boldsymbol{S_{cr,exp}}$ = Experimental flexural crack spacing (mm)

Table 6.1 Summary of tests, number of specimens and testing conditions.

Beams	$(n)_{OL}$	D (mm)	Type of rebar	$(A_s)_{OL}$ $(mm)^2$	Tests and testing conditions						Abbreviation
					20 ℃		40 ℃		60 ℃		
					S_{cr}	w	S_{cr}	w	S_{cr}	w	
Control	----	----	Deform	----	2	1	1	1	1	----	Con-T
	2	6	Plain	56.10	2	2	2	2	2	----	2Ø6-T
Overlaid	3	6	Plain	84.15	2	2	2	2	2	----	3Ø6-T
beams	4	6	Plain	112.20	2	2	2	2	1	----	4Ø6-T
	2	10	Deform	141.50	2	2	2	2	2	----	2Ø10-T

$(n)_{OL}$ = Number of rebar in overlay; D = diameter or rebar $(A_s)_{OL}$ = Area of steel in overlay; S_{cr} = Flexural crack spacing; w = Crack width; T = Testing temperature, 20, 40 or 60 ℃

Crack width was measured from extreme tensile side of concrete during various loading points at 20 and 40 ℃ by crack measurement device, which can measure crack width of 0.2 mm to 2.0

mm, while crack width was not measured during testing at 60 ℃. In case of overlaid beams, two beams were tested at one temperature level. Among two beams, one beam was prepared by using primer at concrete-PCM interface, while the other beam was prepared without using primer. For overlaid beams, similar procedure was adopted for evaluating crack spacing and crack width. Crack width was measured from extreme tensile side of PCM and concrete. Table 6.1 shows the summary of tests, testing conditions and number of specimens for evaluating flexural crack spacing and crack width of beams.

6.3 EXPERIMENTAL DISCUSSION ON CRACK SPACING

6.3.1 Effect of Temperature in RC Beam without Overlay

Fig. 6.4 presents the flexural crack spacing (S_{cr}) of RC beams tested at 20, 40 and 60 ℃. S_{cr} of 89 mm was observed in the beam tested at 20 ℃, while it was 90 and 92 mm of the beams tested at 40 and 60 ℃, respectively. At 20 and 40 ℃, cracks were continuously monitored during loading till failure. But at 60 ℃, all cracks were marked after cooling down of environmental chamber down to room temperature of 20 ℃. Since concrete strength, geometry, type of reinforcement and concrete cover that affect flexural crack spacing were kept constant [10-12], the change in crack spacing was considered to take place only due to change in temperature. Temperature affects the mechanical properties of concrete and bond between concrete and steel. More slippage was observed at high temperature in a previous study reported by Khan [7]. Degradation in compressive strength, tensile strength and bond strength was also reported by Bazant and Kaplan [6], which summarized the work of many researchers. Bond strength was also evaluated by pull-out test, in which degradation in bond strength was observed with the increase in temperature. Duration of temperature exposure also influenced the bond strength and reduction in bond strength was observed with increase in the duration [13-15]. In this study, all specimens were exposed to elevated temperature for more than 16 hours and the loading test was conducted at similar condition. Therefore, the reduction in bond strength due to temperature exposure should be considered as responsible for increase in crack spacing.

6.3.2 Effect of Overlaying Reinforcement

Steel reinforcement area, spacing between steel reinforcements and concrete cover directly affect the crack spacing. Such parameters are used in various codes, which were used for analyzing crack spacing of RC beams [10-12]. Fig. 6.5 presents the crack spacing of overlaid beams and also compares with the flexural crack spacing of control beam. For overlaid beams, reduction in crack spacing was observed with the increase in reinforcement area and perimeter in the overlay part of specimen 2Ø6, 3Ø6 and 4Ø6. Fig. 6.6 presents effect of steel reinforcement area and perimeter on crack spacing. It is clear from Fig. 6.6 that reduction in crack spacing was observed with the increase in total area of all steel reinforcements and increase in total perimeter of all steel reinforcements. For 2Ø6 beam, 13% increase in flexural crack spacing was observed as compared to control specimen. Reinforcement area in overlay part is just 40% of the area of steel in concrete

part. Resistance of crack propagation was resisted by two rebar of diameter 6 mm instead of 10 mm deformed bars. Which assume to be reason for increase in crack spacing. But with further increase in reinforcement area in overlay reduction in crack spacing was observed. And other reason for the reduction in crack spacing of overlaid beams is the decrease in the concrete cover that was reduced from 25 mm to 16 mm.In case of 2Ø10, increase in crack spacing was observed as compared to 3Ø6 and 4Ø6. The increase in the crack spacing as compared to other overlaid beams was due to; (1) Use of deformed bars instead of plain bars and failure of bond between concrete/steel may be split type of failure due to deformed bar instead of pull-out failure. (2) The distance between steel bars is more than 3Ø6 and 4Ø6.

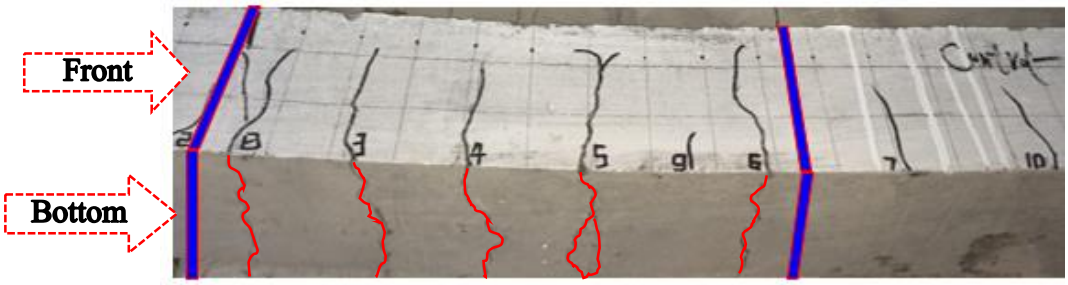

(a) Crack pattern of Con-20

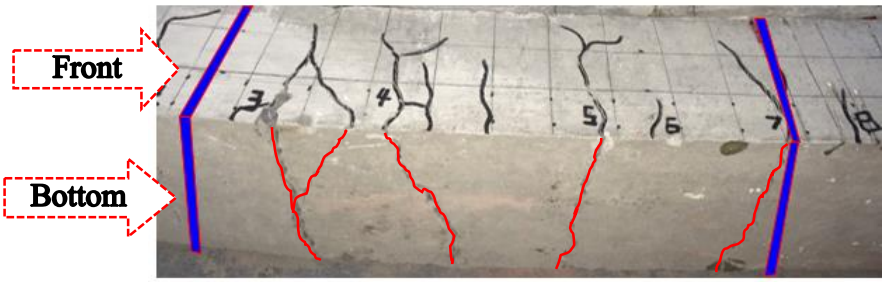

(b) Crack pattern of Con-40

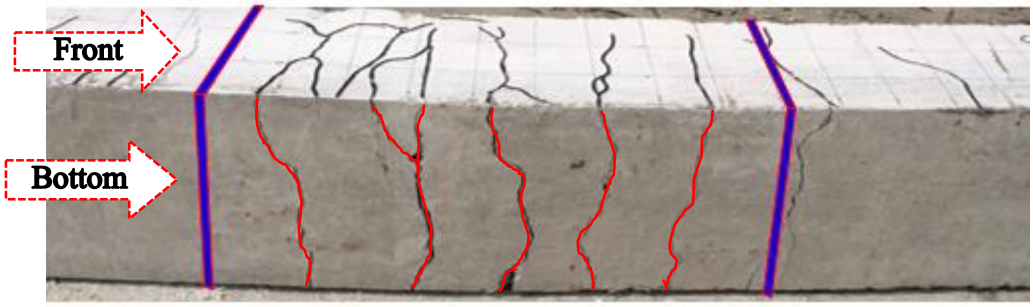

(c) Crack pattern of Con-60

Fig. 6.4. Observed crack pattern of control beams in constant moment zone at different temperature levels.

6.3.3 Effect of Temperature in Overlaid Beams

Fig. 6.7(a) and Fig. 6.7(b) show the flexural crack spacing of control and strengthened

beams at temperature levels of 40 and 60 ℃, respectively. Increase in crack spacing was observed with the increase in temperature. Effect of primer was considered as insignificant. So average of both types of beams, with and without primer, is reported as crack spacing. For 2Ø6, 11% and 12% increase in crack spacing was observed at temperture level of 40 and 60 ℃, respectively, as compared to specimen tested at 20 ℃. Similar trend was observed for rest of beams. Increase in crack spacing at 60 ℃ was 17, 35 and 14% for 3Ø6, 4Ø6 and 2Ø10, respectivly. Crack length and number of cracks were increased by increase in load and also due to ductile behavior of beams.

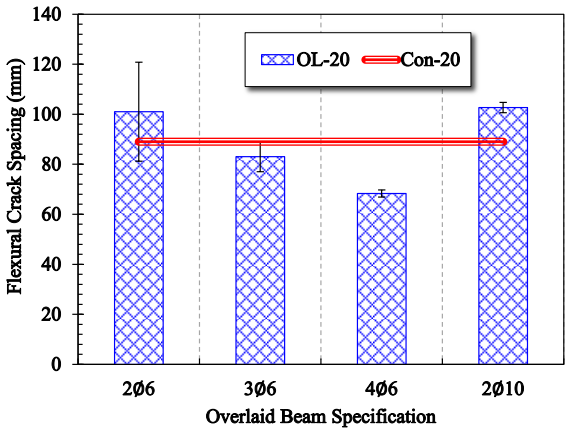

Fig. 6.5 Effect of overlaying on flexural crack spacing at 20 ℃.

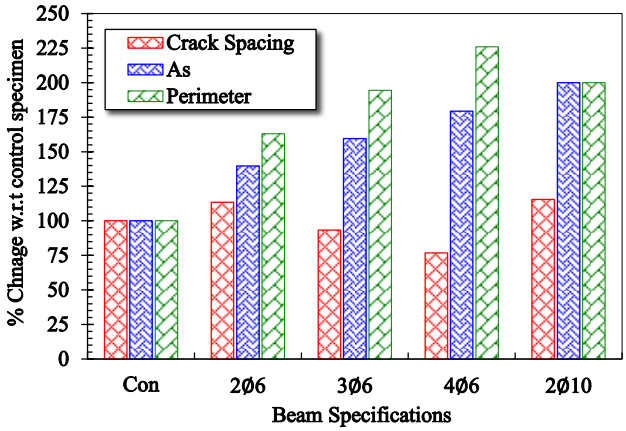

Fig. 6.6 Effect of steel reinforcement area and perimeter on flexural crack spacing.

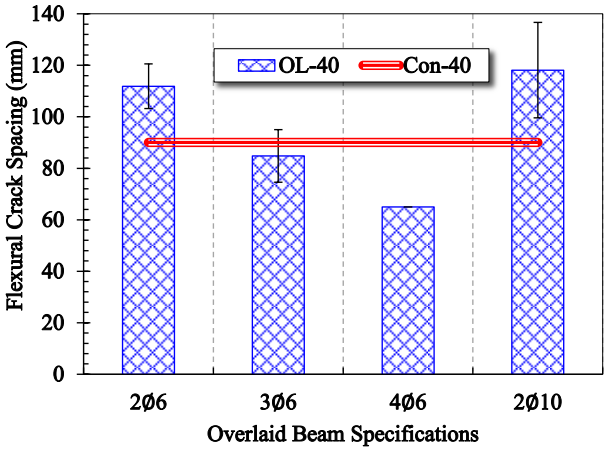

(a) At 40 ℃

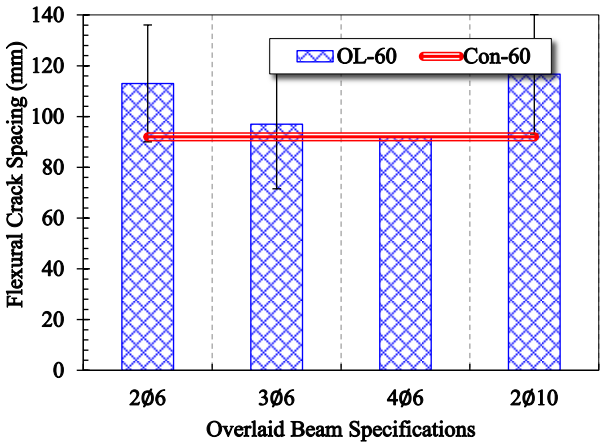

(b) At 60 ℃

Fig. 6.7 Comparison of flexural crack spacing of control beams with overlaid beams at elevated temperature.

Fig. 6.8 and Fig. 6.9 summarized the flexural crack spacing of all beams at various temperature levels. Flexural crack spacing increases with increase in temperature level. Cracks initiates just after the tensile stress of overlay at extreme tension end exceeds the tensile strength of PCM, which was observed to reduce significantly with the increase in temperature [5, 16-18]. Reduction in first crack load, yield load and ultimate load was also observed with the increase in temperature [1].

Due to degradation in the mechanical properties of concrete and PCM with temperature, the bond between concrete/steel and PCM/steel also deteriorated, which is considered as responsible for the increase in flexural crack spacing with temperature.

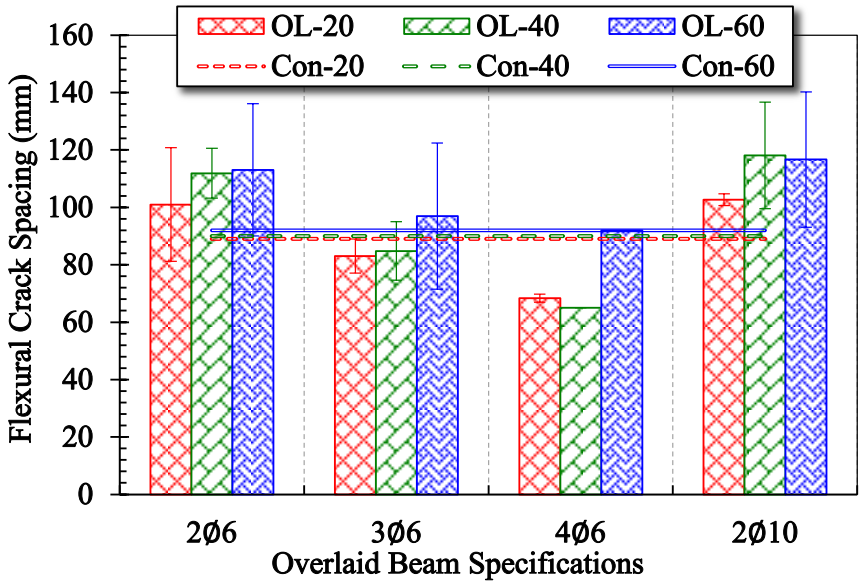

Fig. 6.8 Quantitative summary of flexural crack spacing of all beams at different temperature levels.

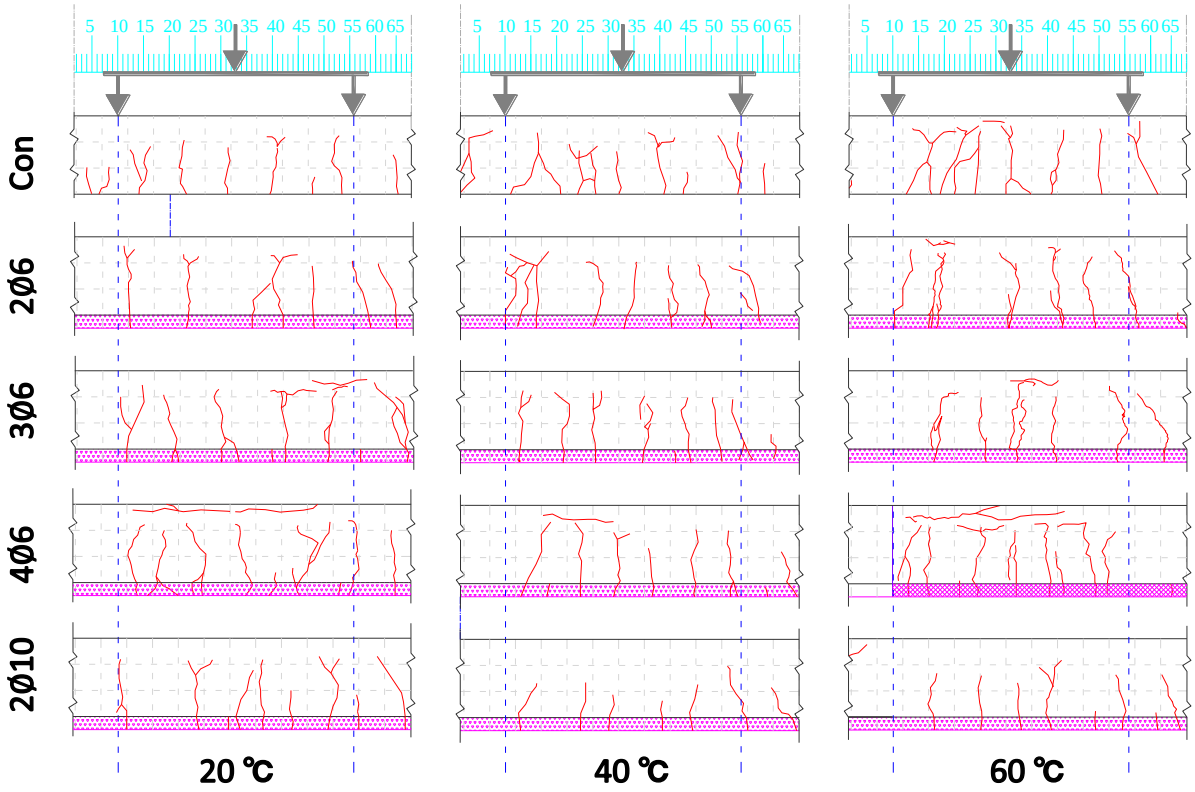

Fig. 6.9 Qualitative summary of flexural crack spacing of all beams at different temperature levels

6.4 ANALYTICAL DISCUSSION ON CRACK SPACING

6.4.1 Prediction of Crack Spacing by Various Codes

Flexural crack spacing was calculated by various codes by considering different approaches [10-12]. Different parameters were considered while calculating crack spacing, like; concrete cover, number and geometry of tensile reinforcement, spacing between rebar and mechanical strength of concrete etc. Proposed equations by various codes are mostly semi-empirical equations and have some contradictions with the observed experimental observations. Zhang *et al*. has summarized the flexural crack spacing calculated by various codes and compared with large data base [4]. It was compared for the conventional as well as overlaid RC beams. It was reported that there were the overestimation and underestimation of flexural crack spacing in overlaid beams by various codes. In this work crack spacing was calculated by JSCE and Eurocode, and then overestimation and underestimation of crack spacing was observed, respectively [10, 11]. According to JSCE, flexural crack spacing was calculated by using Eq. 4. In which, k_1 is surface geometry of bar (1for deformed bar and 1.3 for plain bar); k_2 and k_3 were calculated by using Eq. 5 and Eq. 6, respectively; C is concrete cover in mm; c_s is c/c distance of outer layer of steel reinforcement; $\emptyset$ is diameter of outer layer tensile reinforcement; n is number of layers of tensile reinforcement and f_c' is concrete compressive strength. Fig. 6.10(a) shows the comparison of experimental observed crack spacing with the calculated results by Eq. 4. Overlaid beams by using primer at concrete-PCM interface is presented by "WP" and beams without using primer is presented by "NP". Calculated flexural crack spacing overestimates the experimental crack spacing by more than 40 mm. Overestimation was also observed by Zhang *et al*. and it was reported that the $S_{cr,cal}/S_{cr,exp}$ was 1.29 for large data base of overlaid beams, and even for unstrengthened beams, $S_{cr,cal}/S_{cr,exp}$ was 1.48 [4]. Possible reason for the overestimation was the spacing between rebars. For experimental investigation in this work few rebars were placed in concrete according to desired objectives. In this work, spacing between bars was 140 mm for control beam as well as for 2∅10. And for 2∅6, it was more than 140 mm. But in real structures, to which JSCE equation is applied, mostly the spacing between rebars are maintained less than 100 mm.

$$S_{cr} = 1.1k_1k_2k_3\{4C + 0.7(c_s - \emptyset)\} \quad (4)$$

where

$$k_2 = \frac{15}{f_c^{'} + 20} + 0.7 \quad (5)$$

$$k_3 = \frac{5(n+2)}{7n+8} \quad (6)$$

According to Eurocode EC2 Provisions, Flexural crack spacing was calculated by using Eq. 7 [11]. In which, k_1 is surface geometry of bar (0.8 for deformed bar and 1.6 for plain bar); k_2= 0.5 for bending and 1.0 for pure tension; C is concrete cover in mm; $\emptyset$ is diameter of outer layer

of tensile reinforcement; A_{st} is tensile reinforcement area and A_{ct} is effective area of concrete and is equal to lesser of a) *h/2*, b) 2.5(*h-d*), where "*h*" is height of beam and *d* is effective depth. Underestimation about 50 mm was observed when compared with experimental observations (Fig. 6.10(b)). In Eurocode, bar spacing is ignored that may be reason for underestimation of the flexural crack spacing. Detailed reason for the mismatch with the codes for overlaid beams is provided by Zhang [4].

$$S_{cr} = 2C + k_1 k_2 \frac{\emptyset A_{ct}}{A_{st}} \tag{7}$$

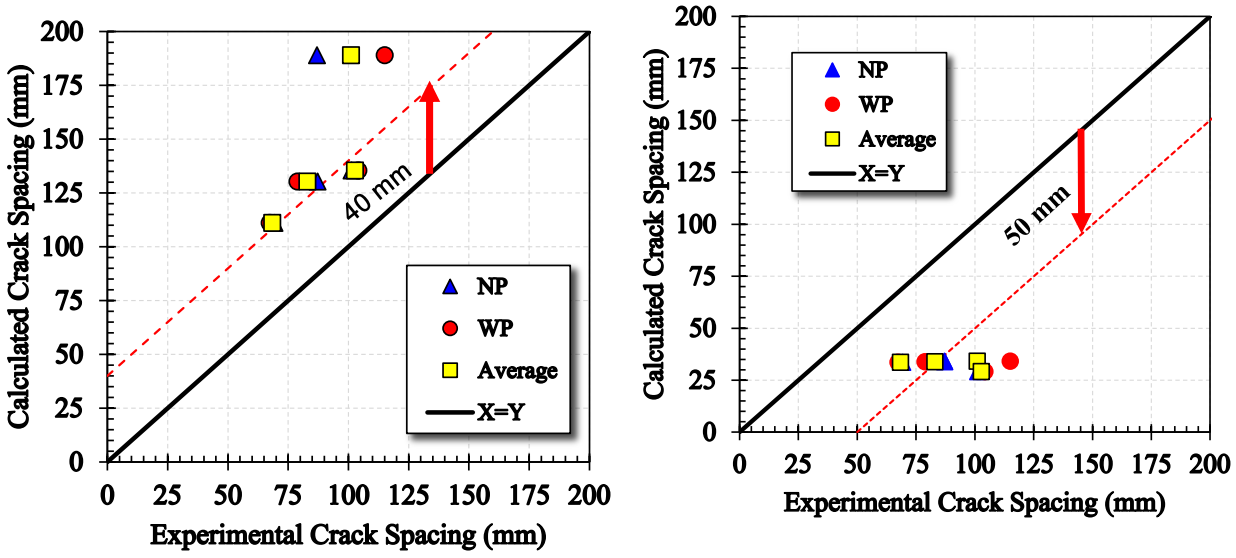

(a) JSCE (b) Eurocode

Fig. 6.10 Comparison of observed crack spacing with calculated by various codes at control condition

6.4.2 Prediction of Crack Spacing for Overlaid Beams at Control Condition

Crack spacing of RC members strengthened by various repairing materials has been discussed in various studies [4, 19-21]. Zhang *et al*. proposed a model for calculating flexural crack spacing of overlaid beams by using simple force equilibrium conditions, in which, uniaxial tensile force is considered between two adjacent cracks as showed in Fig. 6.11. Between two adjacent cracks, bond between concrete/PCM and reinforcement reduces the elongation of reinforcement due to transfer of tensile stress to concrete/overlay. At stabilized crack stage, flexural crack spacing can be calculated by using Eq. 8.

$$S_{RC} = \frac{3f_{ct}(A_{ct} + A_{OL,t}\frac{E_{OL}}{E_c})}{(\sum O_{RC}\tau_{bm,c} + \sum O_{OL}\tau_{bm,OL})} \tag{8a}$$

$$S_{OL} = \frac{3f_{t,OL}(A_{ct}\frac{E_c}{E_{OL}} + A_{OL,t})}{(\sum O_{RC}\tau_{bm,c} + \sum O_{OL}\tau_{bm,OL})} \quad (8b)$$

where;

S =flexural crack spacing; RC = RC beam part; OL =overlay part (PCM); f_{ct} and $f_{t,OL}$ are split tensile strength of concrete and PCM, respectively; E = modulus of elasticity; O = perimeter of steel bars; τ_{bm} = maximum bond strength of concrete/PCM-reinforcement; A=effective tensile area of concrete and PCM

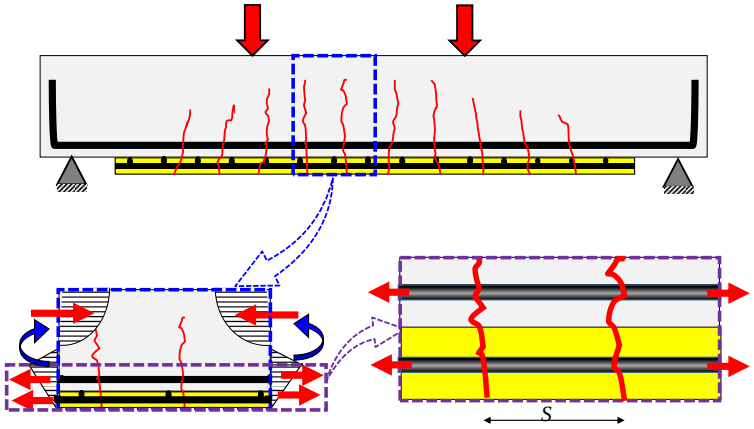

Fig. 6.11 Uniaxial tension between two adjacent cracks of overlaid beams.

$$A_{RCt.max} = \frac{A_{s,RC}.f_{y.RC}}{f_{ct}} \quad (9a)$$

$$A_{OLt.max} = \frac{A_{s,OL}.f_{y.OL}}{f_{pcm.t}} \quad (9b)$$

Table 6.2 Tensile strength evaluation by considering compressive strength

Code	Equation	References	Equation. No.
French Code	$f_t = 0.6 + 0.006f'_{cu}$	[22]	(10a)
JSCE	$f_t = 0.23{f_c'}^{2/3}$	[10]	(10b)
ACI	$f_t = 0.53\sqrt{f_c'}$	[23]	(10c)
where; f_t = Tensile strength (MPa); f'_{cu} = Cubical compressive strength (MPa); f'_c = Cylindrical compressive strength (MPa)			

Effective area of concrete/PCM for certain steel bar within stabilized crack spacing can be achieved by using Eq. 9. In two dimensional consideration, width of the concrete/PCM of beam is constant and effective tensile height can be calculated by using Eq. 9. It must be less than the tensile

height of the beam, detail calculation of other side of effective area of concrete or overlay is provided by Zhang *et al.* [4]. It is clear from Eq. 9 that effective area of concrete/overlay is highly depends upon the concrete/PCM tensile strength. Large variation in the evaluation of tensile strength was observed even calculated by equation proposed by various codes as shown in Table 6.2. At given compressive strength, large variation in tensile strength was observed by using Eq. 10. So, for reliability of analytical calculation of flexural crack spacing, effective area was calculated according to Eurocode provisions [11].

Bond stress between concrete/PCM and reinforcement depends primarily on properties of concrete/PCM, cover thickness and surface geometry (deformed or plain bars). Maximum bond stress between concrete-steel can be evaluated by using Eq. (11) and same equation was used for evaluating bond stress between PCM and steel [4]. Eq. (11a) was used for pull-out failure and it was assumed for all strengthened beams, except 2Ø10, where split type failure was assumed (Eq. (11b)) due to increase in reinforcment diameter and using deformed bar instead of plain bars.

$$\tau_{bm,c} = 1.25\sqrt{f_c^{'}}\ ;\ \tau_{bm,OL} = 1.25\sqrt{f_{PCM}^{'}} \tag{11a}$$

$$\tau_{bm,c} = 5.5\left(\frac{f_c^{'}}{20}\right)^{1/4}\ ;\ \tau_{bm,OL} = 5.5\left(\frac{f_{PCM}^{'}}{20}\right)^{1/4} \tag{11b}$$

where;

f_c' and f_{PCM}' is compressive strength of concrete and PCM in MPa, respectively.

Modulus of elasticity, compressive strength of and tensile strength of concrete and PCM are presented in Table 6.3. Average of three specimens is reported as concerned value.

Table 6.3 Mechanical properties of concrete and PCM at control condition.

Material	Compressive Strength (MPa)	Tensile Strength (MPa)	Modulus of Elasticity (MPa)
Concrete	22.63	3.14	23500
PCM	47.75	6.06	21500

Stabilized crack spacing in concrete part and overlay part was calculated by using Eq. (8a) and Eq. (8b), respectively. Final crack spacing was calculated by using Eq. 12, in which, k_1 is strain gradient coefficient and can be calculated according to CSA [24]. Values of k_1 vary from 1 to 0.5 (1 for tension and 0.5 for bending). In this work k_1 was equal to 0.5.

$$S_{cr,ana} = k_1.\min(S_{RC}, S_{OL}) \tag{12}$$

Experimental flexural crack spacing was compared with the analytical values and is presented in Fig. 6.12. Calculated values slightly overestimate the experimental crack spacing that was only due to variation of tensile strength of materials. Observed tensile strength was 3.14 MPa, while the calculated value according to ACI 318-02 [23] is 2.54 MPa. By using 2.54 MPa in Eq. 8, calculated crack spacing values slightly underestimate the experimental crack spacing (Fig. 6.12). At control condition, calculated flexural crack spacing shows satisfactory agreement with the experimental observations. Flexural crack spacing is sensitive to split tensile strength so more attention must be paid to evaluate the split tensile strength accurately.

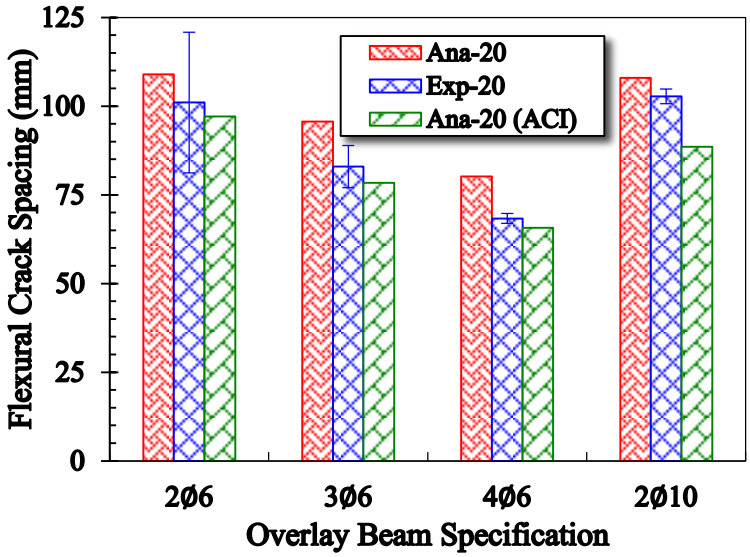

Fig. 6.12 Comparison of experimental crack spacing with predicted values at control condition.

6.4.3 Prediction of Crack Spacing for Overlaid Beams at Elevated Temperature

Eq. 8 was used for the calculation of flexural crack spacing at control condition. At elevated temperature, the variation will be observed in properties of concrete and PCM and the bond between concrete/PCM and steel, while the perimeter of steel reinforcement will be constant at all temperature levels. Compressive strength of PCM at concerned temperature level was investigated in this work and it was observed 47.75, 32.84 and 26.96 MPa at 20, 40 and 60 ℃, respectively. Split tensile strength of concrete and PCM was measured at temperature level of 20, 40 and 60 ℃ by authors in their previous works [5, 16, 17]. So normalized tensile strength was used by considering large amount of data (Eq. 13). Tensile strength and compressive strength of concrete vary with temperature and degradation in strengths were observed with the increase in temperature [6]. And for reliability of the current work, compressive strength of concrete at concerned temperature was evaluated by rearranging the relationship reported by ACI 318-02 (Eq. 14) [23]. It is also clear from Eq. (9), that effective tensile area is affected by tensile strength of respective material. Reduction in tensile strength was observed with the temperature, so increase in effective tensile area is obvious. By considering tensile strength reduction with temperature, Eq. (9) was modified and and change in effective area due to temperature can be obtained by using Eq. (15) .

It is impossible to get tensile area of overlay more than 5000 mm^2 so, increased area of overlay was added to the concrete part.

$$f_{t.pcm} = 1.2 f_{to.pcm} exp(-0.0095T) \quad (13a)$$

$$f_{t,conc} = 1.07 f_{to,conc} exp(-0.004T) \quad (13b)$$

$$f_c' = \left(\frac{f_{t,conc}}{0.53}\right)^2 \quad (14)$$

$$A_{ct,T} = 0.96 A_{ct} \exp(0.002T) \quad (15a)$$

$$A_{OLt,T} = 0.96 A_{OL,t} \exp(0.002T) \quad (15b)$$

where;

f_{to} = tensile strength (MPa) at control condition; f_t = tensile strength at concerned temperature (MPa); T = temperature (20 ℃ < T < 60 ℃); f_c' = compressive strength (MPa)

From Eq. (11), it is clear that bond stress highly depends upon the compressive strength of concerned material. At elevated temperature, severe degradation in compressive and tensile strengths of PCM was observed [5, 16, 17]. Due to reduction in tensile strength at elevated temperature, cracks initiate in specimen at lesser load than control condition. And bond stress also decreases due to reduction in mechanical properties of PCM at elevated temperature. Due to deflection of beams, local pull-out may be observed near the cracks opening and it may be more for plain bars (Fig. 6.13). For deformed bars, and with bars have more diameter split type failure was observed [7].

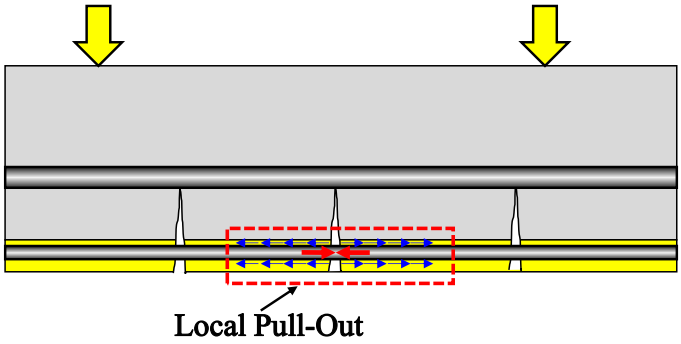

Fig. 6.13 Local pull-out failure in overlay part.

Eq. 8 and Eq. 12 were also used to predict the flexural crack spacing at elevated temperature by incorporating tensile strengths and effective areas at concerned temperature level. At elevated temperature, tensile strength of PCM and concrete was obtained from Eq. (13a) and Eq. (13b), respectively, compressive strength of concrete was obtained by using Eq. 14. And compressive strength of PCM at concerned temperature level was designed in this work. So, bond strength was calculated by using respective values at concerned temperature level. Effective tensile area was obtained by using Eq. (15). Analytical values are compared with the experimental observation and

very close resemblance was observed as shown in Fig. 6.14. Flexural crack spacing is larger in specimens exposed to higher temperature, which presents the deterioration or degradation in performance of strengthened RC member.

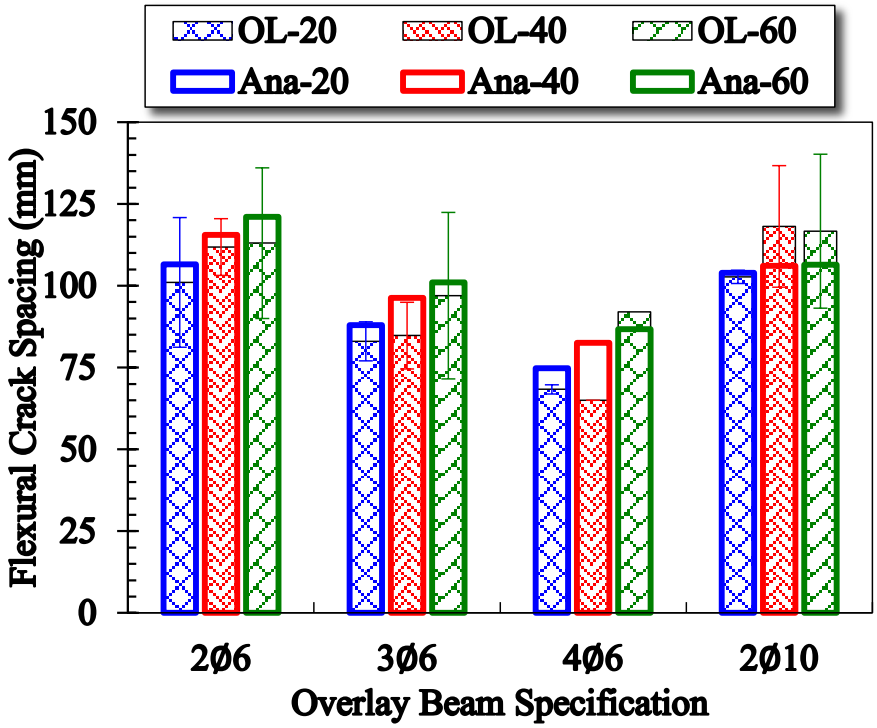

Fig. 6.14 Comparison of experimental crack spacing versus predicted values at different temperature levels.

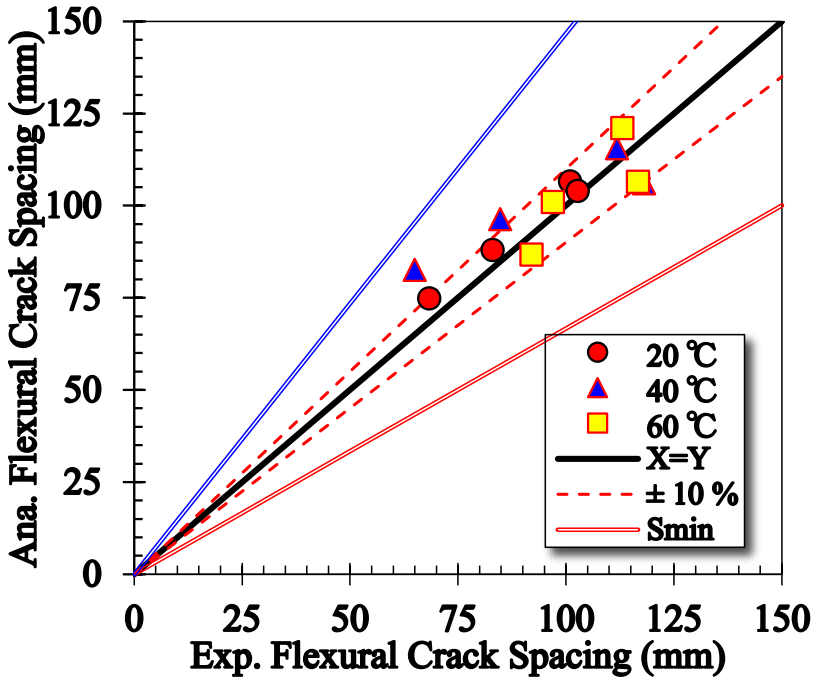

Fig. 6.15 Comparison of experimental and analytical crack spacing

The maximum and minimum crack spacing at the stabilized cracking stage can then be determined by using relationships given in Eq. (16) [4, 25]. Maximum and minimum crack spacing was calculated at control condition and compared with the crack spacing at elevated temperature, as shown in Fig. 6.15. All predicted values, at all temperature levels, of flexural crack spacing lie within the range of ±10% of the experimental observations. At elevated temperature, crack spacing lies within the range of minimum and maximum crack spacing of control condition. Minimum and maximum values of crack spacing can be used for designing or repairing beams for the prediction of crack spacing, which may be very useful for crack width analysis and debonding models etc.

$$S_{cr,max} = \frac{4}{3} S_{cr} \qquad S_{cr,min} = \frac{2}{3} S_{cr} \tag{16}$$

6.5 DISCUSSION ON CRACK WIDTH

6.5.1 Experimental Discussion

Crack width represents the index for the serviceability requirements of RC members. Crack width influences structural performance under several categories viz. aesthetics, tightness and durability. In this work, crack width of all strengthened and unstrengthened beams were measured during testing at 20 and 40 ℃. Crack width was measured from extreme tensile fiber of PCM and concrete at similar load level.

Fig. 6.16 presents the crack width of control beams and overlaid beams at 20 and 40 ℃. For control beams, crack widths in beams exposed at higher temperature level were wider. At 20 ℃ and under the load of 30 kN, 0.12 mm wide crack was observed, while at 40 ℃ and similar load level, the observed crack width was 0.26 mm. Crack width depends on the flexural crack spacing and it was observed experimentally and analytically in previous sections (Section 3 and Section 4) that flexural crack spacing increases with the increase in temperature. So increase in crack width was due to increase in crack spacing with temperature.

Fig. 6.16 also presents the comparison of crack width of control specimen with overlaid beams at control condition and elevated temperature. Crack initiated from the extreme tensile fiber of PCM and propagated towards compression side of beam with further application of load. Which is responsible for larger crack width in PCM than concrete. Although PCM is highly durable material, having higher tensile strength then concrete and have greater resistance against crack width. With overlaying, stiffness and crack initiation load of beams were increased. Crack initiated in overlaid beams at higher load than control specimens at all temperature levels. Even the amount of reinforcement in overlaying is less than control specimen tensile reinforcement, except 2Ø10. And concrete cover was also reduced from 30 mm to 14 mm. At 40 ℃, the crack width in the substrate concrete part and PCM overlay part were greater than in the specimen tested at 20 ℃. At first, crack width was increased proportionally to the increase in load but after yielding crack width increased significantly as compared to load increment. In strengthened beams, having 3Ø6, 4Ø6 and 2Ø10 reinforcement in overlay, crack width were 0.05 mm at 25, 28 and 35 kN, respectively,

at 20 ℃. These load values were reduced to 24, 25 and 30 kN when tested at 40 ℃ (Fig. 6.16). In Fig. 6.16(a), at 20 ℃ the crack widths were measured at load level of 48 kN and it was 0.61 mm and 0.82 mm in the concrete and overlay part, respectively. And at similar load level crack was enlarged to 1.09 and 1.8 mm for the substrate and overlay, respectively, during testing at 40 ℃. Similarly in beam of 3Ø6 (Fig. 6.16 (b)), increase in crack width was observed with the influence of temperature. At load level of 55 kN, crack width widens from 0.28 to 0.50 mm in substrate part and 0.47 to 1.30 mm in overlay part, when temperature level changes from 20 ℃ to 40 ℃ respectively. Tendency of crack width increase is almost same for beams of 4Ø6 and 2Ø10, as shown in Fig. 6.16 (c) & (d).

The increase in crack width with temperature may have similar mechanism for fatigue loading and it was believed that crack width increases with the application of repetitive load [26]. Bond strength between concrete-steel and PCM-steel affected by temperature and significant reduction was observed in bond strength [6, 7]. Elevated temperature reduces the interaction of physical bonding of cementitious material with steel. More slippage is observed at high temperature in past studies which may due to micro-cracking occurring at interface between concrete and steel. Micro-cracking may propagate further with the increase in temperature level and result in weak bond strength. Significant reduction in mechanical properties of PCM with temperature results in increase in crack width. PCM is very sensitive to temperature and softening of PCM at high temperature also affects the crack width. At higher temperature level, significant reduction in tensile strength of PCM was observed [5]. Other reason for the increase in crack width with temperature was due to increase in flexural crack spacing with increase in temperature. Various codes give the prediction formula for crack width which was function of flexural crack spacing [10, 11]. **Fig. 6.17** presents the influence of crack spacing on crack width with the increase in temperature. In section 4 and section 5, it was verified experimentally and analytically that flexural crack spacing increases with increase in temperature level. But it is also clear from **Fig. 6.17** that other factors also influence the crack width, e.g; concrete cover, slippage of rebars and distance between rebars etc. So, increased in crack width was not only due to increase in flexural crack spacing. Summary of observed crack width of control and overlaid beams at 20 and 40 ℃ is presented in Fig. 6.18. In all cases, control and overlaid beams, crack width increases with increase in temperature level, similarly, flexural crack spacing increases with increase in temperature level (Fig. 6.14). It was also observed in Fig. 6.18 that slope of crack width-load relationship also increases with the increase in amount of reinforcement and reduces with the increase in temperature level. Load-deflection relationship of all beams were also established by authors and reported in another study [1]. Initial stiffness increased with the increase in the amount of reinforcement. Crack initiation load was also increased and in the same way yield load and ultimate load was increased. And decay in all above mentioned values were observed with the increase in temperature. Due to similar reason the slope of crack width with load decrease with temperature and increases with increase in amount of reinforcement.

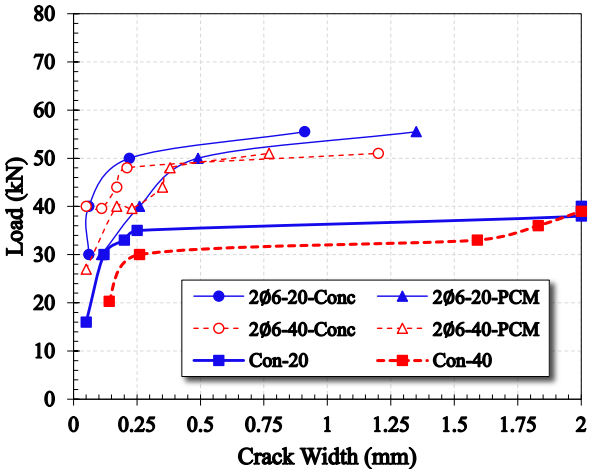

(a) Con and 2Ø6 Specimens

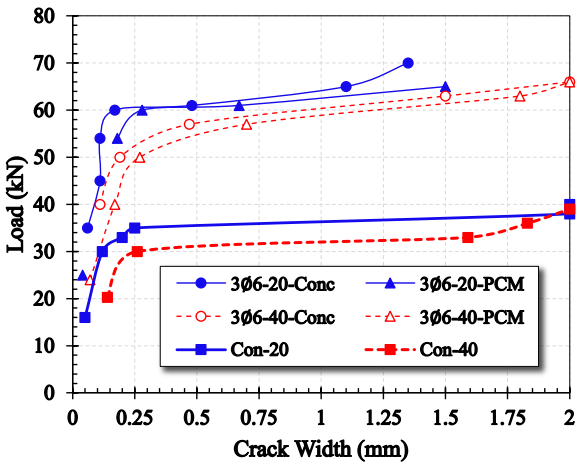

(b) Con and 3Ø6 Specimens

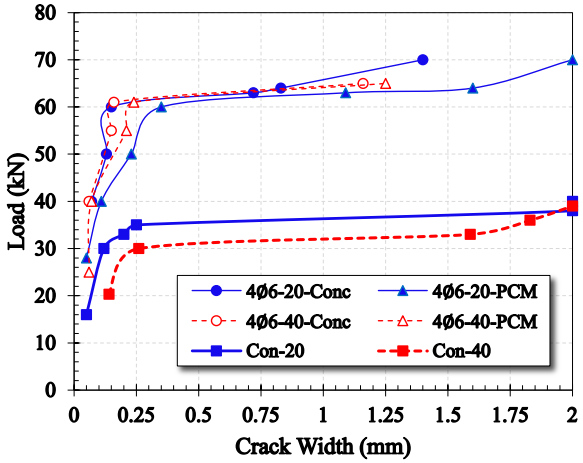

(c) Con and 4Ø6 Specimens

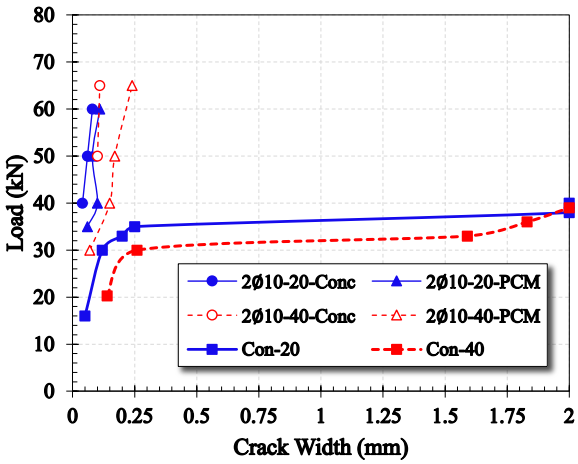

(d) Con and 2Ø10 Specimens

Fig. 6.16 Crack width of control and overlaid beams at 20 ℃ and 40 ℃ .

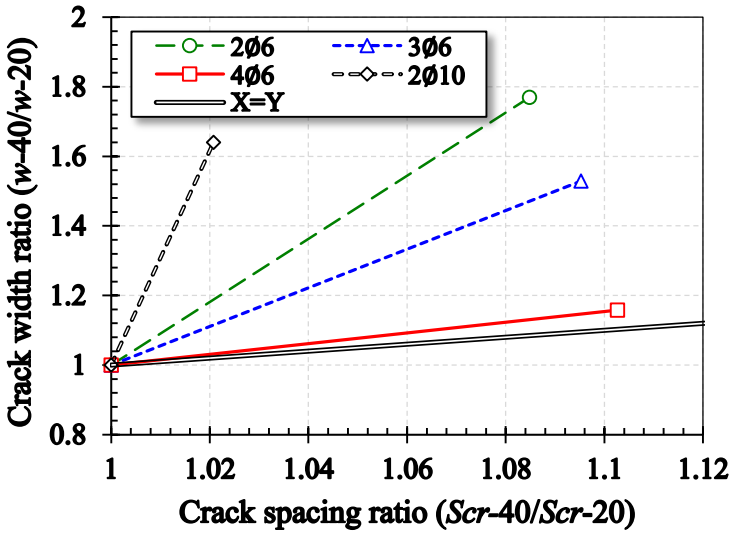

Fig. 6.17 Influence of crack spacing on crack width with temperature.

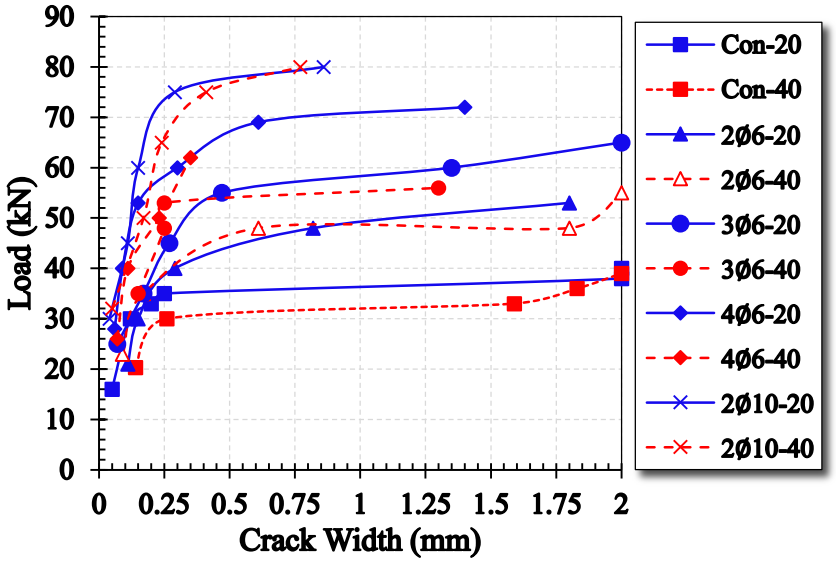

Fig. 6.18 Summary of crack width at 20 ℃ and 40 ℃.

6.5.2 Analytical Discussion

JSCE proposed a model for the predictoin of crack width by incorporating flexural crack spacing and is presented as Eq. (16). where, w is crack width at tension face of member (mm), σ_s and E_s are the stress and elastic modulus of the reinforcment, respectively, and S_{cr} is flexural crack spacing. Concrete cover, transverse reinforcment spacing, surface and geometry which affect the crack width, were incorporated in flexural crack spacing calculated by JSCE method [10]. In propsed method to calculate average crack spacing of overlaid beams (Eq. 8), different mechanism was assumed to predict crack spacing. However, crack width was measured by incorporating flexural crack spacing.

$$w = S_{cr}\left(\frac{\sigma_s}{E_s}\right) \tag{16}$$

Eq. 16 ignores the tensile strain in concrete since it is small, as well as tension stiffening between cracks. Due to tension stiffening, some part of stress is incorporated by cocnrete which results in the reduction in stress beared by steel reinforcement. Modified stress in steel can be obtained by using Eq. 17 that was proposed by by Martin and Khaled [27] for FRP reinforcment and is applicable for other types of reinforcement. ACI also provides the bond paramter k which varies depending on type of reinforcment [23]. ACI equation for crack width prediction was calibrated with defomed bar by using value 1. Here, large data was investigated by using plain bars. So $k = 1$ used for plain bars and 0.8 for deformed bars.

$$\sigma_{sm} = \sigma_s - \frac{0.4\sqrt{f_c^{'}}\,(2bd_c - A_s)}{A_s} \tag{17}$$

$$w = S_{cr} k \left(\frac{\sigma_{sm}}{E_s}\right) \tag{18}$$

$$w = \frac{(H - x_c - c)}{(H - x_c)} S_{cr} k \left(\frac{\sigma_{sm}}{E_s}\right) \tag{19}$$

where, σ_{sm} is mean stress in reinforcment between two cracks, σ_s is stress in reinforcemnet at a cracked section, b is width of beam, d_c is concrete cover, A_s is steel reinforcment area, H is height of beam, x_c is depth of neutral axis and c is the effective height for the position of crack width measurment for concrete part and other terms are as noted previously.

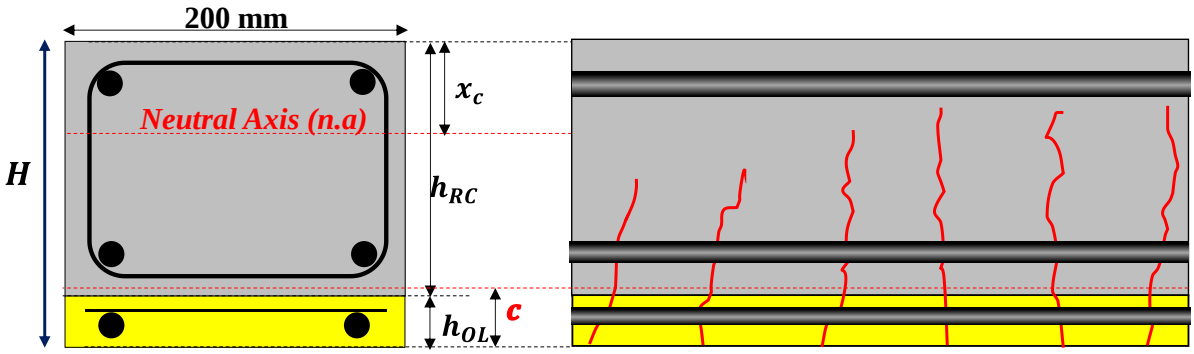

(a) Cross section (b) Longitudnal section

Fig. 6.19 Details of measuring crack width in concrete part.

By using Eq. (17), Eq. (16) was modified and also multiplied by k factor and Eq. (18) was obtained, which was used for measuring crack width of control and overlaid beams at control and elevated temperature. Crack spacing was calculated at all temperature level by using Eq. (8). **Fig. 6.20** presents the comparison of experimental crack width versus predicted crack width, which was predicted by using Eq. (18). Various codes stated 0.5 mm as crack width limit for the aggressive environment. In all cases, observd and predicted crack width were less than 0.5 mm at stablized stage, which verifies the applicability of structure at elevated temperture of 40 ℃. For verification of Eq. (18), a comparison was made by summarizing all data and presented in **Fig. 6.20**. close resemblance was observed with the observed crack width to the calculated crack width. Most of the data lies close to X=Y line, slight overestimation by predicted crack width is acceptable for safe design and serviceability requirement. Fig. 20(a) shows the comparison of crack width of overlay part (PCM), while Fig. 20(b) presents the comparison of crack width in RC beam part (concrete). Eq. (18) was modified to Eq. (19) and effective height for crack width measurment in concrete part was assumed 40 mm from bottom of strengthened RC beams, all details are mentioned in **Fig. 6.19**. Fig. 20 presents satisfactory resembalance of analytical crack width versus experimental crack width in PCM (Fig. 20(a)) and concrete (Fig. 20(b)) at both temperature level. Coefficient of determination (R^2) was observed 0.74 for PCM crack width comparison ((Fig. 20(a)), and 0.71 for concrete (Fig. 20(b)). Further improvement is needed for prediction of crack width by incorporating

other parameters, which may affect the crack width, like concrete cover, modulus of materials etc.

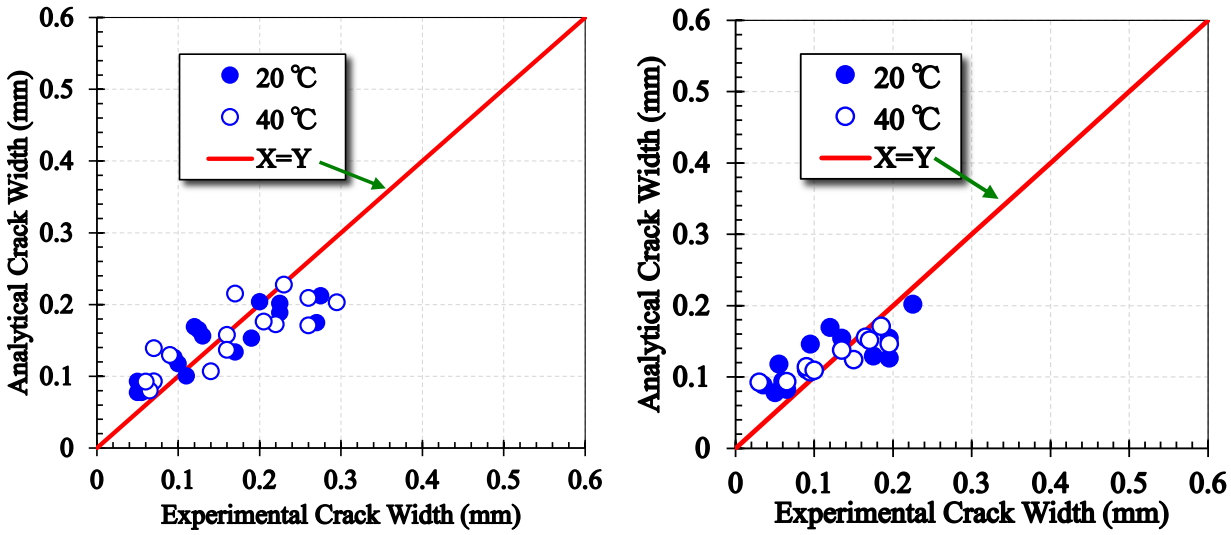

(a) PCM (b) Concrete

Fig. 6.20 Summary of crack width of all beams at both temperature level

6.6 CONCLUSIONS

In the present work, influence of temperature was investigated on the serviceability issue of PCM-overlaid RC beams. Flexural crack spacing was measured by conducting four point bending test on RC and overlaid RC beams at 20, 40 and 60 ℃, while crack width was measured during testing at 20 and 40 ℃ only. Total 27 beams were tested for reliability and applicability of this work, and selected temperature range cover climatic conditions in most of the regions having abundant RC structures. From experimental observation and analytical work, the following conclusions were extracted:

(1) Flexural crack spacing was reduced with increase in reinforcement level in overlay part and increased with the increase in temperature level for both strengthened and unstrengthened beams.

(2) The method to calculate flexural crack spacing was proposed for overlaid beams at all temperature levels and verified with experimental observations. Most of the calculated data lie within ±10% of experimental results.

(3) Crack initiated from tensile face of overlay and propagated towards compression side of beam. Crack width of PCM was wider than the crack width of concrete since PCM overlay was at tension face of the substrate RC beam. Crack width also increased with the increase in temperature level.

(4) Crack width was predicted by incorporating predicted flexural crack spacing at temperature level of 20 and 40 ℃. The predicted crack width was also verified by the observed crack width. Close agreement was observed between experimental and analytical crack width at both level of temperature.

Large amount of data was presented in this work and can be used by structural designers and researchers for further investigations and to produce guidelines for repairing of RC structures in the specific regions.

REFERENCES

[1] Rashid K, Ueda T, Zhang D. Study on strengthening of RC beam by overlaying with polymer cement mortar at elevated temperature. Symposium on Reliability of Engineering System. Hangzhou, P.R. China2015 (5 Pages).

[2] Zhang D, Ueda T, Furuuchi H. Intermediate Crack Debonding of Polymer Cement Mortar Overlay-Strengthened RC Beam. Journal of Materials in Civil Engineering. 2011;23(6):857-65.

[3] Zhang D, Ueda T, Furuuchi H. Concrete cover separation failure of overlay-strengthened reinforced concrete beams. Construction and Building Materials. 2012;26(1):735-45.

[4] Zhang D, Ueda T, Furuuchi H. Average crack spacing of overlay-strengthened RC beams. Journal of Materials in Civil Engineering. 2011;23(10):1460-72.

[5] Rashid K, Ueda T, Zhang D, Miyaguchi K, Nakai H. Experimental and analytical investigations on the behavior of interface between concrete and polymer cement mortar under hygrothermal conditions. Construction and Building Materials. 2015;94:414-25.

[6] Bazant PK, FM. Concrete at high temperature-Material properties and mathematical methods,: Harlow:longman; 1996.

[7] Khan MS, Prasad J, Abbas H. Bond strength of RC beams subjected to cyclic thermal loading. Construction and Building Materials. 2013;38:644-57.

[8] Ohama Y. Handbook of polymer-modified concrete and mortars-properties and process technology. New Jersy: Noyes Publications; 1995.

[9] ACI 318-02. Building code requirements for structural concrete (318-02) and commentary (318R-02). USA: American Concrete Institute (ACI); 2002.

[10] JSCE-2007. Standard specification for concrete structures: Design. JGC 15, Tokyo: Japan Society of Civil Engineers; 2007.

[11] Design of concrete structures, Part I: General rules and rules for buildings. European Committee for Standardization (CEN). Eurocode , Paris, 2004.

[12]C-Fm. Comité Euro-Internationale du Béton et Fédération Internationale e la Précontrainte (CEB-FIP). Lausanne, Switzerland.1990.

[13] Chiang C-H, Tsai C-L. Time–temperature analysis of bond strength of a rebar after fire exposure. Cement and Concrete Research. 2003;33(10):1651-4.

[14] Chiang C-H, Tsai C-L, Kan Y-C. Acoustic inspection of bond strength of steel-reinforced mortar after exposure to elevated temperatures. Ultrasonics. 2000;38(1):534-6.

[15] Bingöl AF, Gül R. Residual bond strength between steel bars and concrete after elevated temperatures. Fire Safety Journal. 2009;44(6):854-9.

[16] Rashid K, Ueda T, Zhang D, Fujima S. Tensile strength and failure modes of concrete repaired by polymer cement mortar in hot region. In: ACF, editor. 6th International Conference of Asian Concrete Federation. Seoul, Korea 2014:1338-45.

[17] Rashid K, Ueda T, Zhang D, Fujima S. Study on behavior of polymer cement mortar in severe

environmental conditions. 37th Annual Conventionof Japan Concrete Institute (JCI). Chiba, Japan 2015: 1597-1602.

[18] Rashid K, Ueda T, Zhang D, Miyaguchi K. Study on influence of temperature on bond integrity between polymer cement mortar and concrete. Advances in Construction Materials. Whistler, BC, Canada2015 (9 Pages).

[19] Ceroni F, Pecce M. Design provisions for crack spacing and width in RC elements externally bonded with FRP. Composites Part B: Engineering. 2009;40(1):17-28.

[20] Pecce M, Ceroni F. Modeling of tension-stiffening behavior of reinforced concrete ties strengthened with fiber reinforced plastic sheets. Journal of Composites for Construction. 2004;8(6):510-8.

[21] Sato Y, Vecchio FJ. Tension stiffening and crack formation in reinforced concrete members with fiber-reinforced polymer sheets. Journal of Structural Engineering. 2003;129(6):717-24.

[22] BAEL. Re`gles techniques de conception et de calcul des ouvrages et constructions en be ́ton arme ´suivant la me ́thode des e ́tats limites: French Concrete Code Eyrolles ed. ; 1992.

[23] ACI 318-02 ; Building code requirements for structural concrete (318-02) and commentary (318R-02). USA: American Concrete Institute (ACI) 2002.

[24] Canadian Standard Associations (CSA). S474 concrete structures. CSA-S474, Mississauga, Ontario, Canada, 2004.

[25] Kankam CK. Relationship of bond stress, steel stress, and slip in reinforced concrete. Journal of Structural Engineering. 1997;123(1):79-85.

[26] 224R-01 A. Control of Cracking in Concrete Structures. American Concrete Institute, Farmington Hills, Mich 2001.

[27] No ̈l M, Soudki K. Estimation of the crack width and deformation of FRP-reinforced concrete flexural members with and without transverse shear reinforcement. Engineering Structures. 2014;59:393-8.

Chapter 7

CONCLUSIONS AND RECOMMENDATIONS

7.1 CONCLUSIONS

Four types of polymer cement mortar (PCM) were used in this extensive experimentation and exposed to several environmental deterioration mechanisms. PCMs as bulk and also after adhesion with concrete were exposed to such environmental conditions. Concrete in all experimentation was ordinary concrete and compressive strength varies from 23 MPa to 45 MPa. Several conclusions were extracted from the experimental and analytical results and described with respect to behavior at material level and member level respectively.

7.1.1 Material Level

The following conclusions were drawn out from experimental results along with analytical results of concrete, PCM, concrete-PCM specimens under exposure of several environmental conditions. Both parameters of environment, temperature and moisture, were considered at material level testing.

1) Compressive and tensile strength of concrete and PCM were reduced with the increase in temperature level from 20 to 60 ℃ within 16 hours. Degradation in strength of PCM was observed more than strength of concrete. Exposure of constant temperature of 60 ℃ for 30 days also affected but influence of short duration of temperature exposure have severe effect than long term constant temperature exposure.

2) Along with the exposure condition, testing condition also influences the strength of PCM and composite specimens. Little recovery was observed in tensile strength of PCM when tested after cooling down the specimen to room temperature. More recovery in PCM tensile strength was observed when testing temperature was close to the glass transition temperature of polymers in PCM.

3) Day night variation and seasonal variation were also incorporated while considering the environmental condition of arid regions. Degradation in interfacial tensile strength was observed when tested at elevated temperature as compared to other testing conditions. Effect of temperature combined with moisture have severe effect among all other environmental and testing conditions.

4) Influence of temperature, under dry and wet condition was investigated. It was found that dry and wet conditions do not change significantly effects of temperature on tensile strength.

Tensile strength reduces linearly with the increase in temperature from 20, 40 to 60 ℃ under both dry and wet condition. More reduction was observed in PCM at all temperature as compared to concrete and composite specimens.

5) Influence of short duration is severe as compared to long exposure and cyclic temperature condition. 30% reduction in interfacial split tensile strength was observed after 24 hour exposure and reduction was only 8% and 28% for constant and cyclic exposure condition for 30 days, respectively.

6) It was confirmed that the main environmental parameter for degradation of strength of constituent and composite specimens were only temperature but not moisture. Specimens submerged in water for several days and also under several wetting and drying cycles did not show much influence of moisture on the interfacial tensile.

7) Interfacial tensile strength of all specimens were observed about 60% of the tensile strength of concrete specimen. Although roughness level at interface was also improved and primer was applied at interface but very small improvement in interfacial strength was observed. Failure mode of all types of composite specimens were adhesive interface failure specimens. At meso-scale cohesive PCM failure was observed along with adhesive interface failure after testing at elevated temperature.

8) Shear strength of bulk as well as composite specimen were also observed by conducting Bi-surface shear strength. Significant reduction in shear strength was observed with the increase in temperature level and observed failure mode was adhesive interface failure at all temperature levels.

9) Differential Scanning Calorimetry (DSC) analyses were performed to investigate the glass transition temperature (T_g) and melting point (T_m) of polymers after exposure to several environmental conditions. Gel permeation chromatography (GPC) analyses were also conducted to measure molecular (M_n) weight of polymers. T_g of polymers, after and before exposure, was observed in same range from 2 to 8 ℃, similar trend was observed in T_m, and values of T_m were less than 60 ℃. Insignificant variation in M_n were observed under all exposure conditions.

10) Prediction formula for interfacial tensile strength and shear strength were proposed, which were applicable at temperature range from 20 to 60 ℃. Selected temperature range covers the T_g and T_m of polymers and also climates in vast regions of the world. Prediction formula have close agreement with the experimental observations and all data lies within ±10% of experimental results. Proposed prediction formula is just a function of the respective strength (tensile or

shear) of both constituent material at 20 ℃ temperature and concerned temperatures.

7.1.2 Member Level

For direct practical application of repairing of RC structure by PCM, member level testing was performed on RC beams strengthened by various amount of reinforcement at bottom of beam which was embedded in PCM overlay. It was concluded from testing at material level that temperature influences on strength of PCM. So elevated temperature was considered as exposure and testing condition at member level testing. The following conclusions were extracted after conducting detailed experimentation and analytical study.

1) At temperature level of 20, 40 and 60 ℃, the beams were tested in four points loading condition. Failure load was increased with the increase in area of strengthening reinforcement and decreased with the increase in temperature level. Even in control specimen (without overlaying) reduction in failure load was observed. But in all cases of the strengthened specimens, observed failure loads were more than that of control specimen. Load carrying capacity was increased by more than 100% in some cases.

2) Observed failure mode was similar to the classical failure mode of RC beam viz. flexural, shear and flexural-shear, at temperature level of 20 ℃. However, at elevated temperature debonding type of failure mode was observed, which is very common in strengthen beams. Debonding was occurred at overlay end (support end) after big crack in flexural shear zone appeared and propagated towards interface of concrete-PCM.

3) First crack load, yield load, ultimate load and load deflections relationships were observed at all temperature levels. And reduction in those loads were observed with the increase in temperature and increase in those loads were observed with increasing strengthening reinforcement area. All the loads of strengthened beams were higher than the unstrengthen beam. Ductility also reduces with the increase in strengthening reinforcement area.

4) Prediction model for debonding strength of strengthened beams was proposed by incorporating interfacial shearstrength between concrete and PCM at concerned temperature. And the existing truss analogy approach was used for the prediction of ultimate shear load and failure modes. All predicted ultimate shear loads and failure modes were verified by the experimental observations.Ultimate shear load lie within ±10% of experimental observations at concerned temperature level.

5) Cracking pattern was observed in detail at elevated temperature. At all temperature levels crack was initiated in PCM part and was propagated towards substrate concrete side. Crack spacing in constant moment zone decreased with the increase in flexural reinforcement and increased

with the increase in temperature. Greater flexural crack spacing was observed in the unstrengthen beam than the all strengthened beams.

6) Crack widths of unstrengthened as well as strengthened beams were measured at 20 and 40 ℃ temperature during testing. Crack width was increased with the increase in temperature. Crack width in concrete was less than the PCM at similar load and temperature level.

7) Crack spacing and crack width was predicted for overlaid beams at elevated temperature and close agreement were observed between experimental and predicted values.

7.2 RECOMMONDATIONS

7.2.1 Suggestions for Engineering Applications

Based on the experimental and analytical study conducted in this study, the following suggestions were made for the application on repairing structure by PCM.

1) No information was available by manufacturers of PCM about the mechanical properties of PCM at elevated temperature, although four types of PCMs were used but all information provided by manufacturers were conducted at 20 to 25 ℃. In real scenario, environmental temperature was varied from 20 ℃ to more than 60 ℃. Current data may be used by manufacturers of PCM for proper selection of PCM in specific region in which it is supposed to apply.

2) In all repaired structures, interfacial stresses in tension and shear were generated at interface between old substrate concrete and PCM. It was observed that interfacial strength is very less as compared to the bulk specimen strength. And at elevated temperature further reduction was observed. So, interfacial strength proposed must be used by designers and researchers while designing of repairing structure.

3) The proposed prediction for debonding strength of beams strengthened with PCM overlay can be used by designers to prevent debonding mode of failure of flexural members. Debonding mode must be prevented due to its brittle failure and also due to safety problem. Influence of temperature should be considered while designing of flexural members strengthened with PCM overlay.

7.2.2 Suggestions for Future Studies

This dissertation describes the interfacial behavior of concrete-PCM at material level and member level at several environmental conditions and more precisely at elevated temperature. Extensive experimentation and analytical study were conducted for application to real structures. According to author knowledge, present work is the first study which describes the performance of

structure with PCM overlaying under environmental conditions. Although, four types of PCMs were used but no data was available for PCM under designed exposure conditions. So, there are still a lot of works that need to be done which are briefly described as follows.

1) Treatment of substrate surface was accomplished in this study by adopting the best method proposed in the literature. But interfacial strength is still less than the strength of constituents. It is suggested here to extend the current work, to improve the interfacial strengths, by using epoxies or adhesive at interface between concrete and PCM.

2) All composite specimens failed at interface and proposed prediction formula was applicable for such failure mode. For other failure modes; concrete cohesive failure or PCM cohesive failure, however, more experimentation and analytical study should be conducted.

3) Day night variation was investigated in this work only for one month (30 days). However, the service life of RC structures is much longer. It is suggested to use long exposure period, at least two years, to predict the service life of strengthened structures accurately.

4) Crack width was predicted only for short duration of temperature exposure. However, long-term effects, like creep and sustained load were ignored and must be considered by extending the current work.

5) Only strengths of materials were evaluated in this work and it is suggested to do more precise investigation of effect of elevated temperature by observation of material changes in micro scale and by stress analysis with consideration of thermal stress, etc.

6) Bond between PCM and steel reinforcement in PCM is of significant importance. It should be evaluated at different temperature levels in order to understand cracking behavior and ultimate failure loads including debonding failure load more precisely.

7) Here only RC beams were tested. This study can be extended for further testing of slabs and columns. And also only static loading was considered in this study. Highway and railway structures are exposed to fatigue loading and repaired by overlaying method in many cases. So, this study should be extended for fatigue at elevated temperature.